Stochastic multiscale modeling of MEMS stiction failure

Truong Vinh HOANG

Liège, Belgium, September 19th, 2017

University of Liège, Belgium

Le Fonds de la Recherche Scientifique

- MEMS: Micro-Electro-Mechanical System
  - Technology to develop microscopic devices
  - Small size: lower power requirement, reduced manufacturing material cost
  - Part of flourishing technology

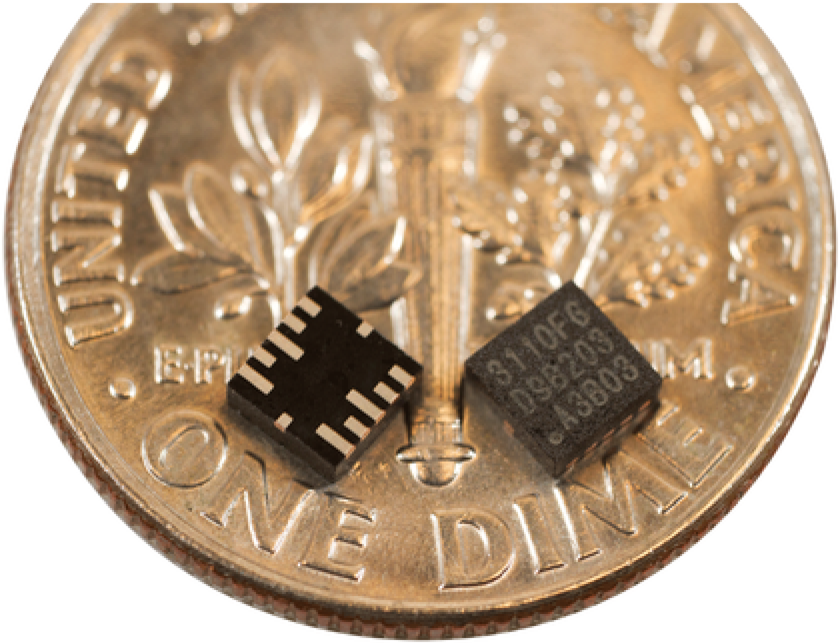

Size of MEMS chips
(Source: mCube)

SEM image of a micro-gears system
(Courtesy Sandia National Laboratories)

Overview

- MEMS: Micro-Electro-Mechanical System
  - Applications: **Accelerometers**, digital mirrors, pressure sensors, gyroscopes, resonators, DNA chips ...

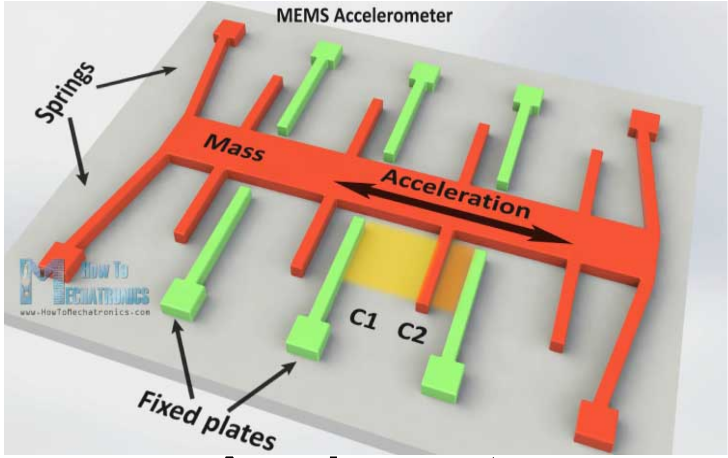

Accelerometer

Measure shock due to accident for airbag system

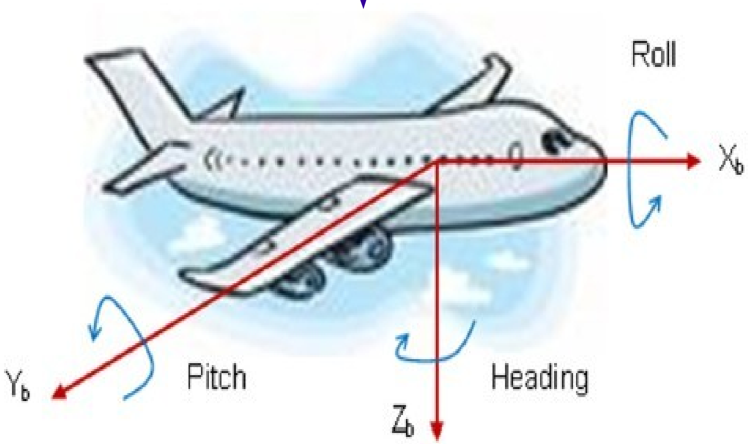

Measure dynamic behavior of airplane

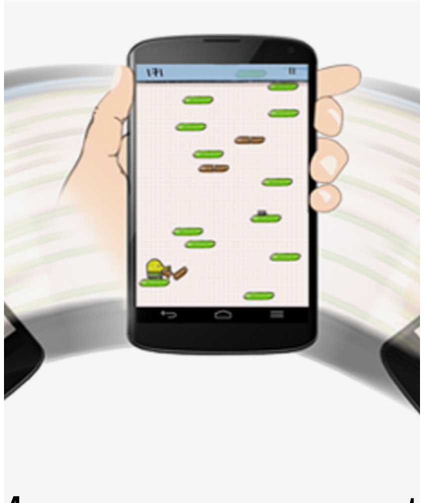

Measure movement of smart phone

Figures sources: contus.com, wiki.seeedstudio.com, carsdirect.com, howtomechatronics.com

Overview

- MEMS: Micro-Electro-Mechanical System
  - Applications: Accelerometers, **digital mirrors**, pressure sensors, gyroscopes, resonators, **DNA chips** ...

Digital mirror for projector
(Epson®)

Affymetrix GeneChip®
(source: wikipedia)

Motivation

- Small volume to area ratio, small gap

$$\frac{\text{volume}}{\text{surface area}} \sim \frac{l^3}{l^2} = l, \quad l \sim 10^{-6}\ \text{m}: \ \text{characteristic length}$$

  - Surface forces become important (one million times more important than at macro scale)
  - Adhesions forces: capillary forces and van der Waals (vdW)
- Stiction phenomenon
  - Two contacting bodies are permanently stuck
  - Common failure of MEMS

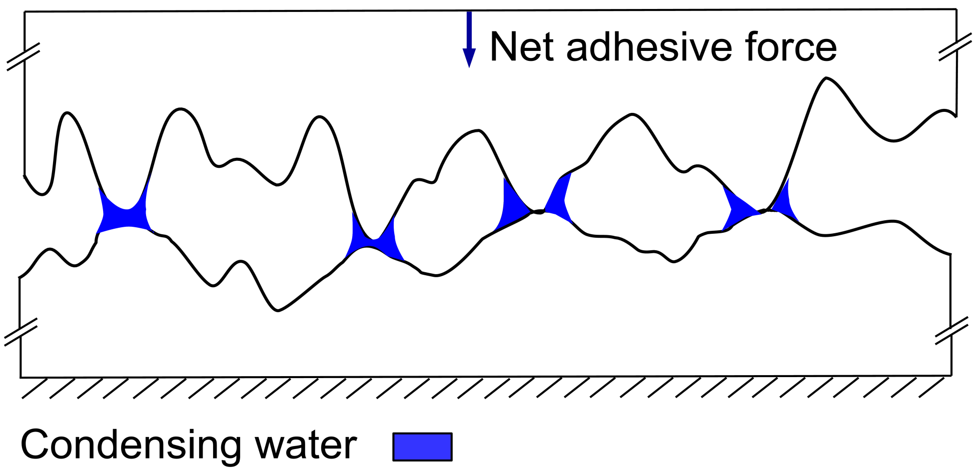

Adhesion of two contacting rough surfaces

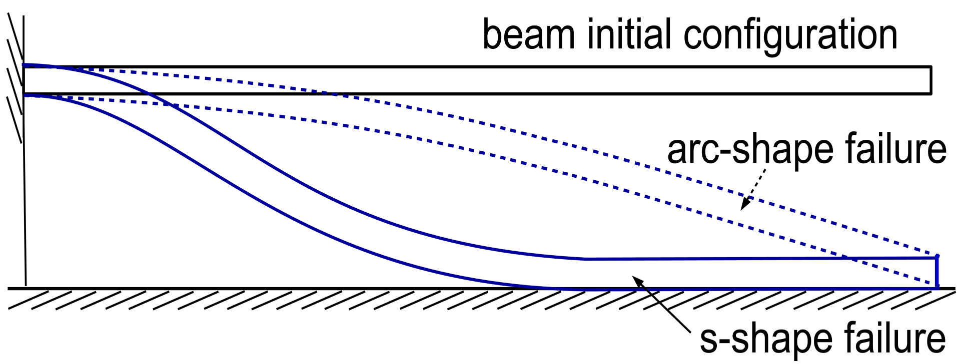

Stiction configurations of micro beams to its substrate

- Small volume to area ratio, small gap

$$\frac{\text{volume}}{\text{surface area}} \sim \frac{l^3}{l^2} = l, \quad l \sim 10^{-6}\ \text{m}: \ \text{characteristic length}$$

  - Surface forces become important
  - Adhesions forces: vdW forces and capillary forces
- Stiction phenomenon
  - Two contacting bodies are permanently stuck
  - Common failure of MEMS

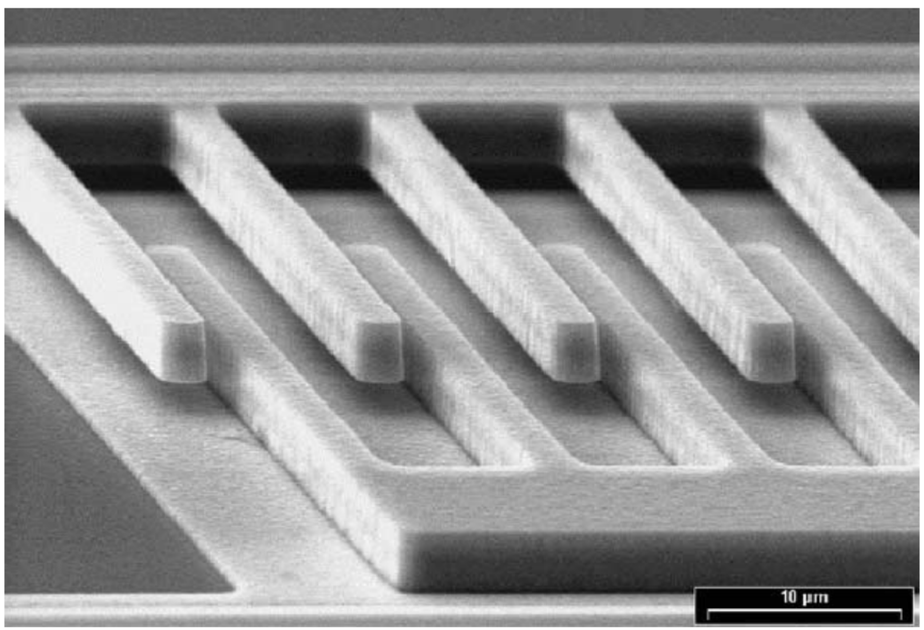

Stiction failure of comb drive
(Courtesy of IMEC)

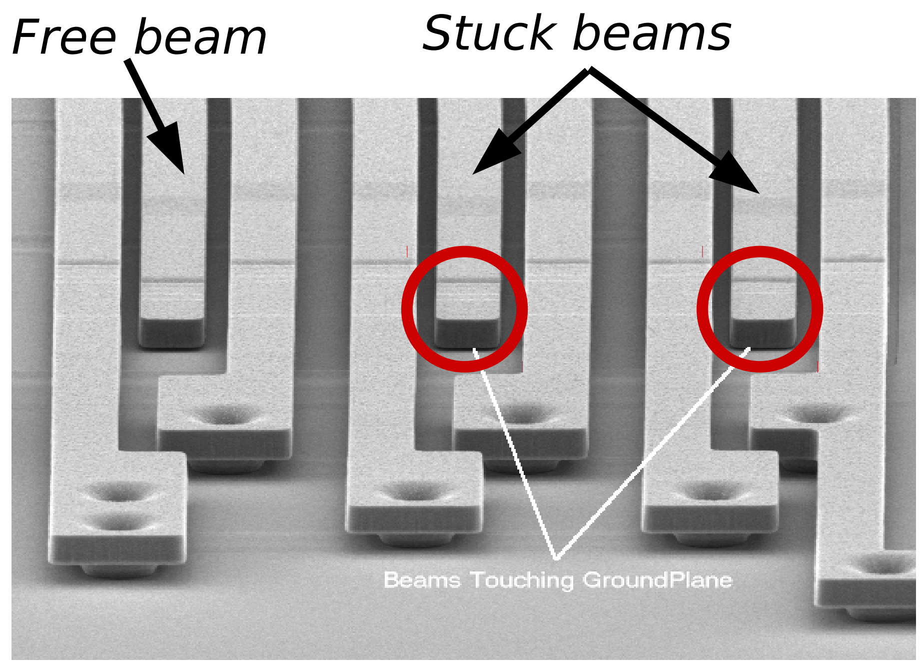

Stiction failure in a MEMS sensor
(Jeremy A.Walraven Sandia National Laboratories. Albuquerque, NM USA)

Motivation

- Multiscale problem
  - Range of adhesive forces (nanometers) << size of structure (micrometers)
  - Effective contact zone is local (**1**) [de Boer et al. 2007]
- Surface roughness
  - Interaction involves only highest asperities (**2**)
- Stiction phenomenon suffers from scatter:
  - (**1**) and (**2**): number of contacting asperities at the effective contact zone is not sufficient to obtain a statistically homogenized behavior
  - Identical design and fabrication process MEMS structures but different stiction behaviors
  - Tested beam arrays: s-shape beams (different crack lengths)

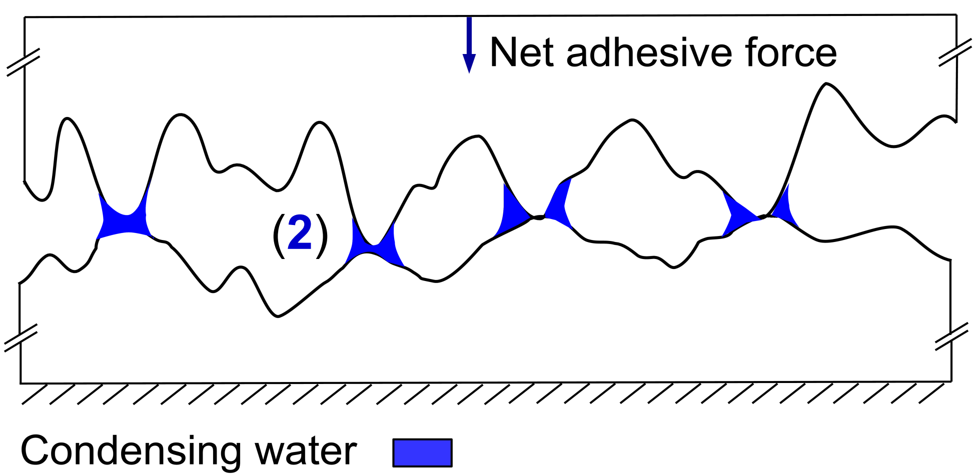

Adhesion of two contacting rough surfaces

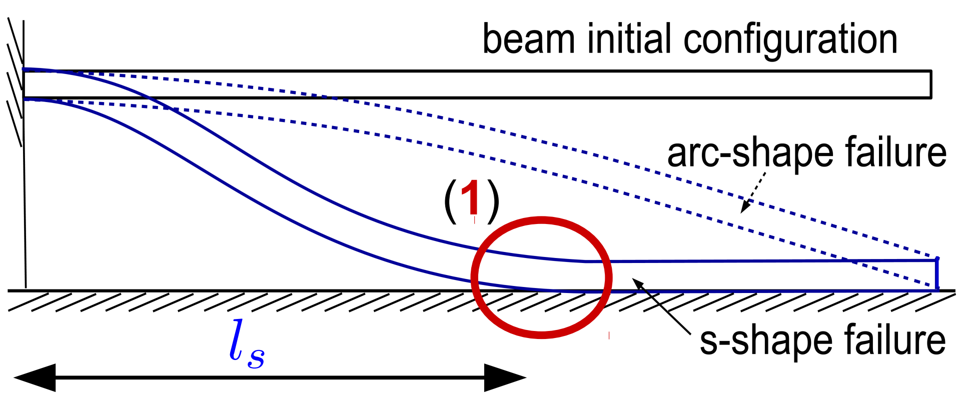

Stiction configurations of micro beam to its substrate

Objectives

- To quantify the uncertainty of MEMS stiction behavior
  - Design a MEMS product striking a balance between costs and stiction failure percentage
- Develop a numerical method
  - Quantifying the uncertainty of the stiction behavior of MEMS
  - Accounting for roughness of contacting surfaces
  - Numerically verified and experimentally validated
  - With acceptable computation cost
- Difficulties
  - Multiple scales, multiple physics
  - Surface roughness characterization
  - Uncertainty quantification across multiple scales and multiple physics
  - High computational costs

Stochastic multiscale model

I. Deterministic multiscale model

- Dealing with the aspects of multiple scales and multiple physics of stiction phenomenon

II. Stochastic analysis

- Dealing with stochastic analysis over multiscale model
- At an acceptable computational cost

III. Numerical verification and experimental validation

IV. Conclusions and perspectives

Contents

Deterministic multiscale

- Goal: evaluate the stiction failure configuration of a MEMS structure
- Brute forte solution: a Finite Element model with a small element size
  - Element size h ~ 1 nm to capture the adhesive stresses of capillary and vdW interactions
  - Structure size L ~ 100 μm
  - L/h ~ 100 million : Expensive computational cost
- Develop a multiscale model
  - To reduce computational cost

Deterministic multiscale model

- Lower-scale: measurement of surface topology
  - Lower scale: using Atomic Force Microscopy (AFM) to measure the contacting surfaces
- Meso-scale: surface contact model
- Upper-scale: MEMS Stiction behavior

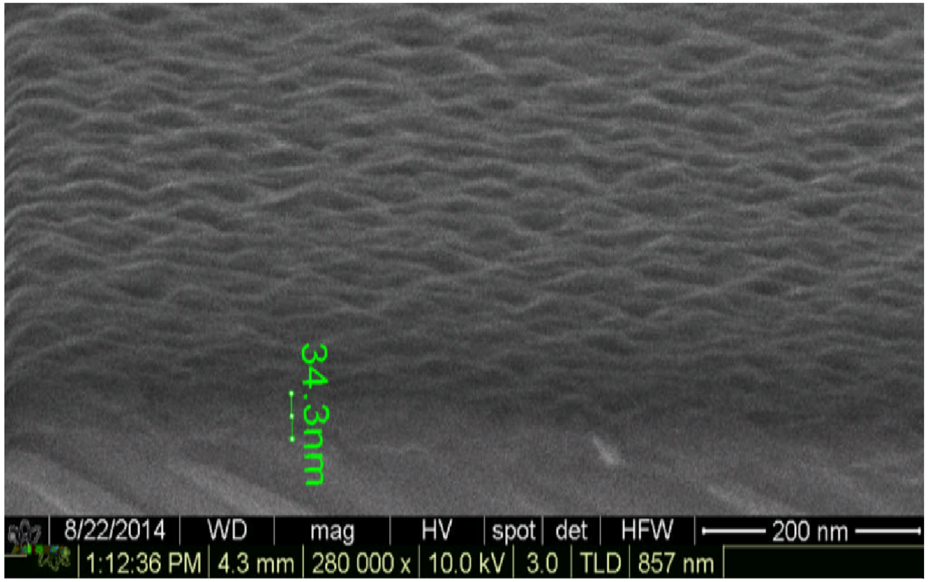

SEM image of surface roughness

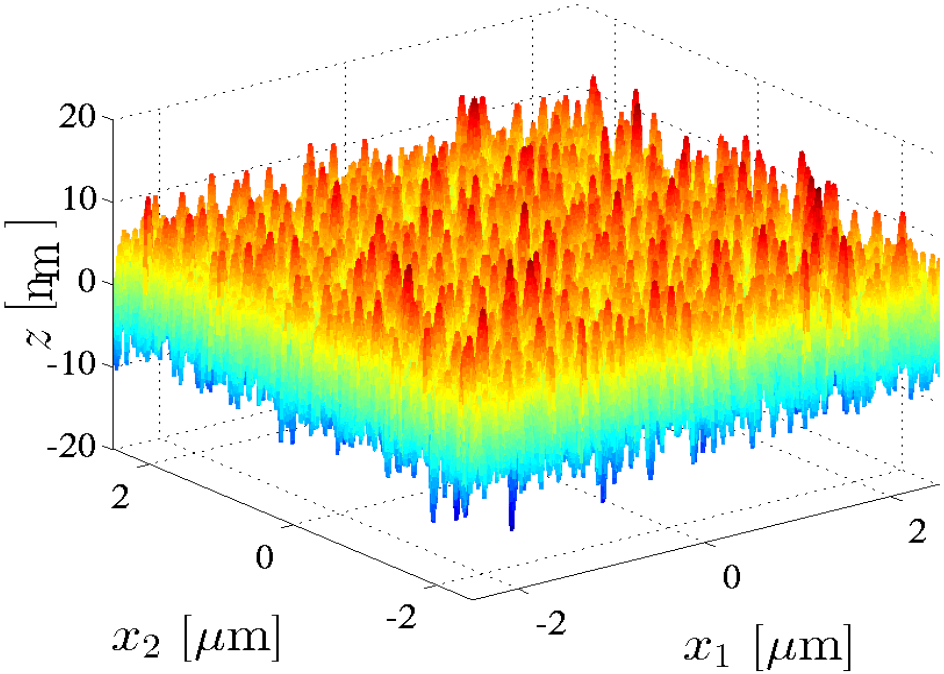

AFM measurement

Samples were fabricated at IMT-Bucharest: National Institute for Resesearch and Development in Microtechnologies, Romania

Deterministic multiscale model

- Lower-scale: measurement of surface topology
- Meso-scale: surface contact model
  - Evaluate the apparent adhesive contact forces between AFM measurements
- Upper-scale: MEMS Stiction model

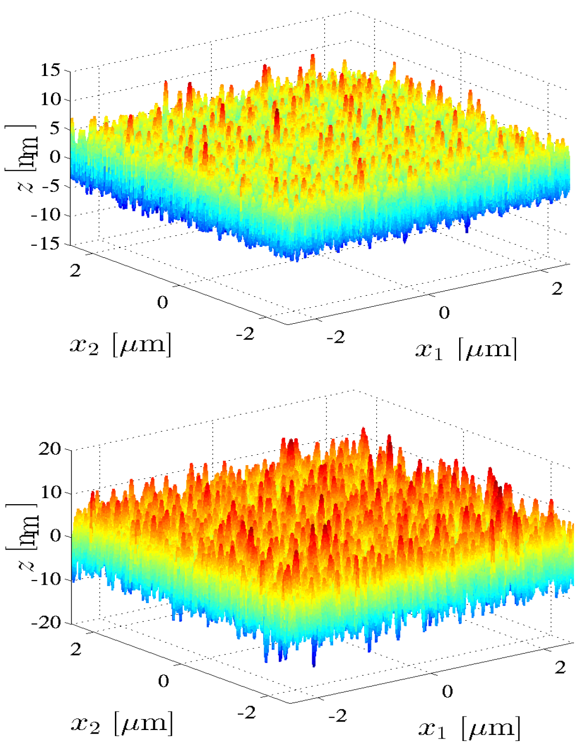

AFM measurements

Meso-scale contact model

roughness, vdW, capillary forces

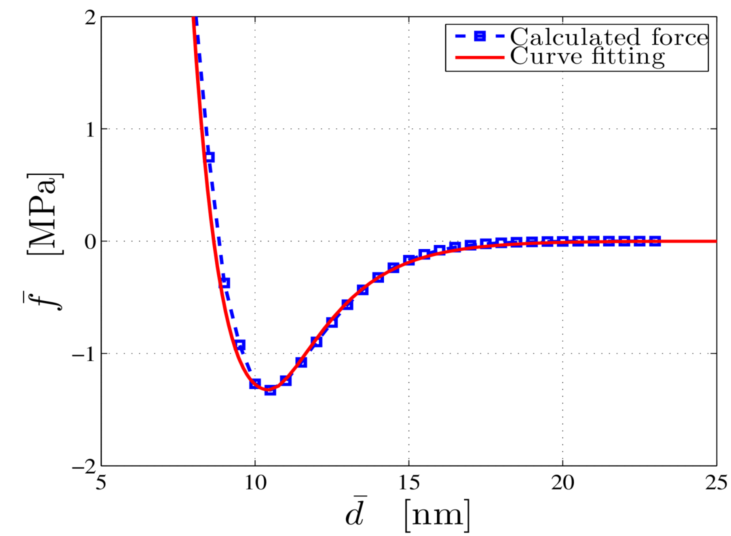

Apparent adhesive forces vs contact distances

Deterministic multiscale model

- Lower-scale: surface roughness
- Meso-scale: surface contact model
- Upper-scale: MEMS Stiction behavior
  - Construct a FE model of the considered MEMS structure to evaluate its stiction behavior
  - Meso-scale contact forces function is considered as contact law associated with integration points
  - Ratio between structure size and element size is reduced (~ 100): computational cost is reduced compare to (single scale model) brute force FE

Meso-scale adhesive contact forces

FE model

Stiction configuration

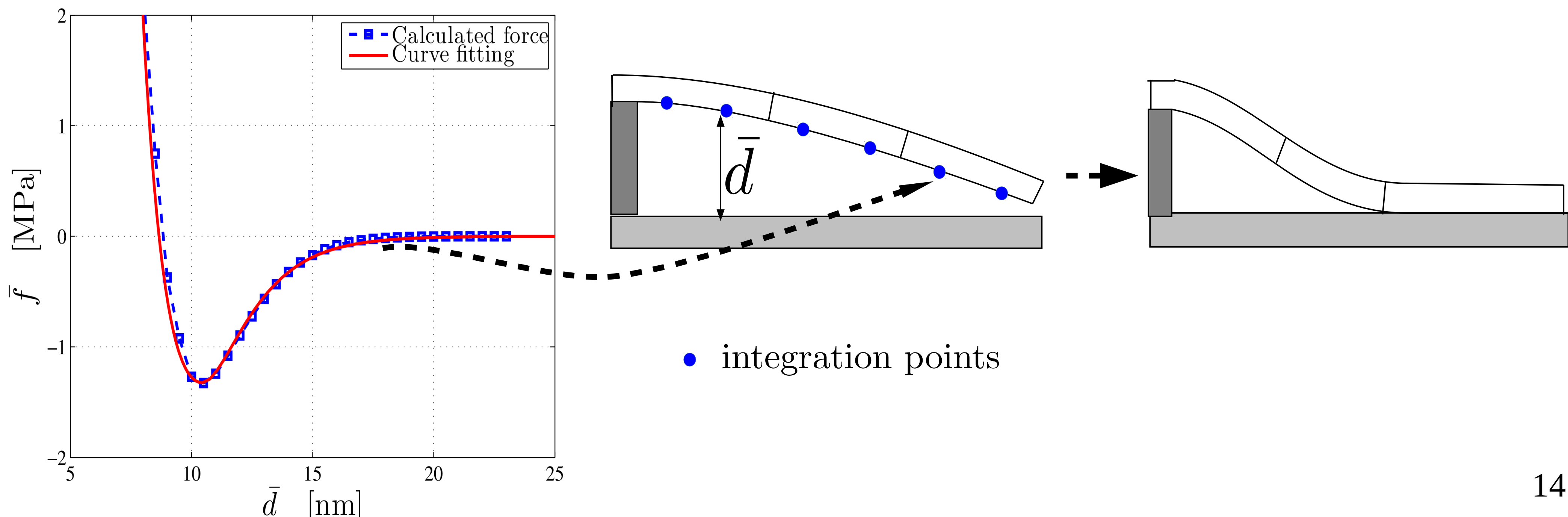

I. Deterministic multiscale model

- Meso-scale contact model
- Upper-scale FE stiction model

Meso-scale contact model

- Physics of adhesive forces
  - vdW interaction is not discussed here (see my thesis for details)
  - Capillary forces: resulting from condensing water including meniscus and absorbed surface layer.

$$\text{Lalace pressure: } \Delta P = \frac{\gamma_{\mathrm{LG}}}{r_K} = \frac{\mathcal{R}T \ln RH}{V_m}, \quad \text{Kelvin radius: } r_K = \frac{\gamma_{\mathrm{LG}} V_m}{\mathcal{R}T \ln RH}$$

(RH humidity level, γ_{LG} liquid vapor energy, V_m liquid molar volume, $\mathcal{R}$ universal gas constant, T absolute temperature)

$$\text{Theoretical adhesion energy is constant: } w_C = h_{\mathrm{water}} \Delta P = 0.144\ [\mathrm{J/m^2}]$$

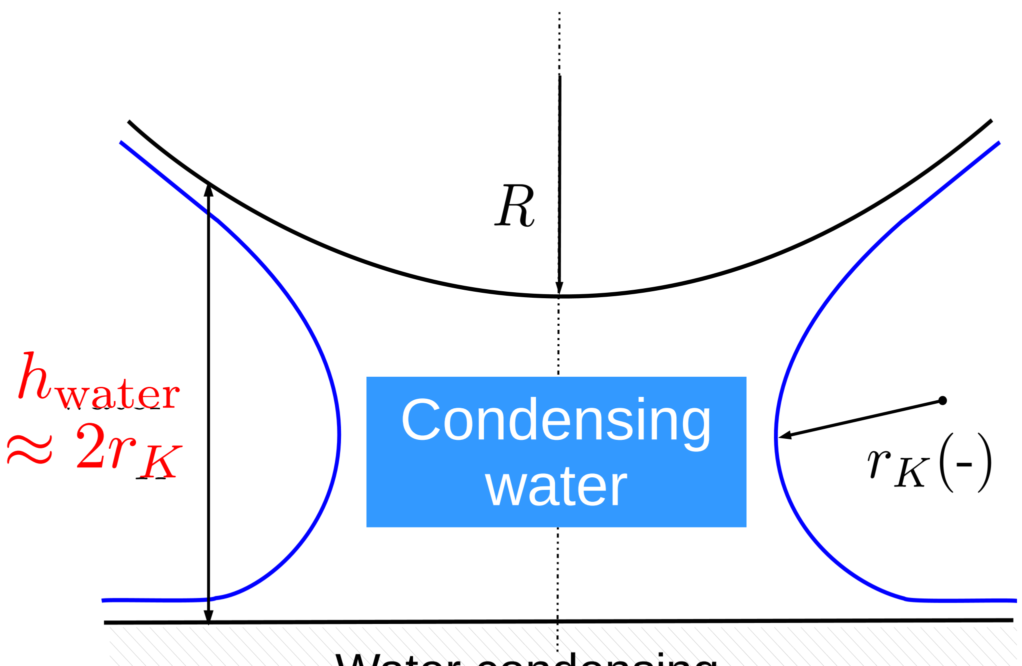

Water condensing between a sphere and substrate

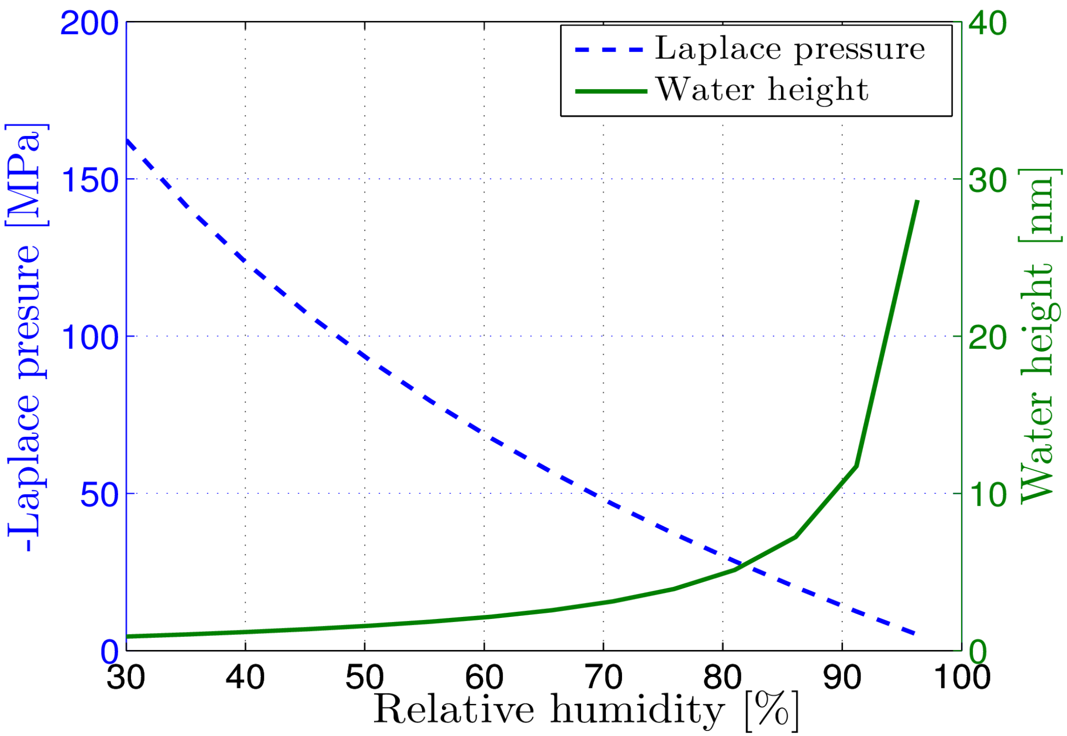

Capillary interaction parameters

Meso-scale contact model

- Contact problem between a rough surface and a flat surface
  - Adhesive stress is weak compared to material stiffness
  - Physical contact happens only at the highest asperities: multiple asperity contact theory
  - Saturation effect: water menisci can be merged together at high humidity levels
    - Menisci could not be treated locally at each asperity

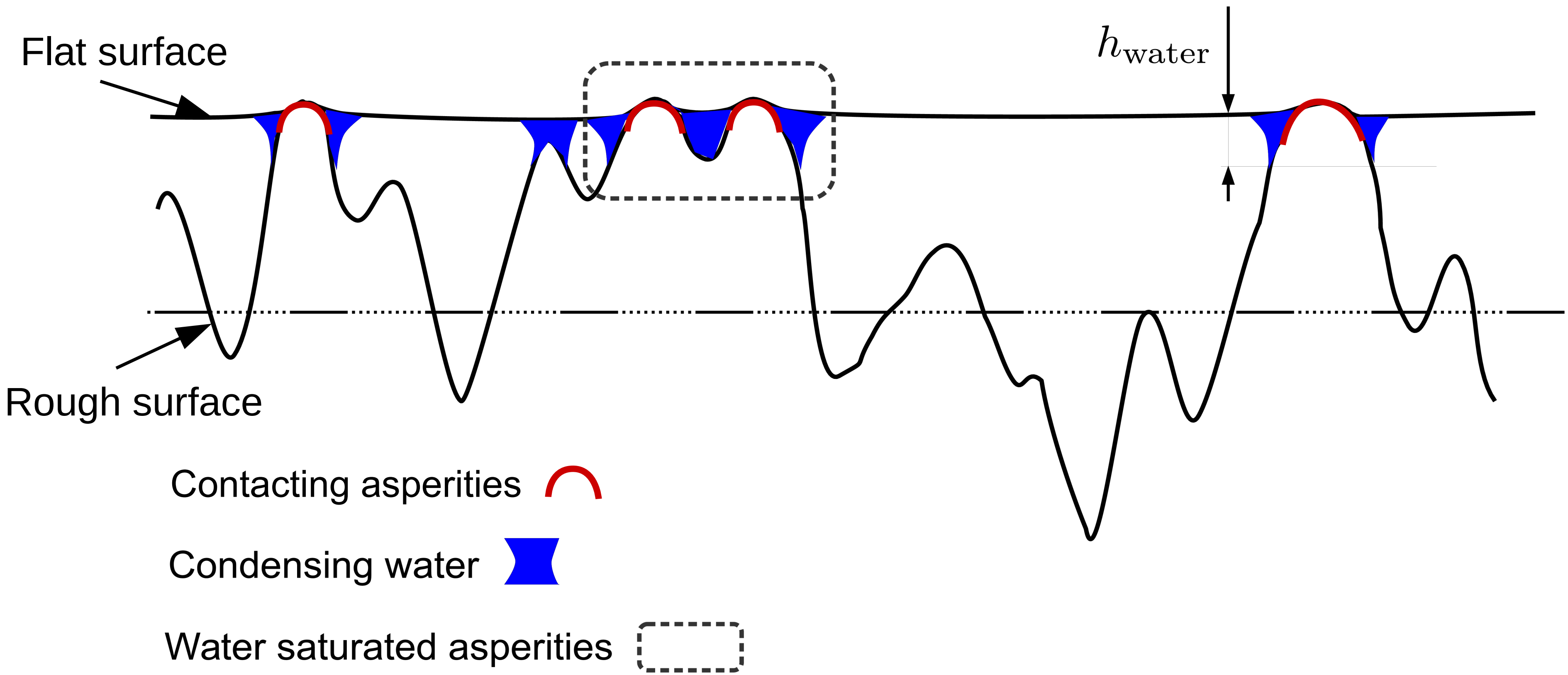

Meso-scale contact model

- FE method [Ardito et al. 2013, 2014]
  - Advantage: accurate
  - Disadvantage: high computational cost
- Analytical model, e.g. Greenwood-Williamson (GW) model [Greenwood et al. 1966]
  - Based on multiple asperity contact theory [Ardito et al. 2016]
    - Evaluate the adhesive contact forces at each contacting asperity
    - Sum all the forces to get the total adhesive contact force
    - Summation is simplified by a statistical average
      - infinite surface size is assumed
  - Advantage: efficient in terms of computational cost
  - Disadvantages:
    - Saturation effect is not accounted for
    - Size effect (for stochastic analysis) is not accounted for since infinite surface size is assumed
- Semi-analytical surface contact model (**in this thesis**)
  - Based on multiple asperity contact theory with low computational cost
  - Adavantages: account for saturation effect and size effect

Asperity contact models

- Spherical asperity contact models
  - Hertz model: non-adhesive elastic contact [Hertz 1882]
  - Derjaguin-Muller-Toporov (DMT) model: long range and weak adhesive stress, hard material [Derjaguin et al. 1975]
  - Johnson-Kendall-Roberts (JKR) model: short range and strong adhesive stress, soft material [Johnson et al. 1971]
  - Maugis model: transition model [Maugis 1992]
  - Modified DMT model (adhesive elastic contact): long range, weak interaction stress, hard material
    - Developed in this thesis

Applicability of contact models			
	DMT	Maugis	**Modified DMT**
Capillary interaction on polysilicon* (hard material)	✓	✓	✓
Extending to surface contact (**with saturation**)			✓

(*) Polysilicon is one of the most important materials in context of MEMS

Asperity contact models

- Hertz model (non-adhesive elastic contact)

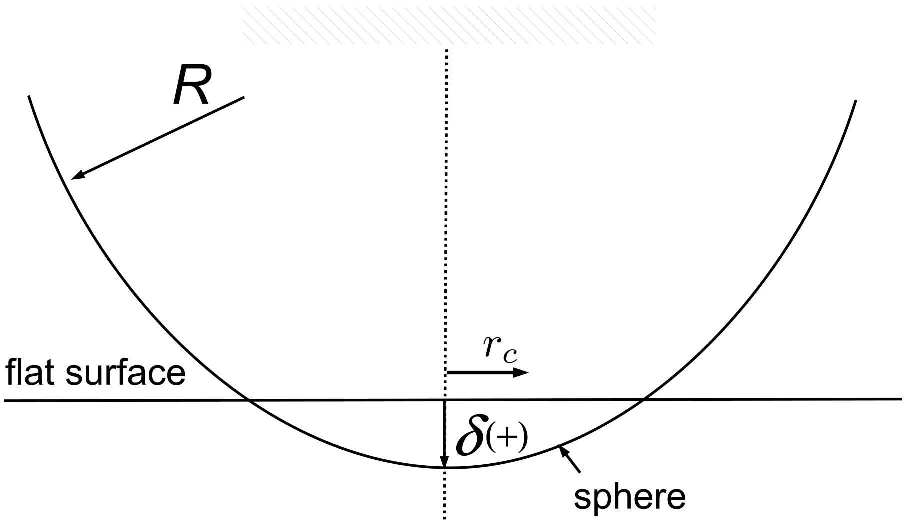

Undeformed configuration

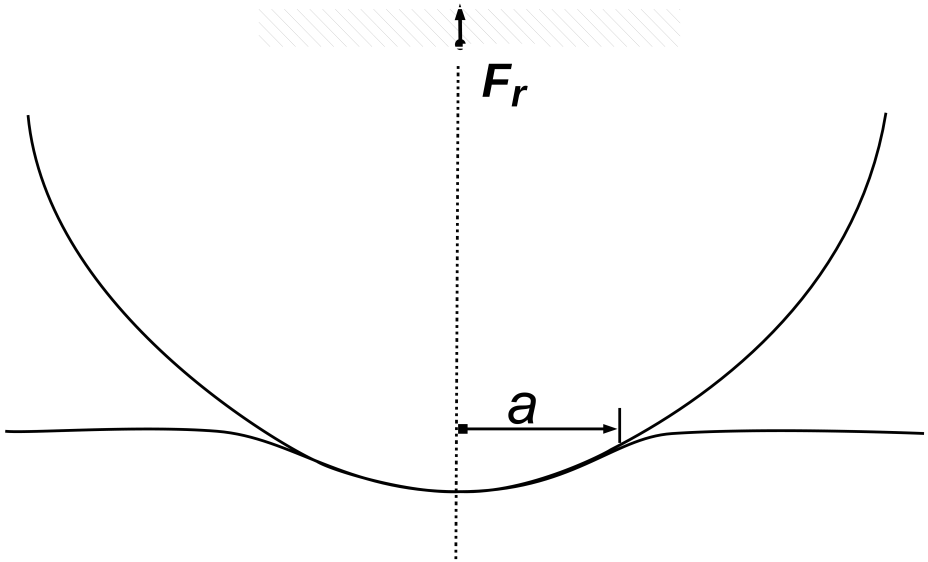

Deformed configuration

Material elastic properties,
Boundary conditions

Hertz model $\longrightarrow$

Deformed configuration of spheres,
elastic repulsive forces

$$\text{physical contact radius:} \quad a = \sqrt{R\delta}$$

$$\text{elastic repulsive force:} \quad F_r = \frac{Ka^3}{R}$$

$$K = \frac{4}{3}\left[(1-\nu_1^2)/E_1 + (1-\nu_2^2)/E_2\right]^{-1}$$

Asperity contact models

- DMT model
  - Assumption: weak and long range adhesive forces, hard material
    - Deformation resulting from adhesive stress is negligible compared to the one from elastic stress
    - Deformed configuration can be evaluated using Hertz model
      - Radius *a*: of physical contact area
      - Radius *c*: the largest radius at which the contact distance is h_{water}
    - Total contact force can be evaluated by adding the elastic repulsive force and capillary force

$F_{\mathrm{r}},\ a,\ c$ are evaluated from Hertz model

Capilary interaction: $\mathrm{F}_C = \Delta P(\pi c^2 - \pi a^2)$

Total force: $F = F_r + F_C$

(area of deformed sphere inside meniscus) (asperities physical contact area)

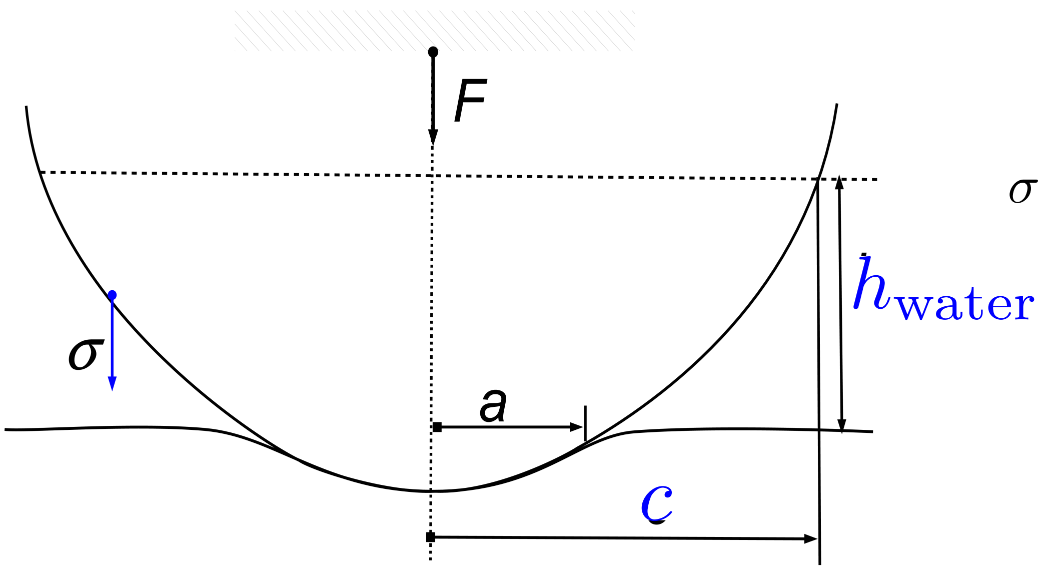

$$\sigma = \begin{cases} \Delta P & \text{if } 0 < h \leq h_{\mathrm{water}} = 2r_K\ ; \\ 0 & \text{if } h > h_{\mathrm{water}} = 2r_K \end{cases}$$

Deformed configuration (evaluated by Hertz model)

- Modified DMT model
  - Additional assumption: at the points (●) whose contact distance is equal to the height of meniscus h_{water} the sphere is not deformed
  - The ability to evaluate radius c solely from undeformed geometry is key to account for the saturation effect.

c evaluated solely using undeformed geometry

$$\left.\begin{array}{l} F_{\text{r}},\ a \text{ are evaluated from Hertz model} \\ \text{Capilary interaction:} \quad F_C = \Delta P(\pi c^2 - \pi a^2) \end{array}\right\} \quad \text{Total force:} \quad F = F_r + F_C$$

(πc^2: area of deformed sphere inside meniscus) (πa^2: asperities physical contact area)

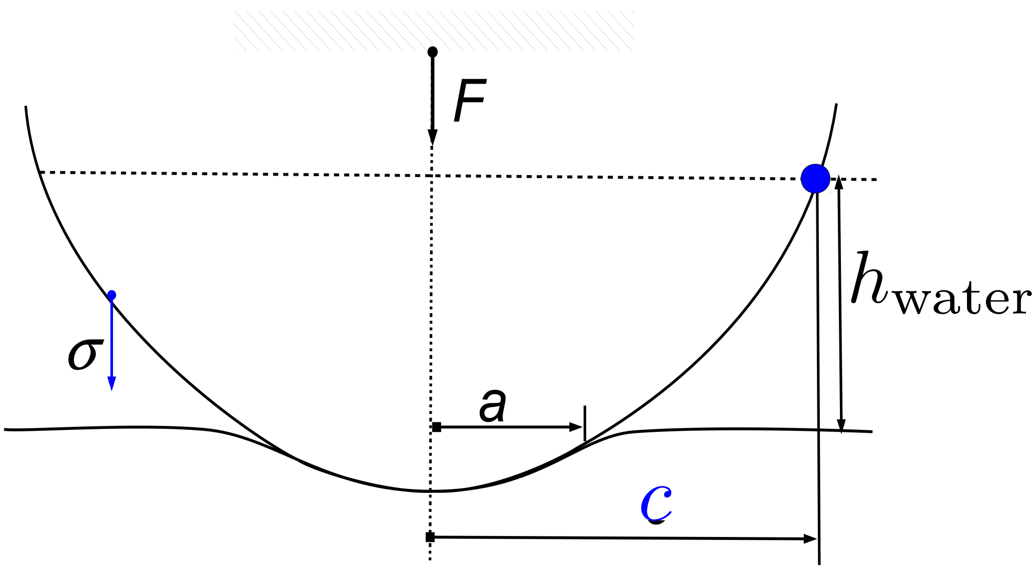

Deformed configuration

$$\sigma = \begin{cases} \Delta P & \text{if } 0 < h \leq h_{\text{water}} = 2r_K \ ; \\ 0 & \text{if } h > h_{\text{water}} = 2r_K \end{cases}$$

- Verification of the modified DMT model
  - Comparison on a sphere vs. flat surface interaction: Modified DMT model, DMT model, Maugis model
  - Good agreements between three models
  - The validity of additional assumption in the modified DMT model is numerically verified

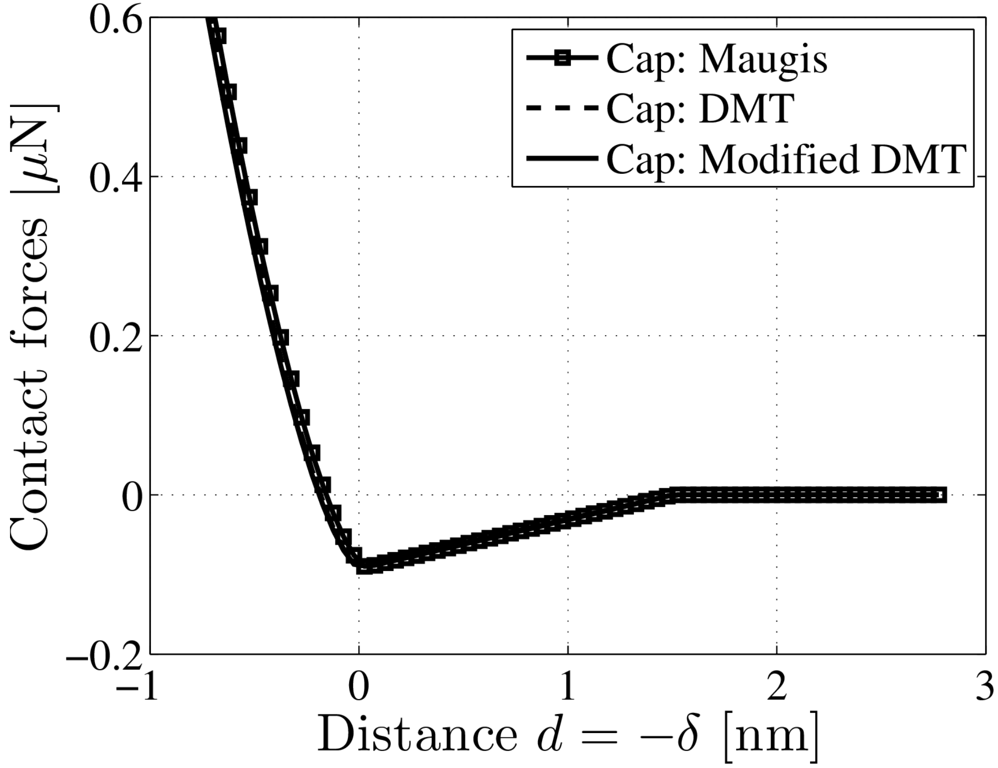

$R = 100$ nm, $RH = 50\%$

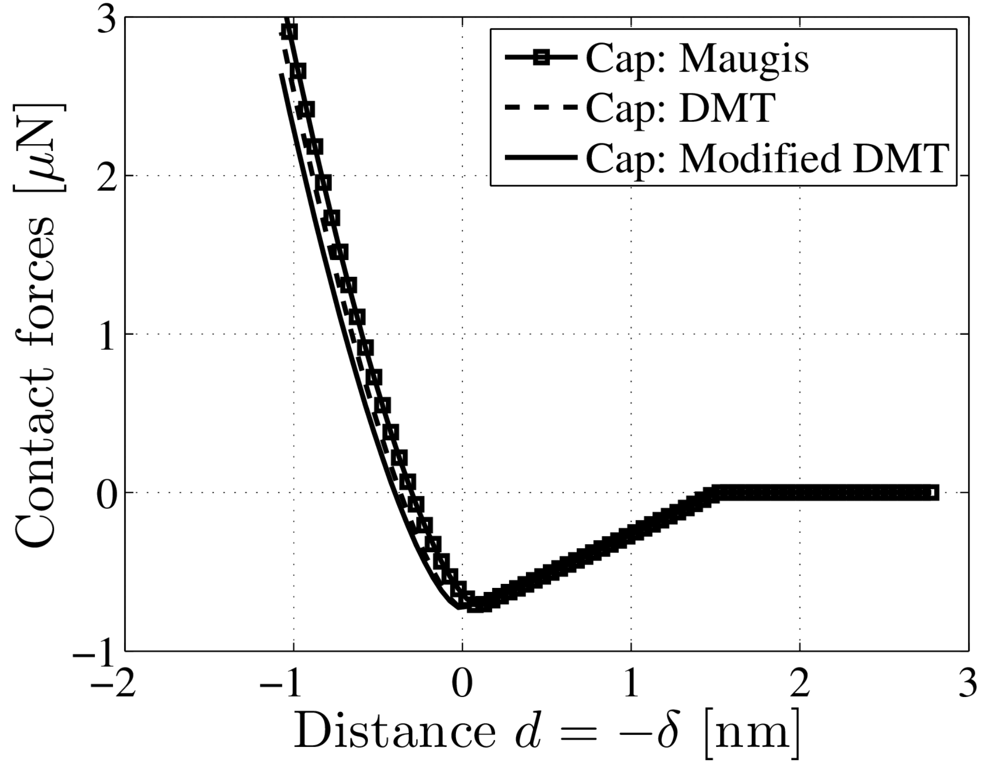

$R = 800$ nm, $RH = 50\%$

Meso-scale contact model

- Semi-analytical model for contact between rough surfaces
  - Equivalent contact problem

z_1 vs. z_1

z_1

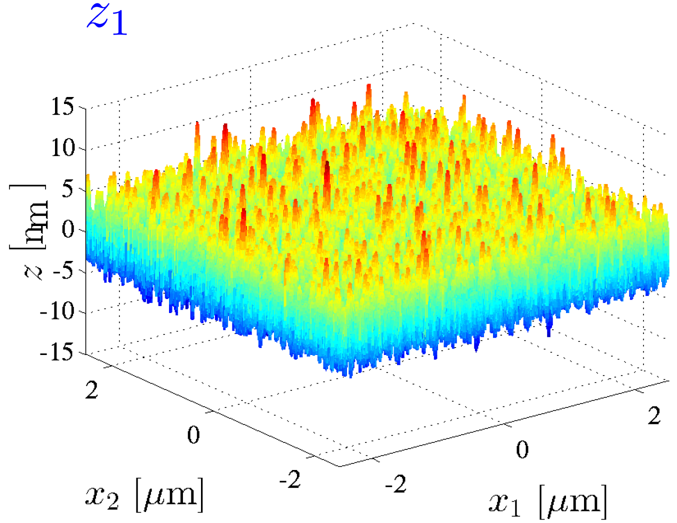

z_2

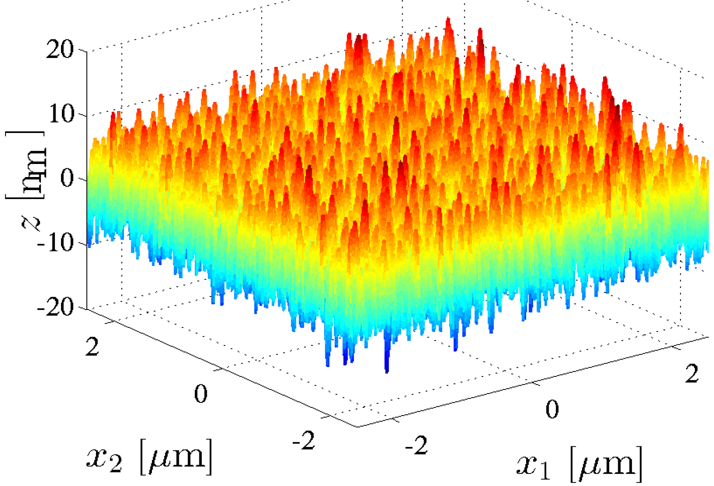

AFM measurements

equivalent to

z_{eq} vs. flat surface

$z_{eq} = z_1 + z_2$

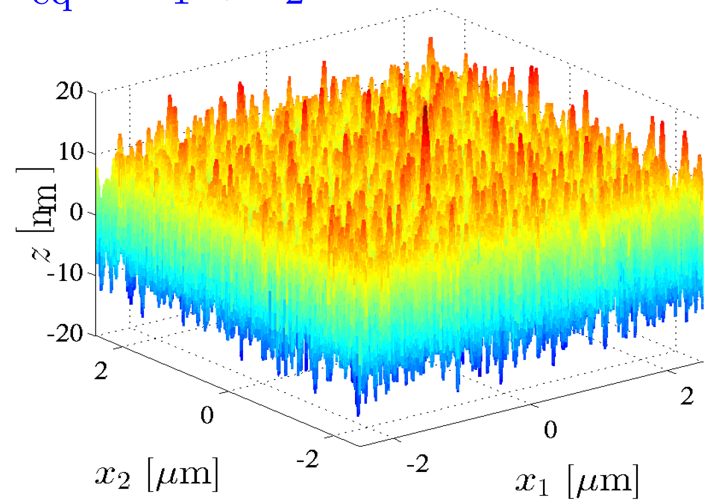

flat surface

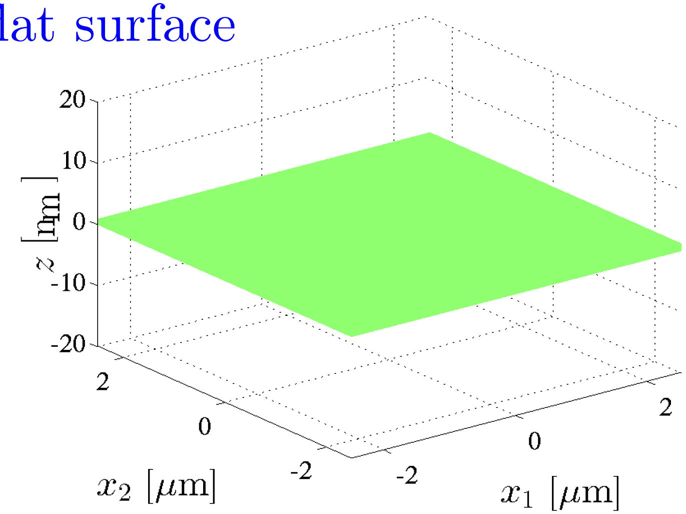

Meso-scale contact model

- Semi-analytical model for contact between rough surfaces
  - Extend modified DMT model to surface contact
  - Repulsive and capillary interactions are evaluated separately
  - Capillary effect is treated in a global way: saturation effect is accounted for

$$\text{total repulsive force } f_r = \sum F_r^{(i)}$$

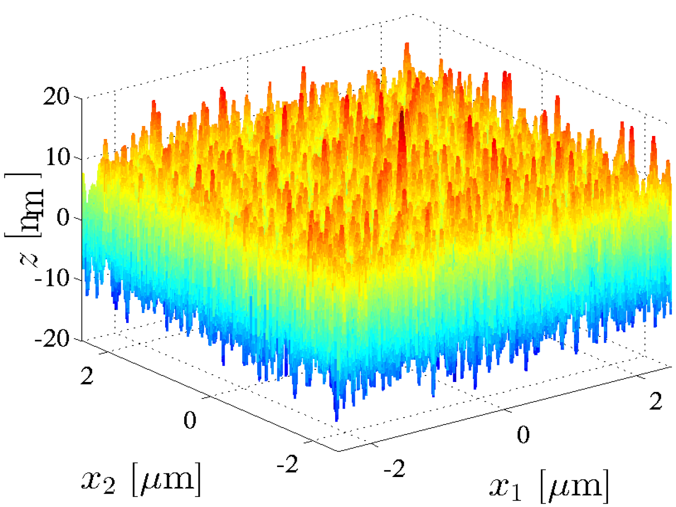

Equivalent rough surface

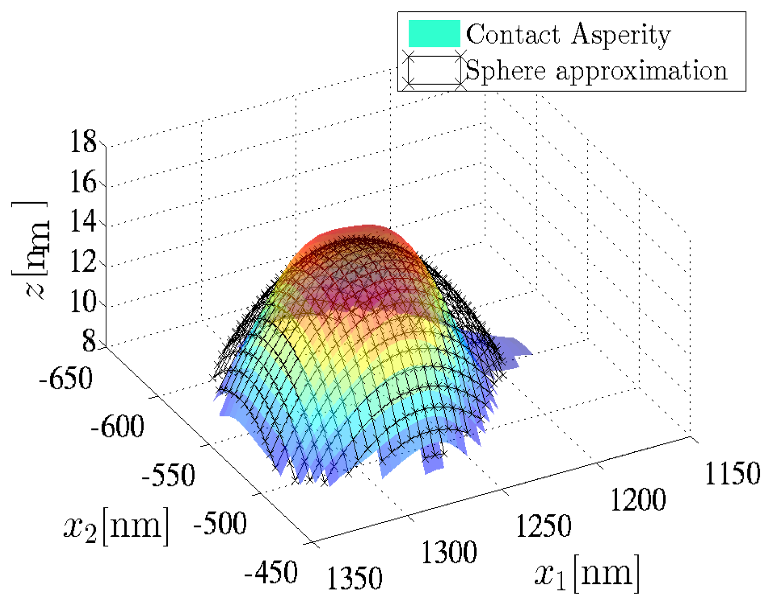

i-th identified contacting asperity, its spherical approximation

$$F_r^{(i)},\ a^{(i)}$$

Hertz model (elastic interaction)

Meso-scale contact model

- Semi-analytical model to contact between rough surfaces
  - Extend modified DMT model for surface contact
  - Repulsive and capillary interactions are evaluated separately
  - Capillary effect is treated in a global way: saturation effect is accounted for

$$\left.\begin{aligned} &\text{total repulsive force } f_r = \sum F_r^{(i)} \\ &\text{capillary force} \quad f_C = \Delta P(A_{h_{\text{water}}} - \sum \pi a^{(i)2}) \end{aligned}\right\} \text{total force } f = f_r + f_C$$

$A_{h_{\text{water}}}$ (area of topology whose contact distance $\leq h_{\text{water}}$)

$\sum \pi a^{(i)2}$ (asperities physical contact area)

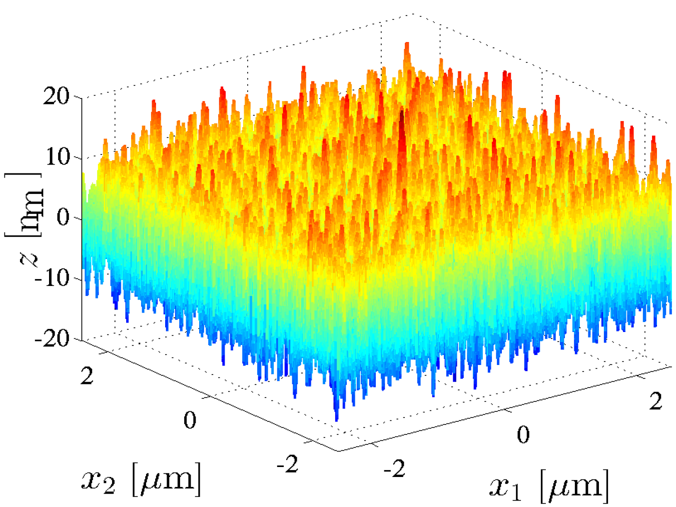

Equivalent rough surface

$A_{h_{\text{water}}}$

evaluated solely using undeformed geometry (as c)

Meso-scale contact model

- Semi-analytical model for contact between rough surfaces
  - A typical evaluated contact forces function has three zones depending on contact distance
    - Two contacting surfaces are far way: no interaction (zero forces)
    - Two contacting surfaces approach each other: adhesive interaction is dominant (negative forces)
    - Two contacting surfaces enter to significant physical contact: elastic compression is dominant (positive forces)

$$\bar{f} = \frac{\text{total force}}{\text{surface area}}$$

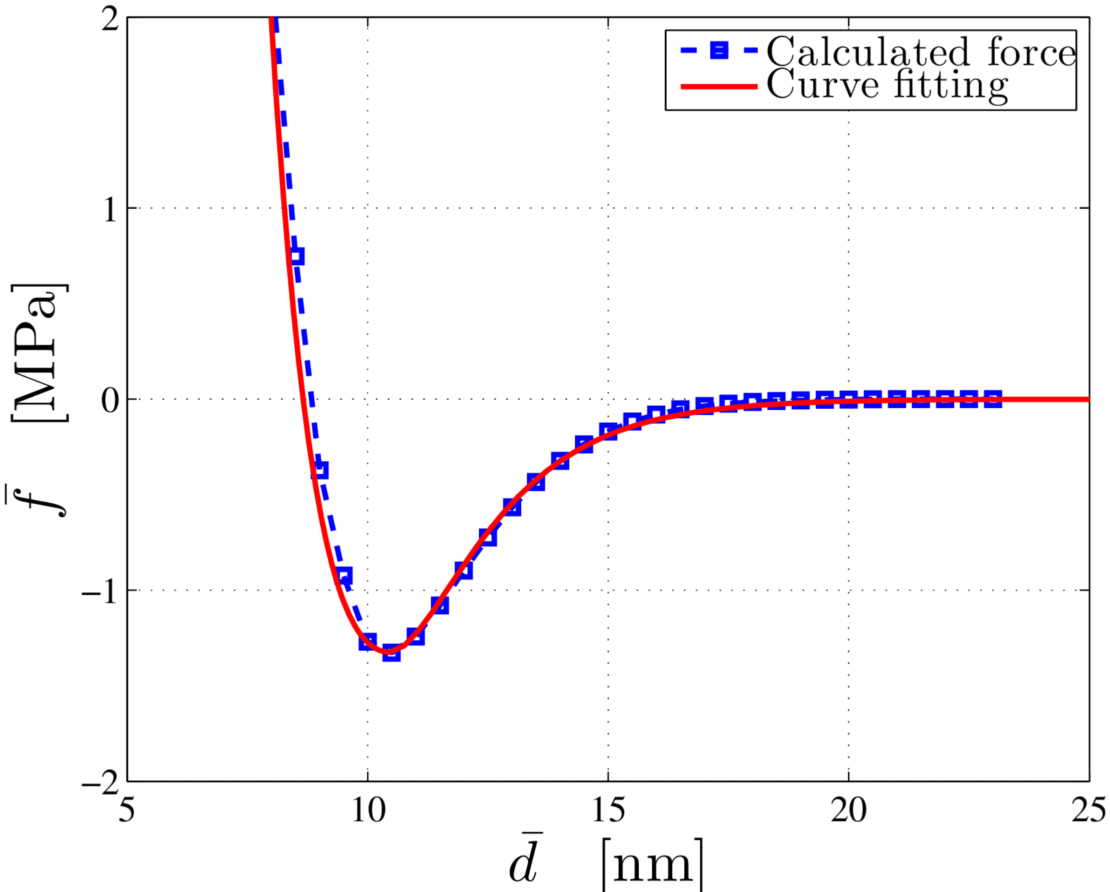

Meso-scale contact model

- Semi-analytical model vs. GW model
  - In GW model: saturation effect is not accounted for
    - The merging parts of menisci are repeatedly counted
    - Overestimating adhesion force that could be not realistic

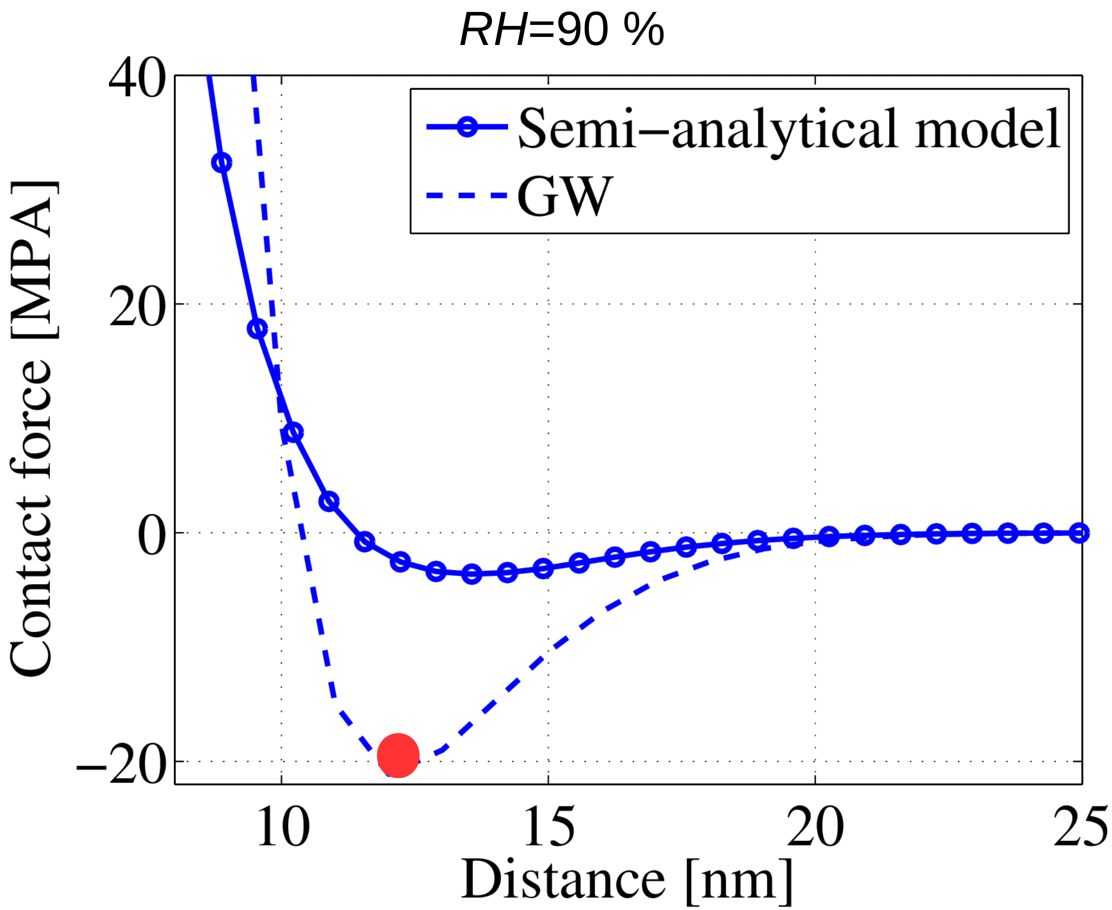

Maximum adhesive stress by GW model: 20 MPa (Not realistic)

(Theoretical maximum adhesive stress of water at *RH*=90%: $\Delta P = 14 \text{ MPa}$)

Meso-scale contact model

- Semi-analytical model vs. GW model
  - GW model: size of contacting surface is considered as infinite
    - GW model might not fully capture the adhesion effect (adhesion effect is only important at microscopic scale)
    - Adhesion force is underestimated (when saturation does not happens e.g. at low humidity levels)
    - Cut-off of surface height can be used in GW model, however which cut-off should be used is still questionable

RH=30 % (low humidity level, no saturation)

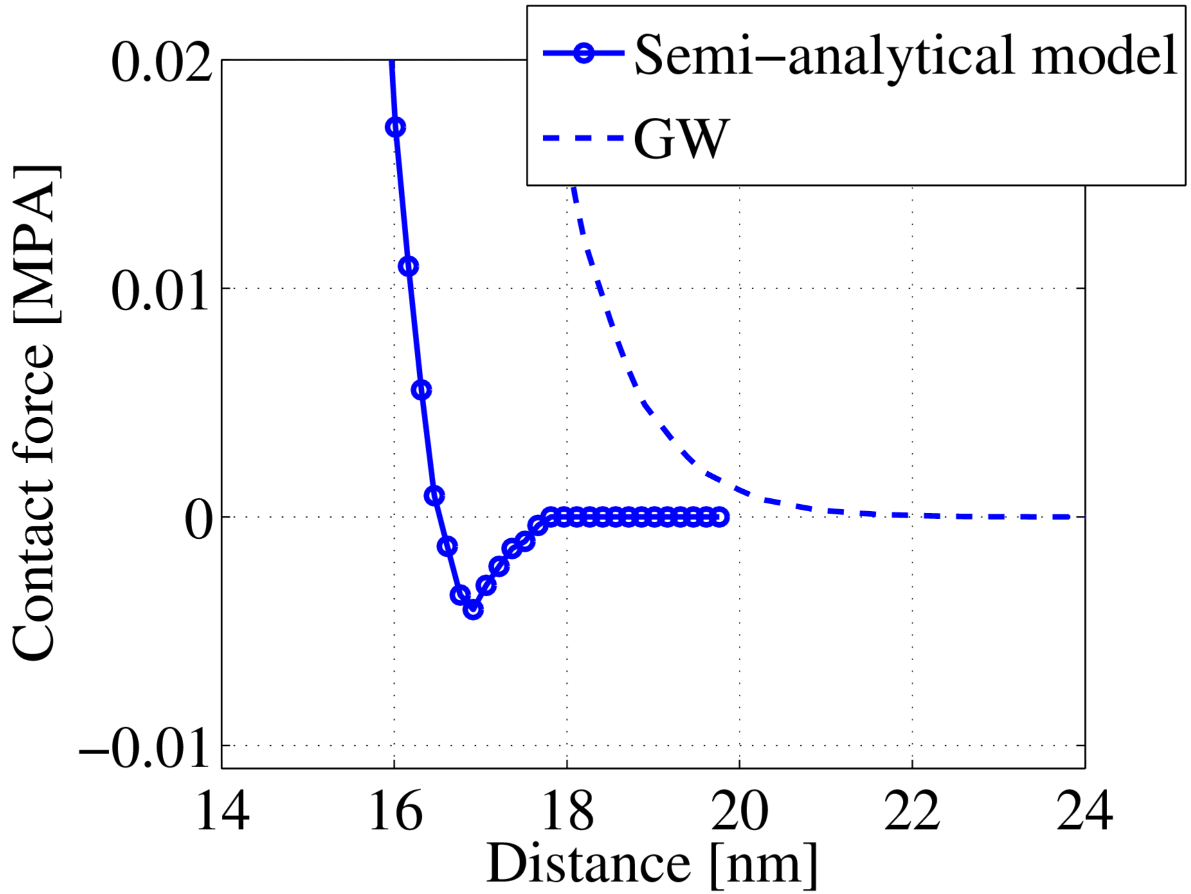

I. Deterministic multiscale model

- Meso-scale contact model
- ▶ Upper-scale FE stiction model

- FE model
  - Governing equation (elastic deformation):

$$\mathbf{K}\mathbf{u} = \mathbf{f}^c(\mathbf{u}) + \mathbf{f}^a$$

$\mathbf{u}$: vector of unknown beam nodal displacements and rotations
$\mathbf{K}$: stiffness matrix (e.g. evaluated using Euler-Bernoulli beam theory)
$\mathbf{f}^c$: nodal forces vector resulting from meso-scale adhesive forces
$\mathbf{f}^a$: nodal forces vector resulting from applied forces

  - Solved using Newton-Raphson method as contact law is non-linear
  - Apply loading–unloading process to obtain the stiction configuration

Meso-scale adhesive contact forces

FE model

Stiction configuration

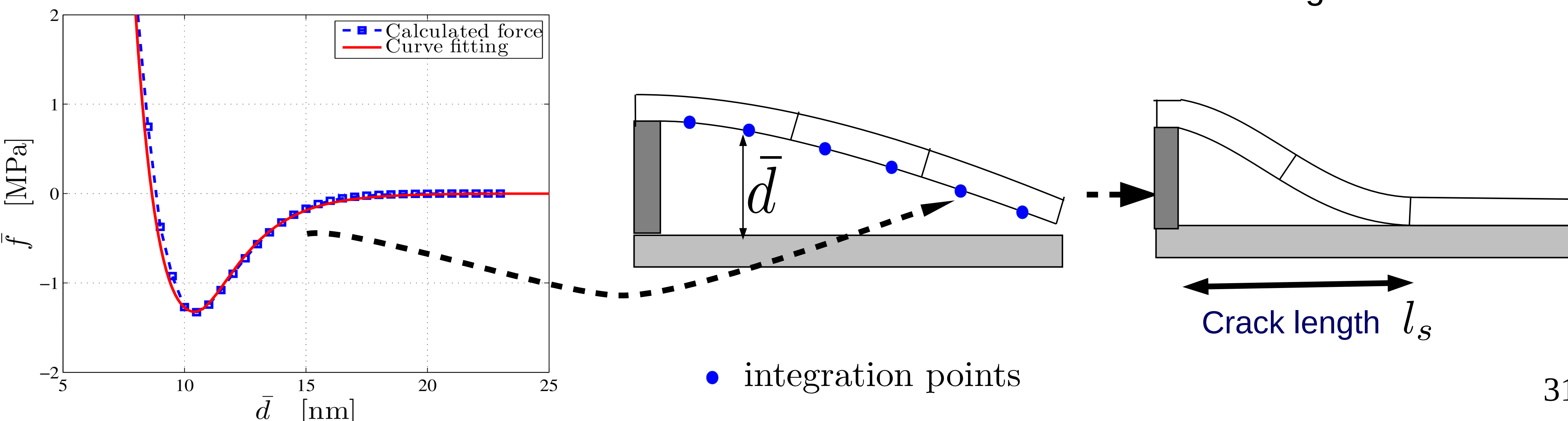

Upper-scale contact model

- FE model
  - Governing equation (elastic deformation):

$$\mathbf{K}\mathbf{u} = \mathbf{f}^c(\mathbf{u}) + \mathbf{f}^a$$

$\mathbf{u}$: vector of unknown beam nodal displacements and rotations

$\mathbf{K}$: stiffness matrix (e.g. evaluated using Euler-Bernoulli beam theory)

$\mathbf{f}^c$: nodal forces vector resulting from meso-scale adhesive forces

$\mathbf{f}^a$: nodal forces vector resulting from applied forces

  - Solved using Newton-Raphson method as contact law is non-linear
  - Apply loading–unloading process to obtain the stiction configuration
    - Range of adhesive stress is small (nanometers)

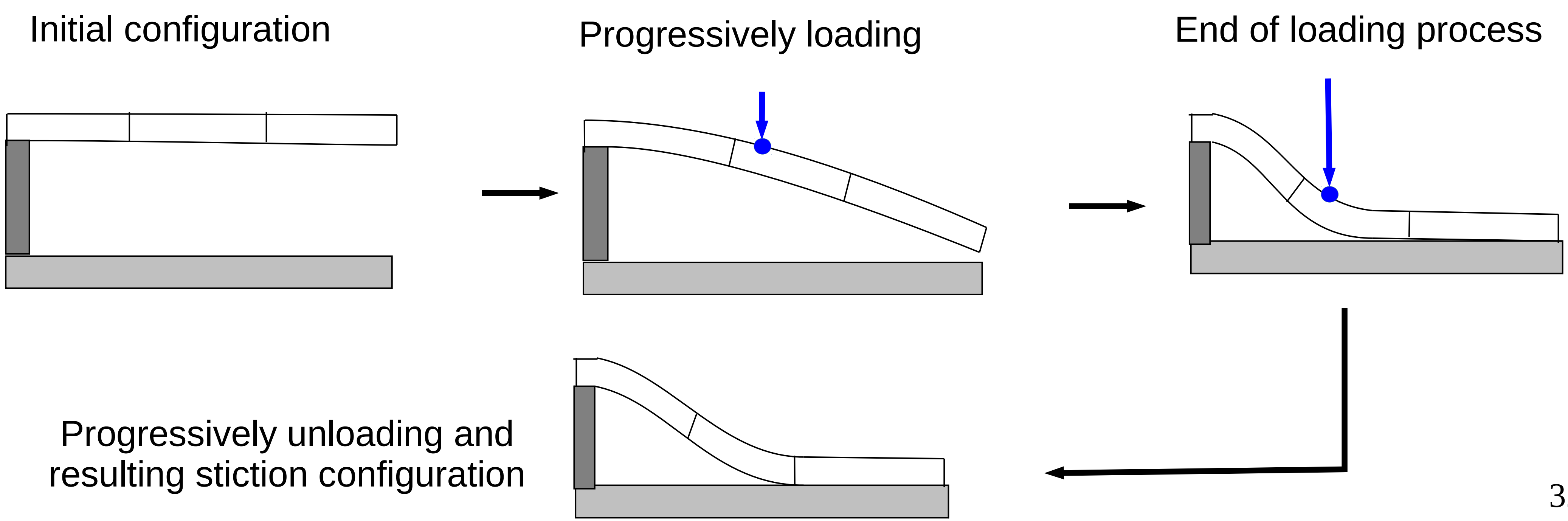

Deterministic multiscale model: summary

Lower-scale:
AFM measurements

Meso-scale:
contact force model

Upper-scale:
structural stiction model

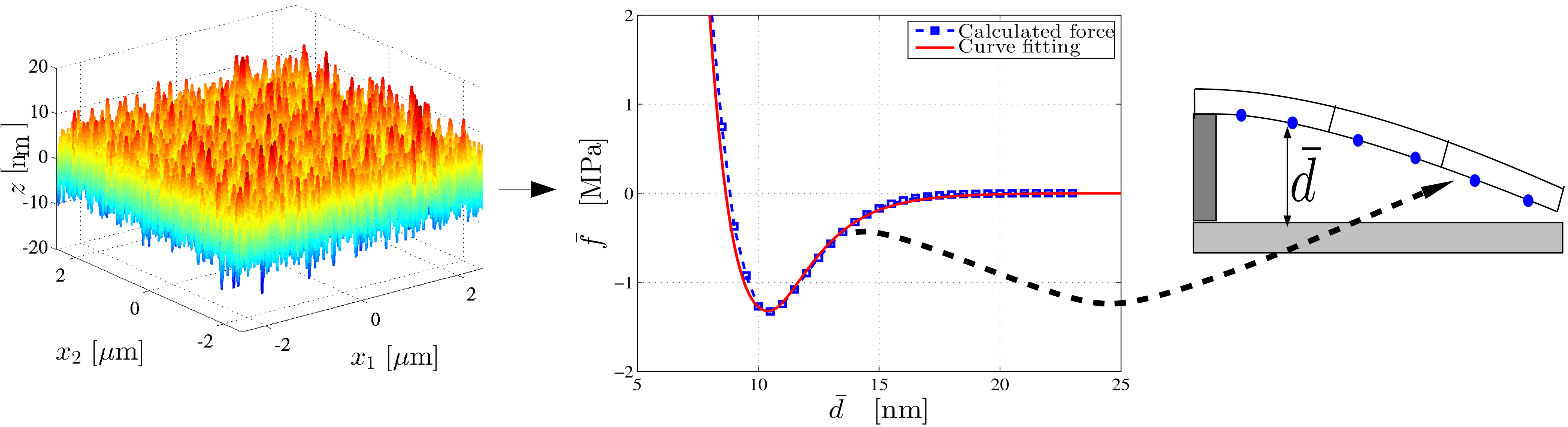

Motivation for Sec. II: Stochastic analysis

Three AFM measurements at three different locations of an identical surface

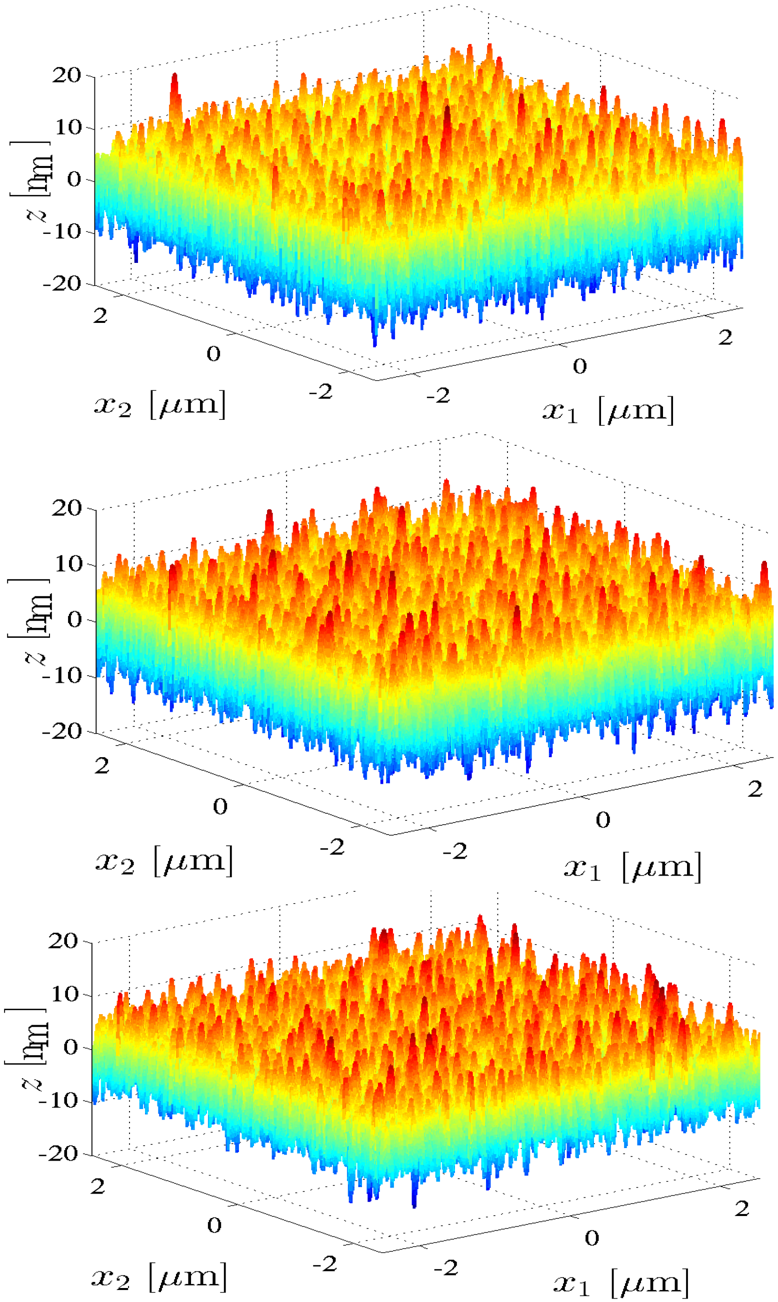

Non-deterministic evaluated contact forces (AFM measurement vs. flat surface)

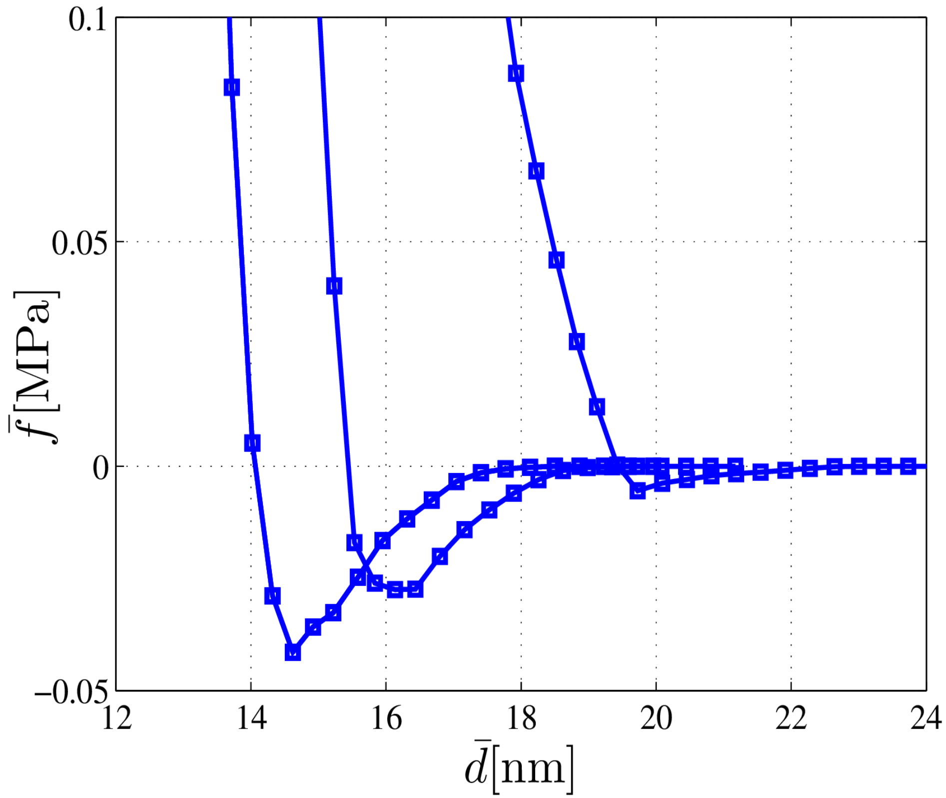

Contents

Scale separation analysis

- Characteristic lengths
  - Lower-scale: l^{m} , the characteristic length of the distances among neighboring asperities
  - Meso-scale: l^{meso} , the characteristic length of the size of surface used to evaluate contact forces
  - Upper-scale: l^{M} , the characteristic length of the size of MEMS structure
- Scale separation conditions (general)

$$l^{m} \ll l^{\mathrm{meso}} \ll l^{\mathrm{M}}$$

  - $l^{m} \ll l^{\mathrm{meso}}$: **number of contacting asperities is sufficient** to derive statistically representative homogenized contact behavior
  - $l^{\mathrm{meso}} \ll l^{\mathrm{M}}$:meso scale contact behavior is applicable to evaluate upper scale behavior
  - **Meso-scale adhesive contact behavior is deterministic and can be applied as deterministic contact law to upper-scale FE model**

Scale separation analysis

- Size of MEMS structure is reduced, to hold: $l^{\text{meso}} \ll l^{\text{M}}$

$$l^{m} \lesssim l^{\text{meso}} \ll l^{\text{M}}$$

  - $l^{m} \lesssim l^{\text{meso}}$: **number of contacting asperities is not sufficient** to derive a statistically representative homogenized contact force
  - ***Meso-scale adhesive contact behavior is nondeterministic***

- Uncertainty quantification of MEMS stiction
  - Account for the randomness of the evaluated contact forces at meso-scale

Independent AFM measurements

(different locations of an identical pair of contacting surfaces)

contact model

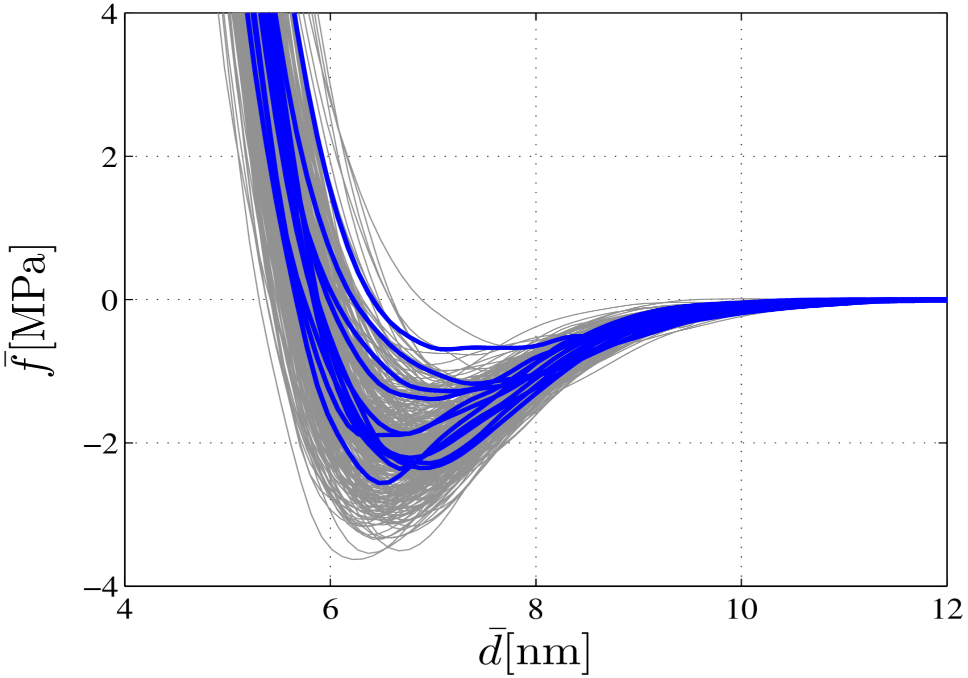

Non-deterministic contact forces

Direct Monte Carlo simulation (MCS)

- MCS: evaluate probabilistic behavior of MEMS structure
  - Evaluate N_{MC} realizations of stiction behaviors of considered MEMS structure
- Straightforward approach: direct MCS
  - Measure the contacting surfaces at the locations corresponding to the integration points
  - Evaluate the corresponding forces and integrate these forces as random contact laws
  - Inefficiency: high computational cost
  - Impractical: Many AFM measurements

N_p AFM measurements located at integration points of contacting surfaces

1 realization

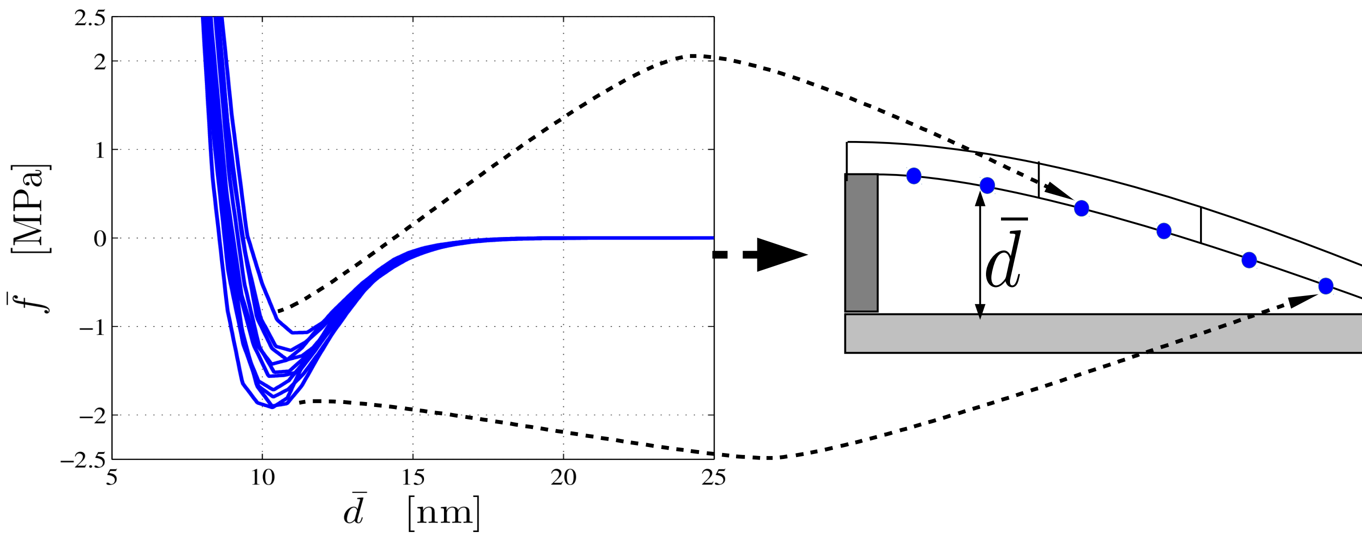

Lower-scale:
AFM measurements

Meso-scale:
Explicitly evaluated forces
(at different integration points)

Upper-scale: FE model
1 Stiction behavior

Direct Monte Carlo simulation (MCS)

- MCS: evaluate probabilistic behavior of MEMS structure
  - Evaluate N_{MC} realizations of stiction behaviors of considered MEMS structure
- Straightforward approach: direct MCS
  - Measure the contacting surfaces at the locations corresponding to the integration points
  - Evaluate the corresponding forces and integrate these forces as random contact laws
  - Inefficiency: high computational cost
  - Impractical: Many AFM measurements

N_p AFM measurements located at integration points of contacting surfaces

1 realization

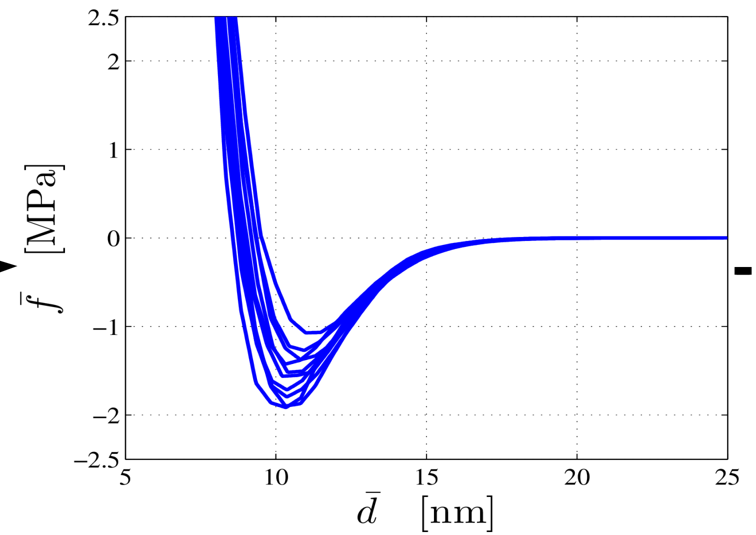

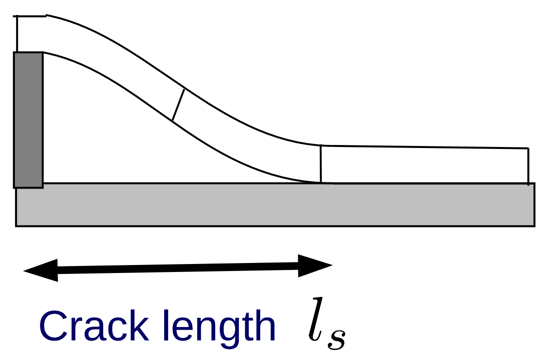

Lower-scale:
AFM measurements

Meso-scale:
Explicitly evaluated forces
(at different integration points)

Upper-scale: FE model
1 Stiction behavior

Direct Monte Carlo simulation (MCS)

- MCS: evaluate probabilistic behavior of MEMS structure
  - To evaluate N_{MC} realizations of stiction behaviors of considered MEMS structure
- Straightforward approach: direct MCS
  - Measure the contacting surfaces at the locations corresponding to the integration points
  - Evaluate the corresponding forces and integrate these forces as random contact laws
  - Impractical: Many AFM measurements
  - Inefficiency: high computational cost

1 realization

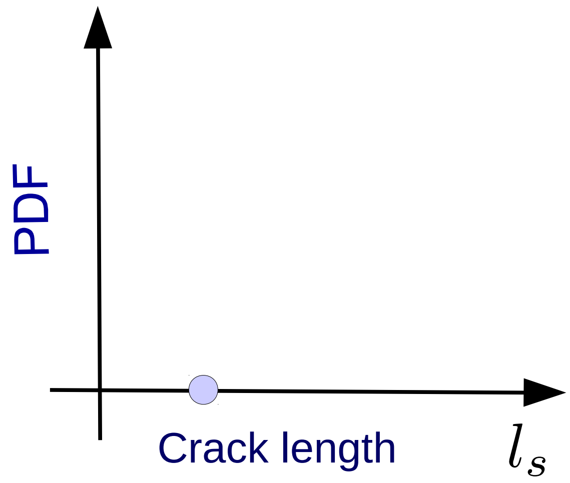

Upper scale:
1 Stiction behavior

Direct Monte Carlo simulation (MCS)

- MCS: evaluate probabilistic behavior of MEMS structure
  - To evaluate N_{MC} realizations of stiction behaviors of considered MEMS structure
- Straightforward approach: direct MCS
  - Measure the contacting surfaces at the locations corresponding to the integration points
  - Evaluate the corresponding forces and integrate the forces as random contact laws
  - Impractical: Many AFM measurements
  - Inefficiency: high computational cost

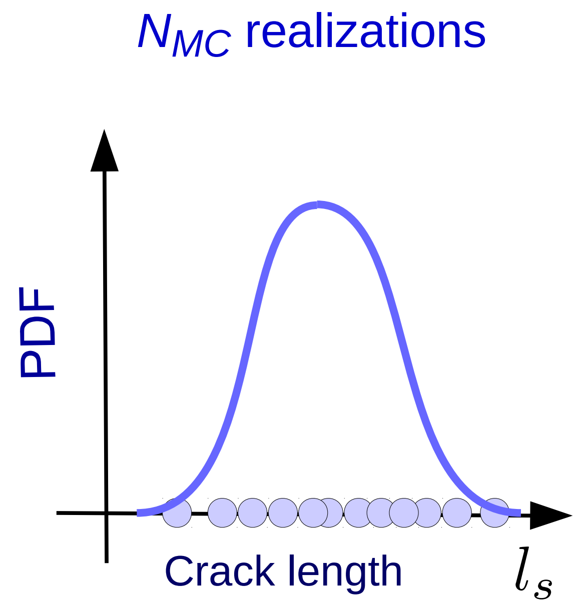

Upper scale:
N_{MC} stiction behaviors

Direct Monte-Carlo simulation (MCS)

- MCS: evaluate probabilistic behavior of MEMS structure
  - To evaluate N_{MC} realizations of stiction behaviors of considered MEMS structure
- Straightforward approach: direct MCS
  - Measure the contacting surfaces at the locations corresponding to the integration points
  - Evaluate the corresponding forces and integrate the forces as random contact laws
  - **Impractical: Many AFM measurements**
  - **Inefficiency: high computational cost**

Estimation of the cost of Direct MCS	
Number of realization	N_{MC}
Number of AFM measurements	$2N_p \times N_{MC}$
Number of explicitly evaluated apparent contact force functions	$N_p \times N_{MC}$

$N_p \sim 200: \text{ number of intergration points in the FE model}$

$N_{MC} \sim 1000: \text{ number of realizations in MCS}$

Stochastic model-based multiscale method (indirect MCS)

- Lower-scale model: **surface generator**
  - Surface generator: generate a large number of numerical surfaces with approximated statistical properties characterized from measurements
  - Some AFM measurements (~ 3) are required
- Meso-scale model
  - Evaluate the *m* apparent contact forces between *m* pairs of generated contacting surfaces
- **Stochastic model of contact forces**
  - Input data: $m(\ll N_p \times N_{MC})$ explicitly evaluated apparent contact forces
  - To generate $N_p \times N_{MC}$ apparent contact forces
- Upper-scale model: MCS
  - Contact laws are generated from stochastic model
  - Performing MCS with FE model using the generated contact laws

Estimation of the cost of MCS		
Method	Direct MCS	Stochastic multiscale
Number of AFM measurement scans	$2N_p \times N_{MC}$	2×3
Number of explicitly evaluated apparent contact force functions	$N_p \times N_{MC}$	m

II. Stochastic analysis

- Surface generator
- Stochastic model of contact forces

Surface generator

- Input data:
  - AFM measurements
- Characterization:
  - Identify the statistical properties using random field method
- Simulations:
  - Generate numerical surfaces respecting the identified statistical properties

AFM measurements (1D illustration)

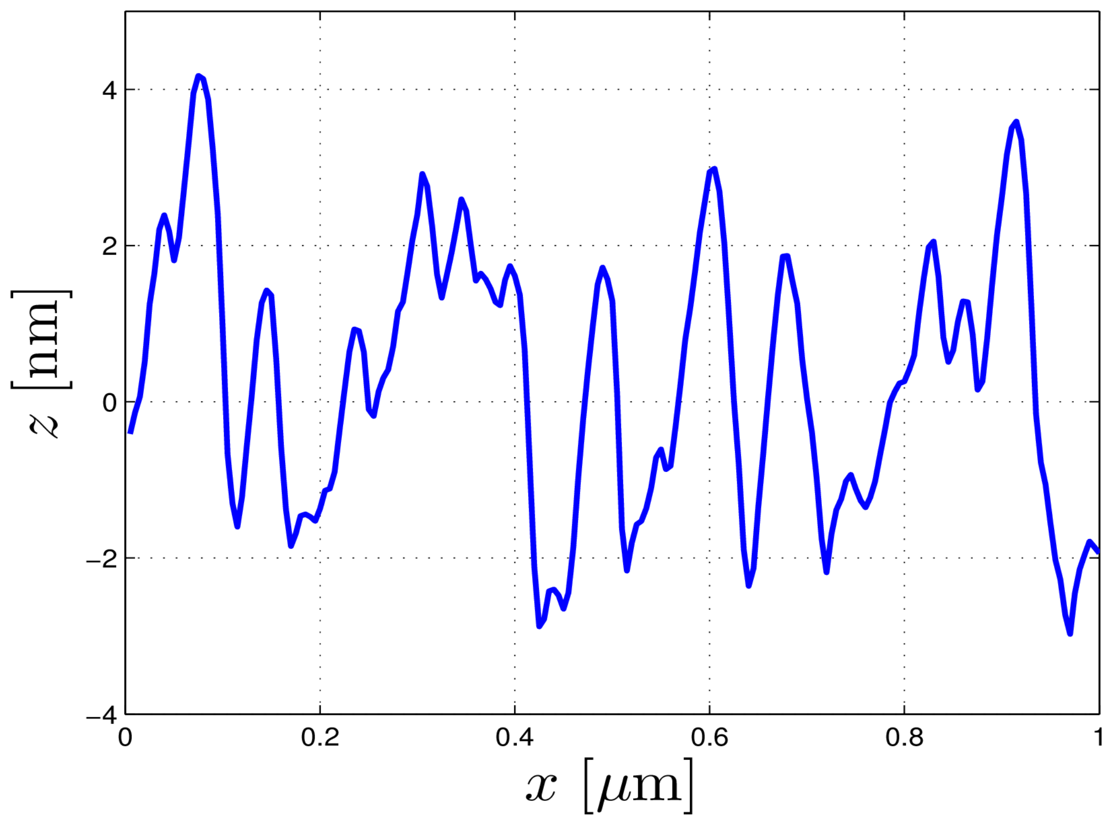

Surface generator

- First order marginal probability density function (mPDF),

AFM measurements (1D illustration)

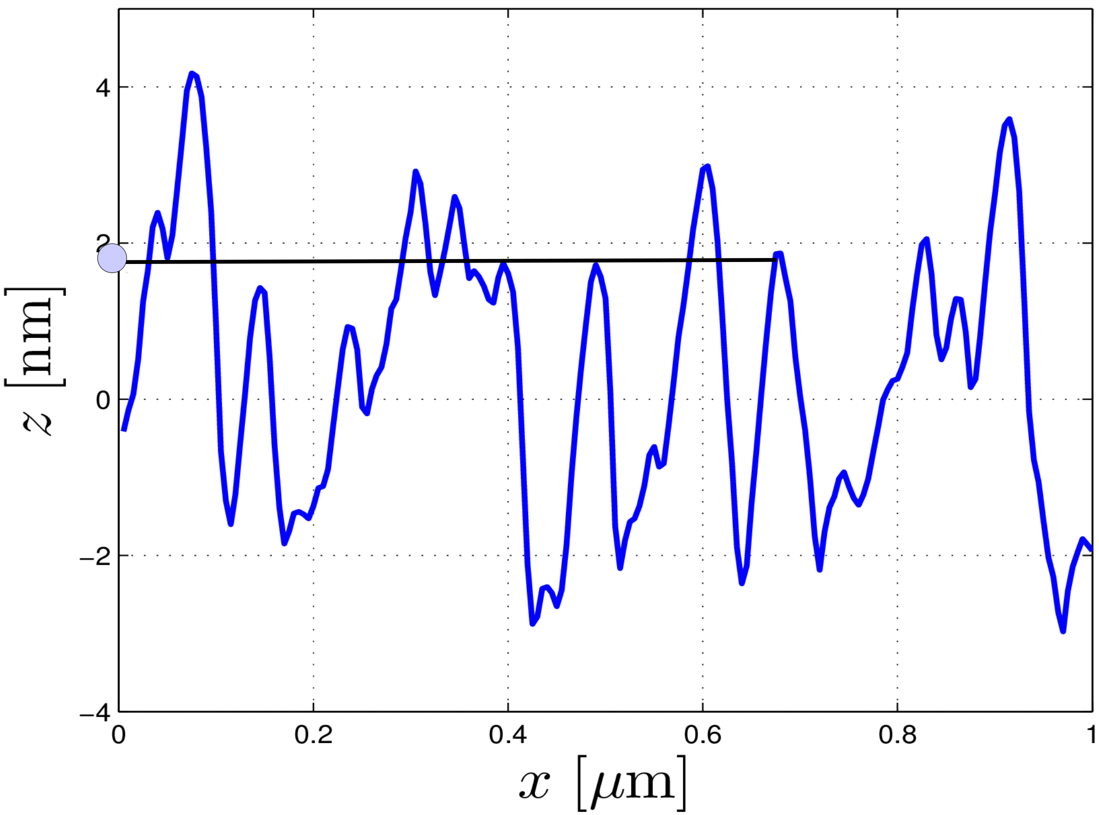

First order mPDF

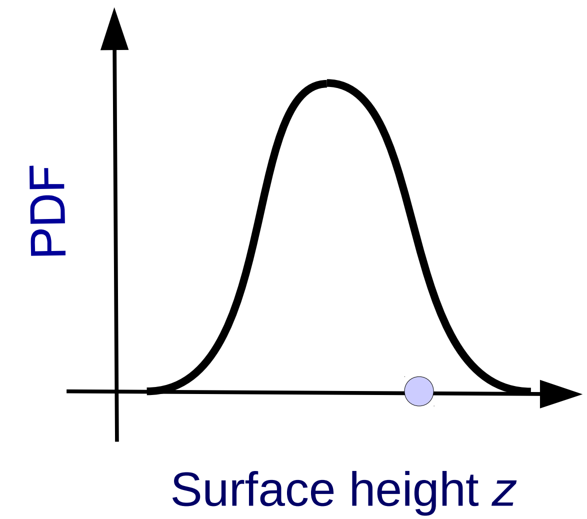

Surface generator

- Evaluate the first order mPDF
  - Statistical moments: mean, roughness, skewness, kurtosis evaluated from AFM data

$$\text{roughness } rms = \sqrt{m_2} = \mathbb{E}[z^2]^{1/2}$$

$$\text{skewness } \gamma = \frac{m_3}{rms^3} = \frac{\mathbb{E}[z^3]}{rms^3}, \qquad \text{kurtosis } \beta = \frac{m_4}{rms^4} = \frac{\mathbb{E}[z^4]}{rms^4}$$

$$\mathbb{E}: \ \text{Expectation}$$

  - Method: maximum entropy principle [Shannon1949]
    - Search for the PDF that maximizes its entropy and matches the statistical moments

$$\boxed{\mathrm{p}_Z(z) = \exp(-\lambda_0 - \sum_{i=1}^{4} \lambda_i z^i).}$$

$$\lambda_i \quad \text{coefficients to find using constraints}$$

  - Neglecting skewness and kurtosis: Gaussian distribution
  - Accounting for skewness and kurtosis: Non-Gaussian distribution

- Evaluate the first order mPDF
  - Non-Gaussian estimated PDF is in better agreement with measurements histogram
  - Contact happens at only the highest asperities, accuracy of first order mPDF when getting to the high asperities is crucial.

Compare estimated PDF with histogram

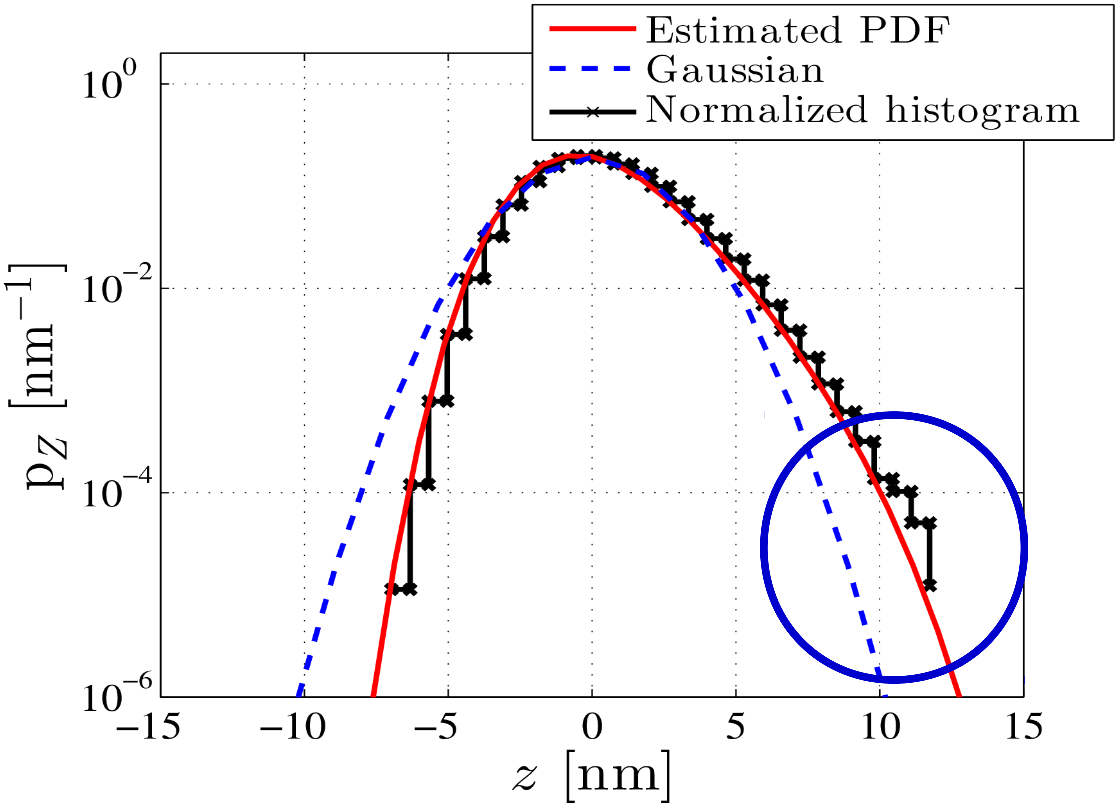

roughness $rms = 2$ nm

skewness $\gamma = 0.53$

kurtosis $\beta = 3.4$

Surface generator

- Spatial correlation
  - Auto-covariance function (ACF) characterizes the spatial correlation of two points at a given distance

$$r_Z(\tau) = \mathbb{E}[z(\mathbf{x}), z(\mathbf{x}+\tau)]$$

AFM measurement (1D representation)

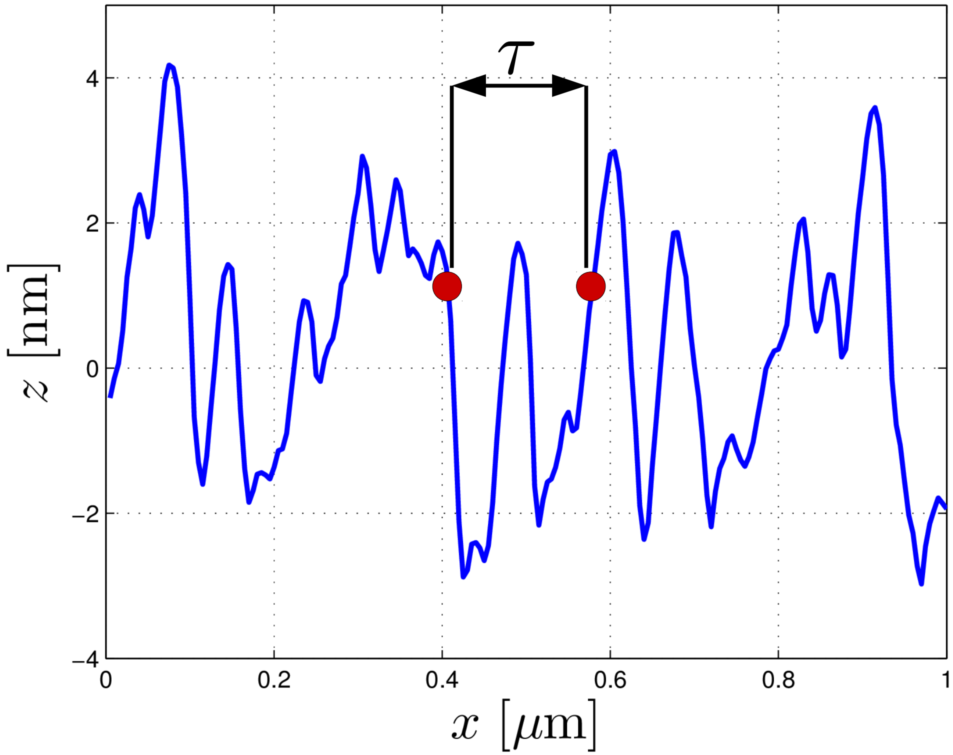

Auto-covariance function

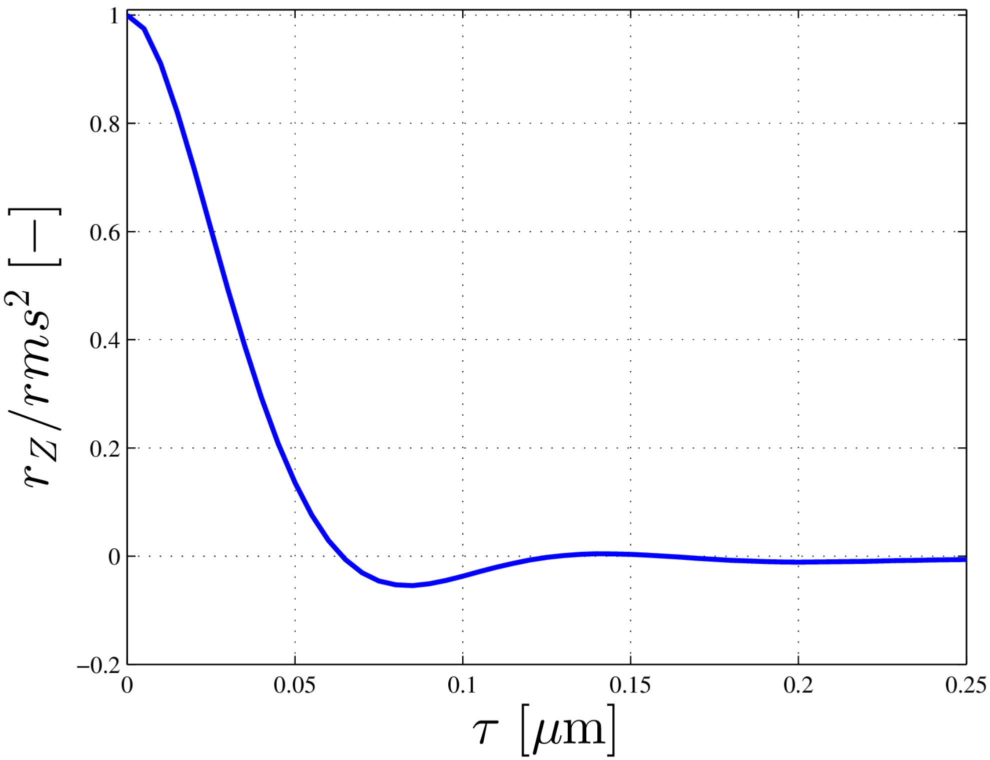

Surface generator

- Evaluate the power spectrum density (PSD) function
  - ACF is the inverse Fourier transform of the PSD function
  - PSD function characterizes the density of variance in wave number space
    - PSD function decreases when increasing wave number

$$s_Z(\zeta) = \int_{\Re^2} \exp(-\mathrm{i} < \zeta\tau >) r_Z(\tau) \mathrm{d}\zeta \quad \text{(Fourier transform of ACF)}$$

PSD function
(Polar representation)

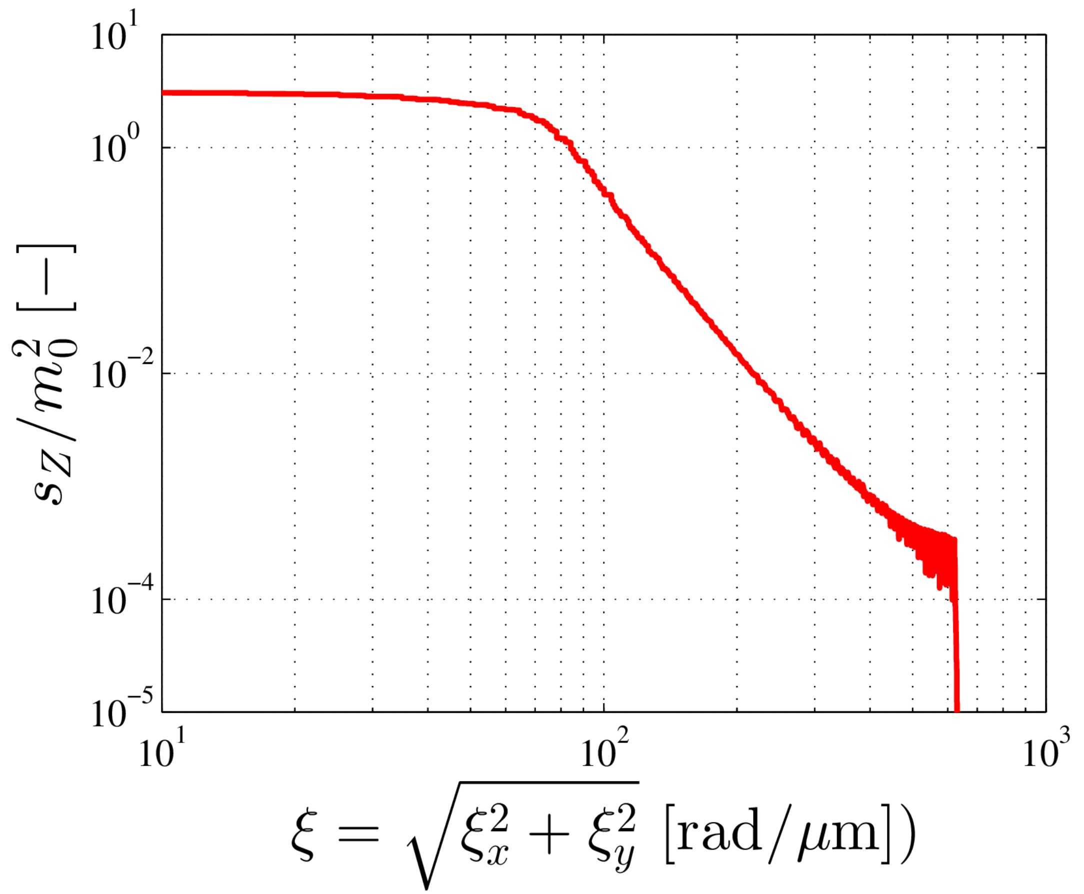

Surface generator

- Non-Gaussian surface generator from the first order mPDF and PSD function
  - Generate Gaussian surfaces (1) and map them to Non-Gaussian surfaces (2)
    - The generated non Gaussian surfaces well respect the first order mPDF

$$s_Z \xrightarrow{(1)} z_{\mathrm{G}}(\theta) \xrightarrow{(2)} z_{\mathrm{NG}}(\theta)$$

(1) Generate Gaussian surface [Poiron et al. 1995]

$$z_{\mathrm{G}}(\mathbf{x},\theta) = \sqrt{2\Delta\zeta^2}\,\mathfrak{Re}\left[\sum_{l_1=1}^{\mu}\sum_{l_2=1}^{\mu} v_{(l_1,l_2)}(\theta)\sqrt{\frac{1}{(2\pi)^2} s_Z(\zeta_{l_1},\zeta_{l_2})}\exp\left(\mathrm{i} < \mathbf{x},\zeta > +\mathrm{i}\psi_{(l_1,l_2)}(\theta)\right)\right]$$

Random variable

PSD function

Random phases

Sum of sinus functions whose phases are random and weighted by square root of PSD function

Surface generator

- Non-Gaussian surface generator from the first order mPDF and PSD function
  - Generate Gaussian surfaces (1) and map them to Non-Gaussian surfaces (2)
    - The generated non Gaussian surfaces well respect the first order mPDF

$$s_Z \xrightarrow{(1)} z_{\mathrm{G}}(\theta) \xrightarrow{(2)} z_{\mathrm{NG}}(\theta)$$

(2) map Gaussian surfaces to non-Gaussian surfaces using iso-probabilistic transformation [Shinozuka 1971]

Gaussian Cumulative Distribution Function (CDF)

Non-Gaussian CDF (from 1st order mPDF)

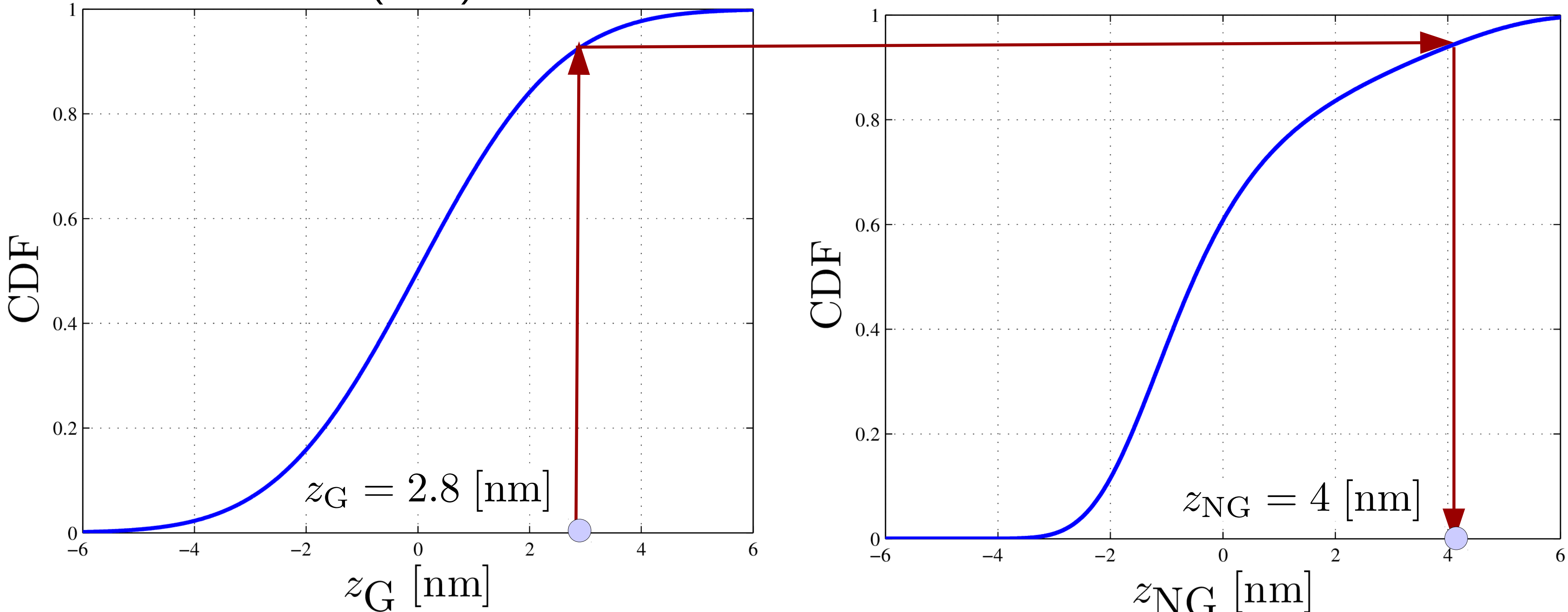

Surface generator

- Non-Gaussian surface generator from the first order mPDF and PSD function
  - Generate Gaussian surfaces (1) and map them to Non-Gaussian surfaces (2)
  - The generated non-Gaussian surfaces well respect the first order mPDF identified from AFM measurements
  - The PSD function of non-Gaussian surfaces is no longer the input one
    - Iterative process is required [Shinozuka 1971]: PSD function of the Gaussian surfaces is iteratively updated

$$\underset{\text{(Iteratively updated)}}{s_Z^{(i-\text{th iteration})}} \xrightarrow{(1)} z_{\mathrm{G}}(\theta) \xrightarrow{(2)} z_{\mathrm{NG}}(\theta): \quad \underset{\text{(End criteria)}}{s_{Z_{\mathrm{NG}}} \approx s_Z}$$

Random apparent contact forces

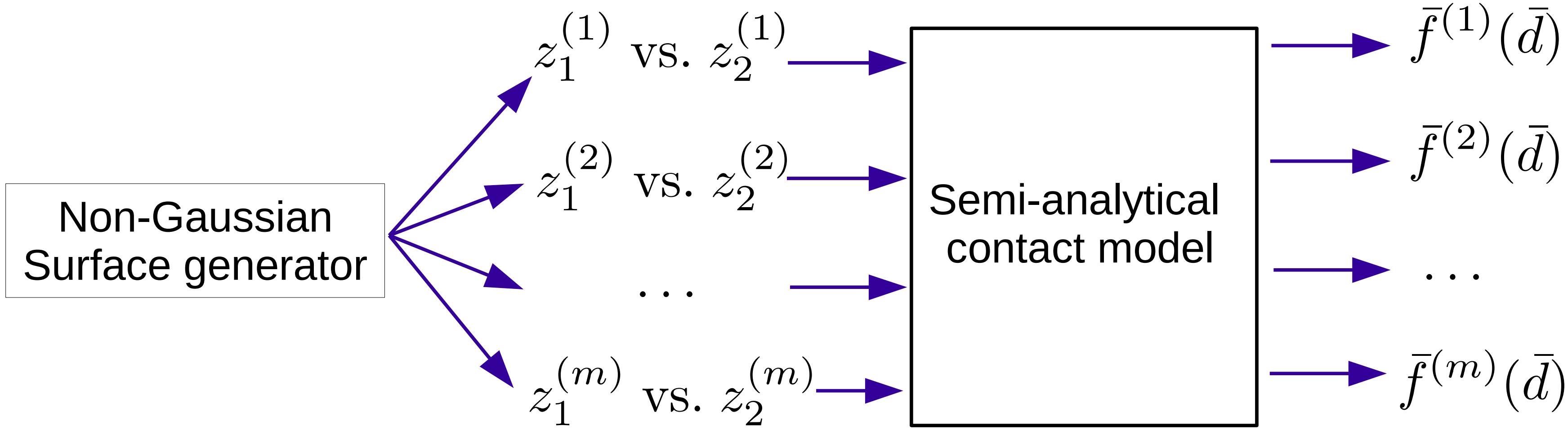

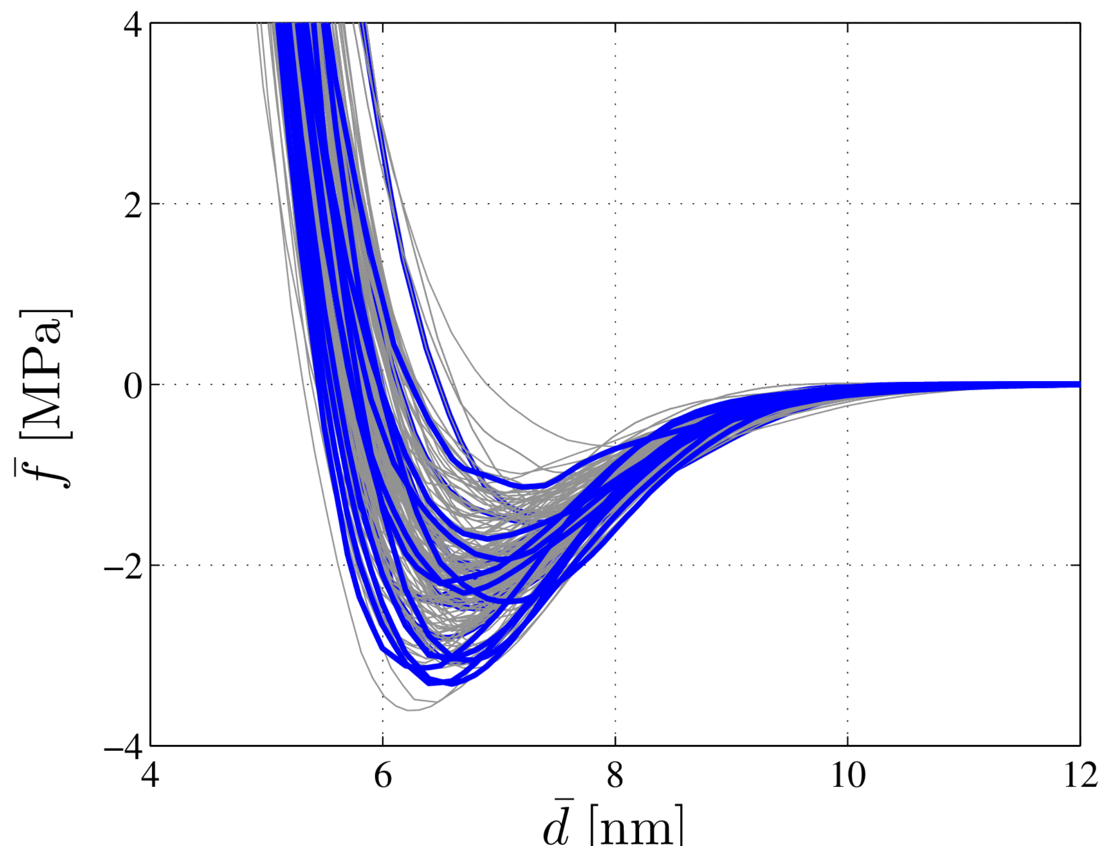

explicitly evaluated apparent contact forces

II. Stochastic analysis

- Surface generator
- ▶ Stochastic model of contact forces

Stochastic model of apparent contact forces

- Input: m explicitly evaluated apparent contact forces
- To generate $N_p \times N_{MC}$ apparent contact forces required for MCS with an approximated distribution
- Because $m \ll N_p \times N_{MC}$, the computation cost to evaluate contact forces is significantly reduced
- **Requirement**: the distribution of generated forces must well approximate the distribution of explicitly evaluated forces.

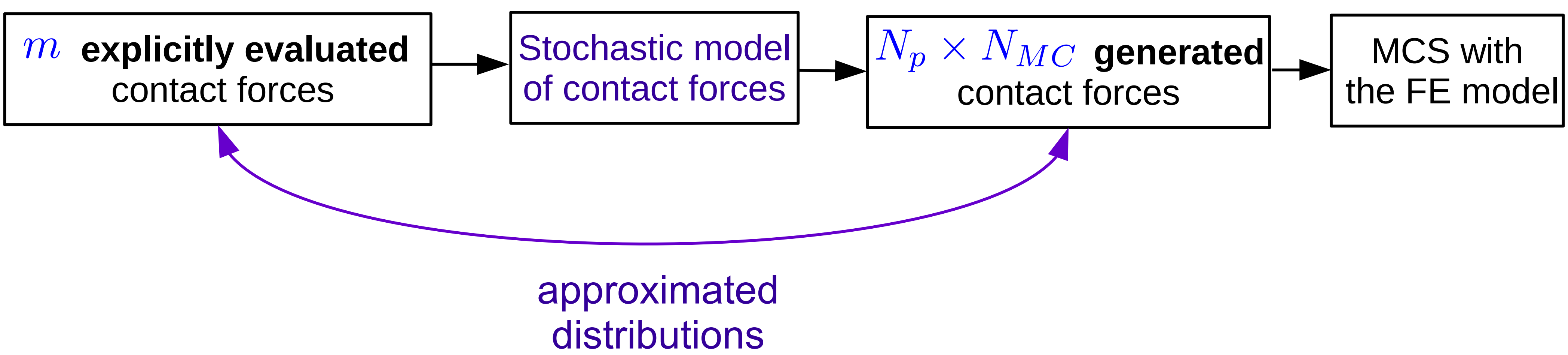

Stochastic model of apparent contact forces

- Parameterization

Force-distance curves

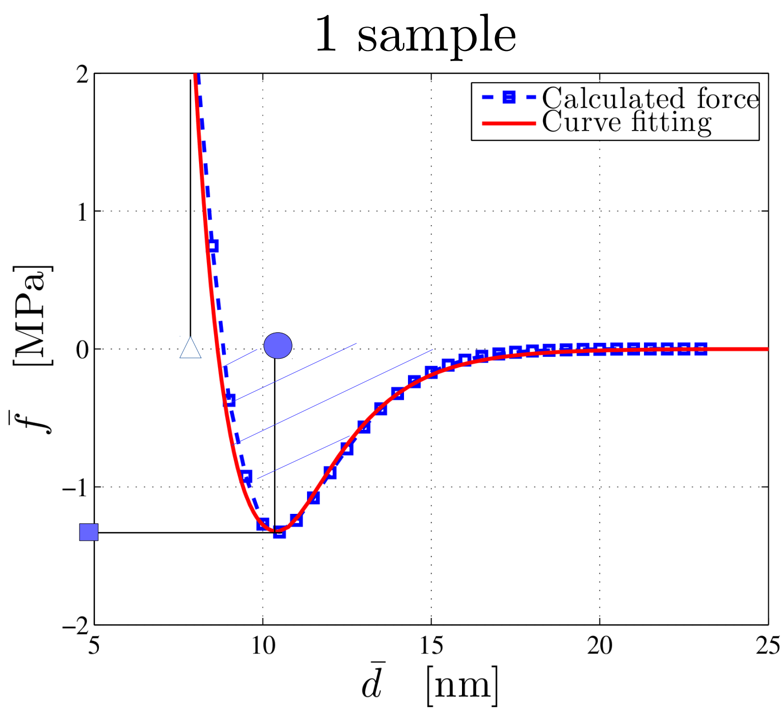

Parameterization

Parameter vectors

$$\mathbf{v} = \begin{pmatrix} -\bar{f}_{\mathrm{max}} \\ -\bar{e} \\ \bar{d}_{\mathrm{max}} \\ \bar{d}_{\mathrm{limit}} \end{pmatrix}$$

$$\bar{f}(\bar{d}) = \Phi(\bar{d}; \mathbf{v})$$

Curve fitting analytical function

Stochastic model of apparent contact forces

- Parameterization

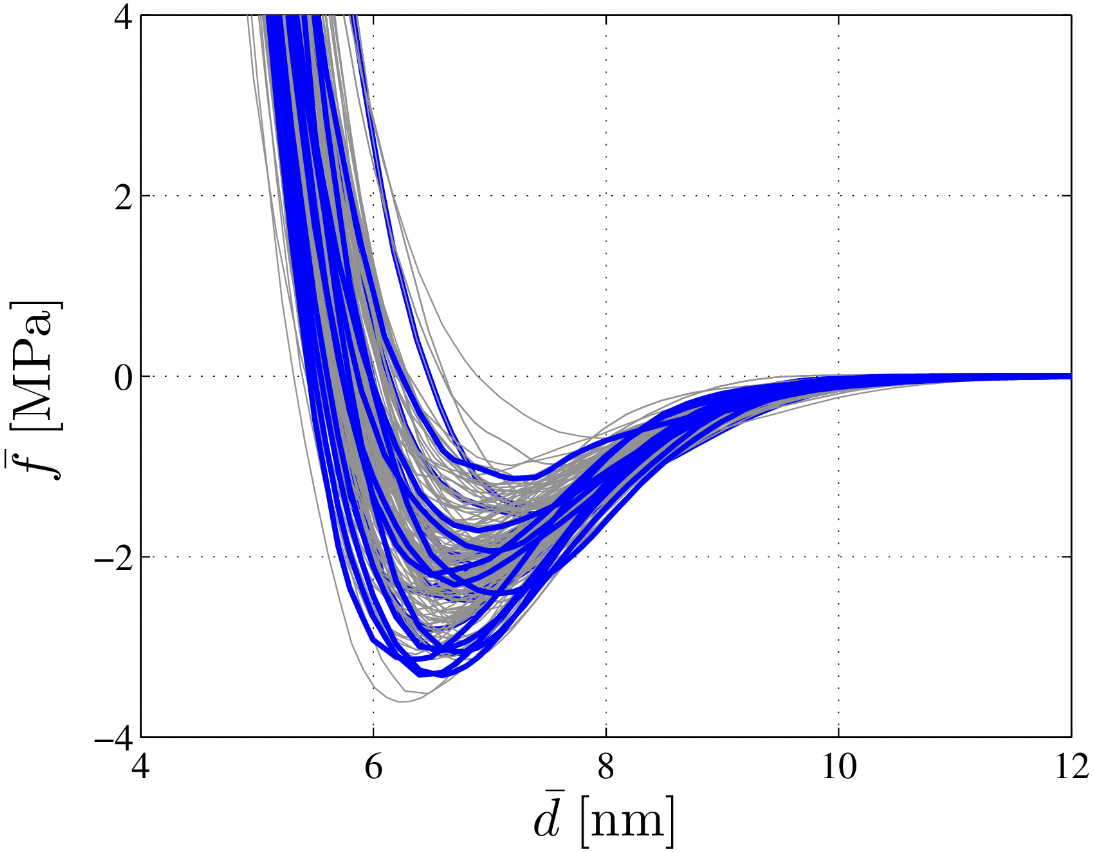

$$\{\mathbf{v}^{(1)}, \cdots, \mathbf{v}^{(m)}\}$$

m explicitly evaluated
adhesive contact forces curves

m parameter vectors

Stochastic model of apparent contact forces

- Data preprocessing procedures

$$\mathbf{v}^{(k)} \xrightarrow{(1)} \mathbf{q}^{(k)} \xrightarrow{(2)} \eta^{(k)}$$

- (1) account for physical conditions
  - By definition, energy and maximum pull-out forces must be always positive
  - Maximum force contact distance must be larger than threshold force contact distance
  - Using log-scale to enhance the positiveness

$$\mathbf{v}^{(k)} = \left[\bar{e}^{(k)}, \bar{f}^{(k)}_{\mathrm{max}}, \bar{d}^{(k)}_{\mathrm{max}}, \bar{d}^{(k)}_{\mathrm{limit}}\right]^{\mathrm{T}} \text{ subject to physical constraints}$$

$$\mathbf{q}^{(k)} = \left[\frac{\log(\bar{e}^{(k)})}{\mathrm{const}_1}, \frac{\log(\bar{f}^{(k)}_{\mathrm{max}})}{\mathrm{const}_2}, \frac{\bar{d}^{(k)}_{\mathrm{max}}}{\mathrm{const}_3}, \frac{\log(\bar{d}^{(k)}_{\mathrm{max}} - \bar{d}^{(k)}_{\mathrm{limit}})}{\mathrm{const}_4}\right]^{\mathrm{T}} \in \Re^4$$

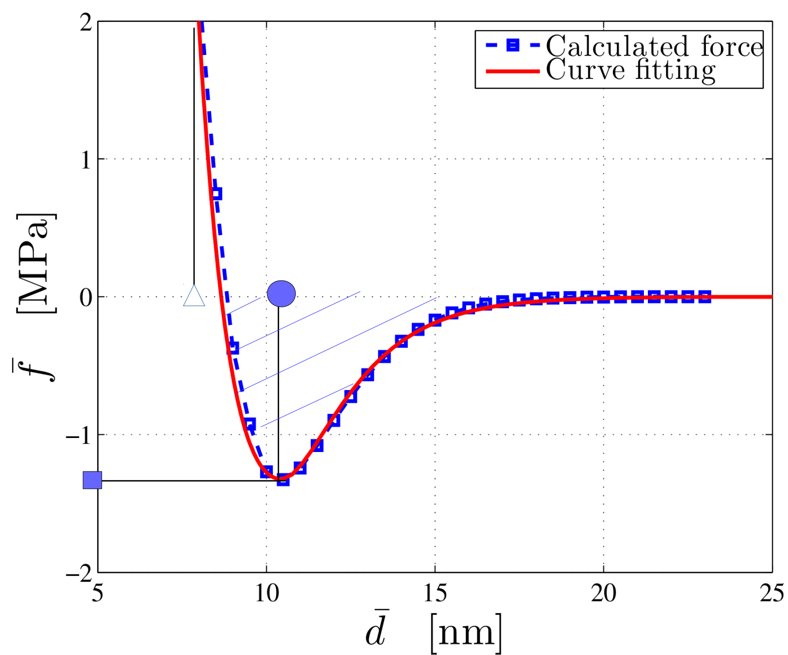

physical conditions $\longrightarrow$

$-\bar{f}_{\mathrm{max}} > 0$

$-\bar{e} > 0$

$\bar{d}_{\mathrm{max}} - \bar{d}_{\mathrm{limit}} > 0$

Parameterization

- Data preprocessing procedures

$$\mathbf{v}^{(k)} \xrightarrow{(1)} \mathbf{q}^{(k)} \xrightarrow{(2)} \eta^{(k)}$$

- (2) Dimensional reduction: reduce effect of the curse of dimensionality
  - To reduce the computational cost
  - Using principal component analysis (PCA) [Jolliffe 2002]

$$q_i^{(k)} \xrightarrow{\text{PCA}} \{\eta_1^{(k)}, \cdots, \eta_4^{(k)}\}$$

  - $\eta_i^{(k)}$ has unit variance, and its importance is weighted by corresponding eigenvalue of covariance matrix of ***q***
  - the obtained vectors have a reduced number of dimensions however still representative for the evaluated contact forces

$$\text{Reduced dimension vectors:} \quad \eta^{(k)} = \{\eta_1^{(k)}, \cdots, \eta_{N_g}^{(k)}\}, \quad N_g \leq 4$$

- Generalized polynomial chaos expansion (gPCE) to represent the randomness of reduced dimension vectors [Ghanem et al. 2003, Xiu et al. 2002]

$$\eta^{\mathrm{PC}} = \sum_{\alpha=1}^{N} \mathbf{c}_\alpha \Psi_\alpha(\xi)$$

Uniform distribution random vector in $[0,1]^{N_g}$

Coefficients Vector

Legendre polynomial

$$\text{Find } \mathbf{c}_\alpha \quad \text{s.t.} \quad \mathrm{p}(\mathbf{x}|\eta^{\mathrm{PC}}) \approx \mathrm{p}(\mathbf{x}|\eta^{(1)}, \cdots, \eta^{(k)})$$

(approximation in terms of distribution)

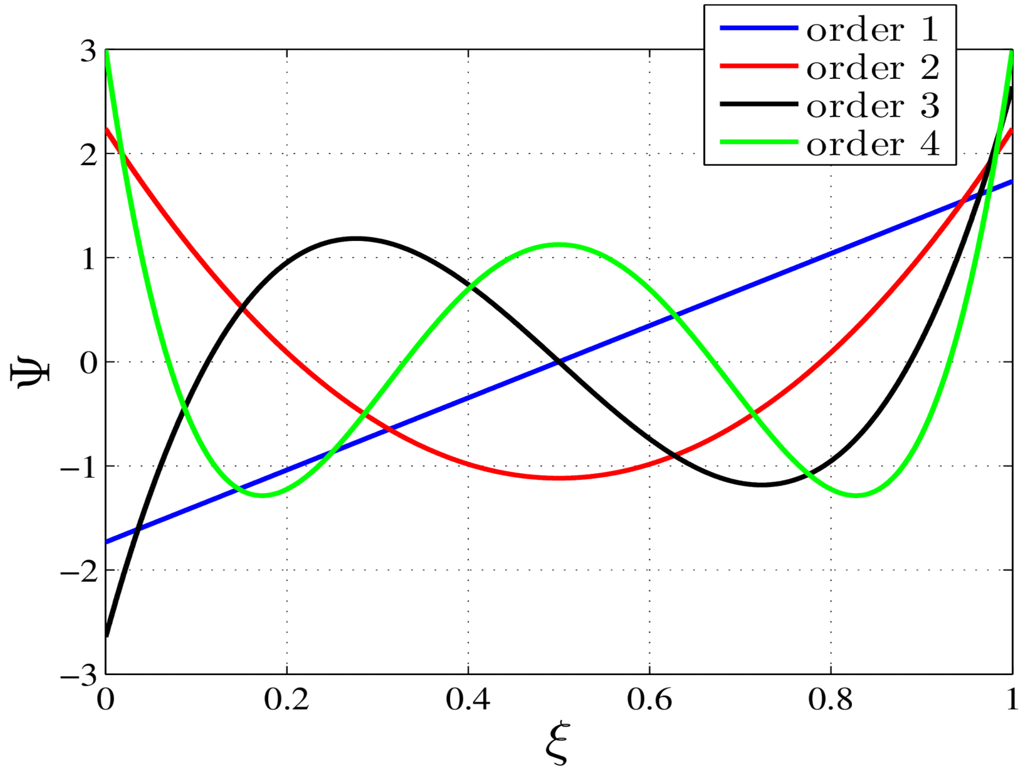

Example of Legendre polynomials in 1D

Stochastic model of apparent contact forces: summarize

- Generate contact forces
  - Generate a large number of contact force functions with a negligible computational cost

$$\text{sampling } \xi \rightarrow \eta^{\text{PC}} = \sum_{\alpha=1}^{N} \mathbf{c}_\alpha \Psi_\alpha(\xi) \rightarrow \mathbf{v}(\xi) \rightarrow \bar{f}(\bar{d}, \xi) = \Phi(\bar{d}, \mathbf{v}(\xi))$$

gPCE model

Parameter vector

Curve fitting analytical function

Explicitly evaluated contact forces

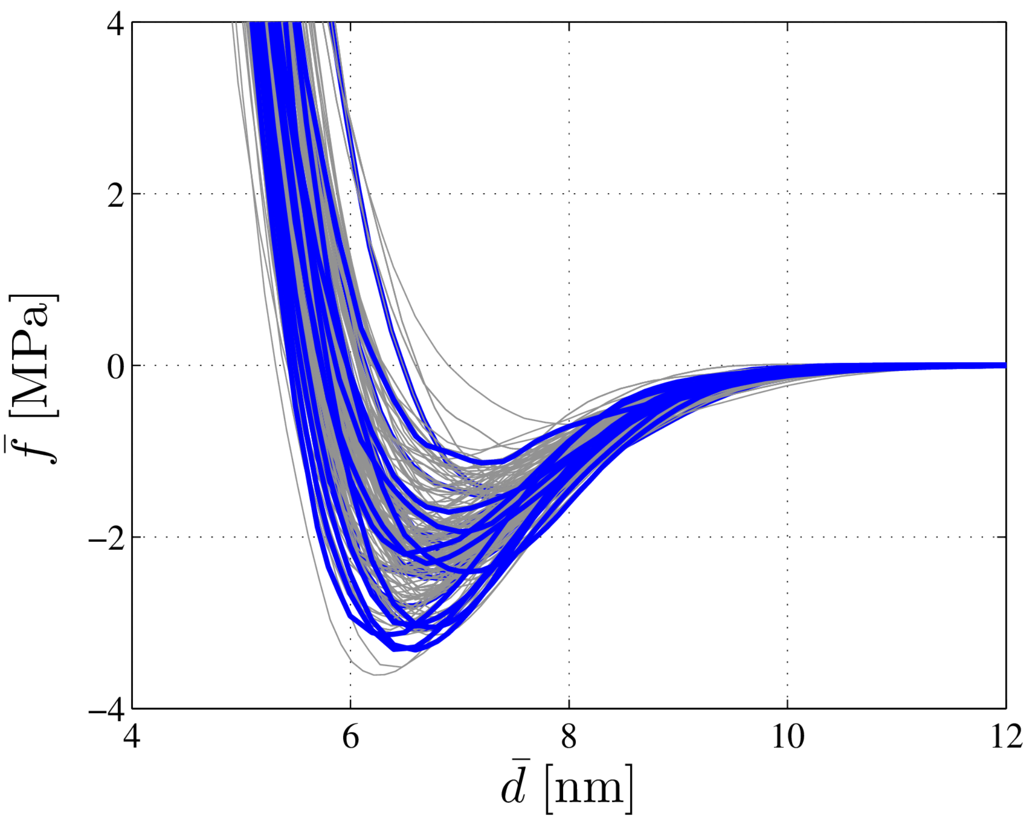

Generated contact forces

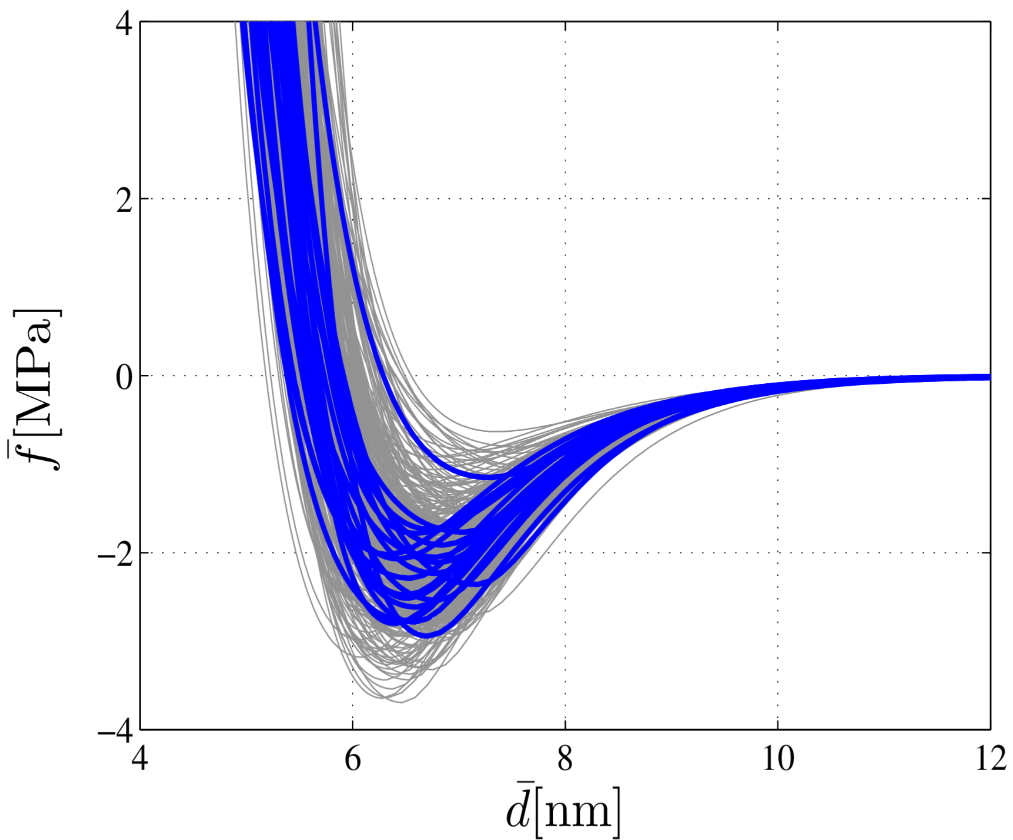

Stochastic model of apparent contact forces: comparison

- gPCE model approximates well the distribution of the reduced dimension vectors

Joint PDF of $\eta_1, \ \eta_2$

(reference: explicitly evaluated forces)

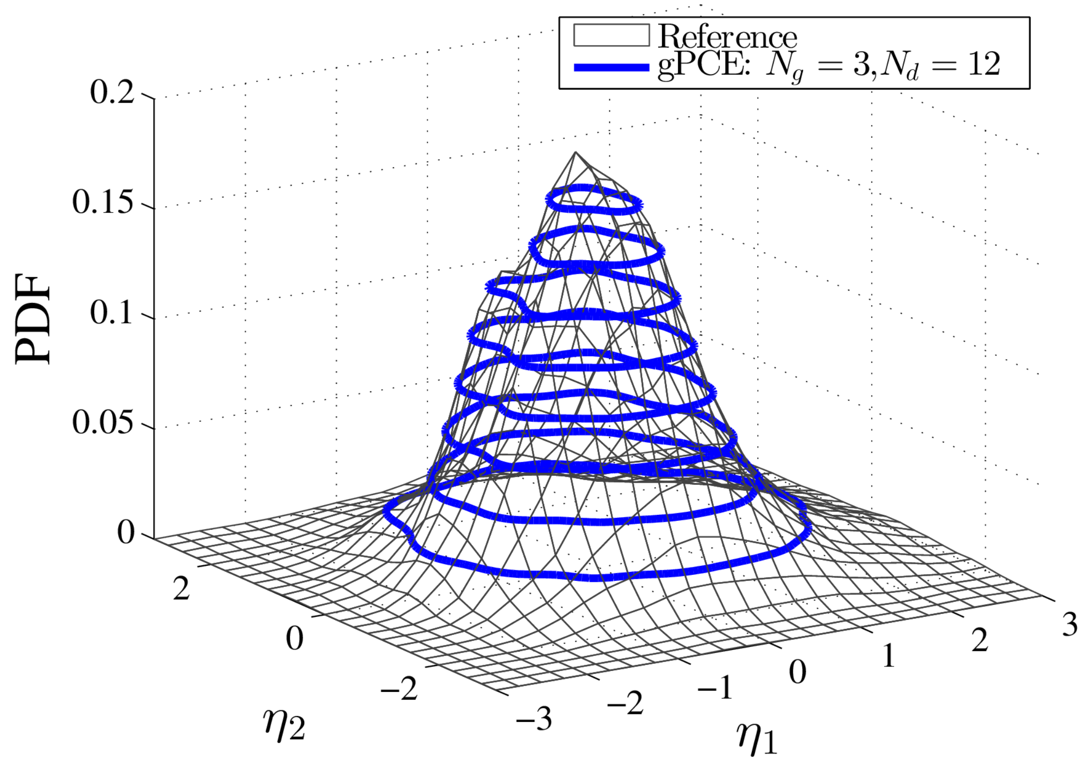

Relative mean square error:

$$\frac{\int_{[0,1]^{N_g}} \left\| \mathfrak{T}^{-1}(\xi) - \sum_{\alpha=1}^{N} \mathbf{c}_\alpha \Psi_\alpha(\xi) \right\|^2 \mathrm{d}\xi}{\int_{[0,1]^{N_g}} \left\| \mathfrak{T}^{-1}(\xi) \right\|^2 \mathrm{d}\xi} = 5\%$$

Stochastic model of apparent contact force: overview

Generated contact forces
using stochastic model

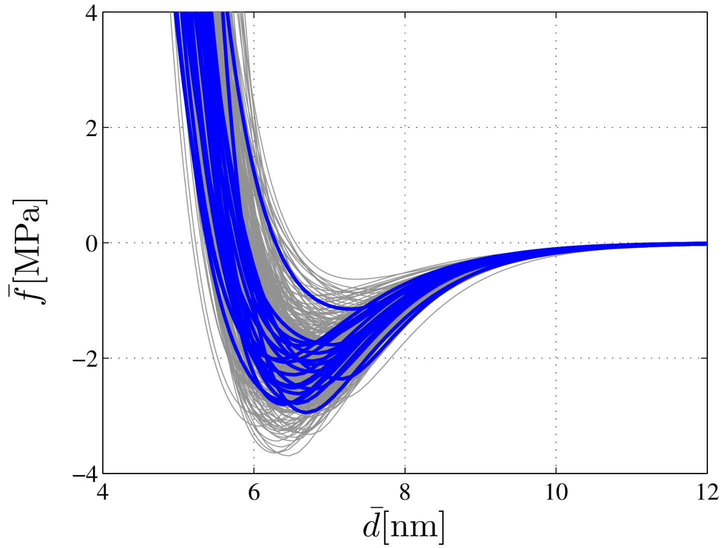

Numerical prediction:
PDF of stiction behavior

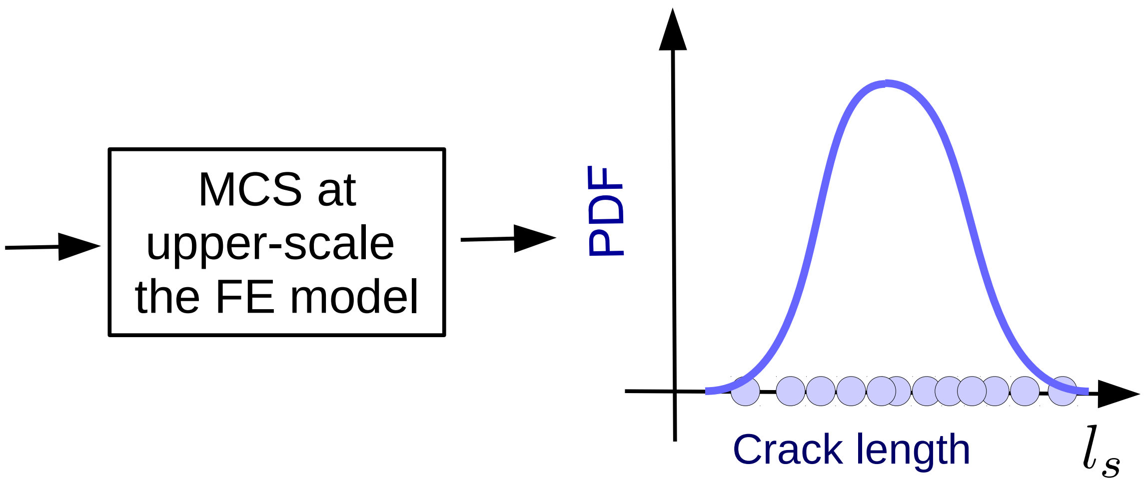

- Generated contact forces:
  - Computational cost is significantly reduced compared to the direct MCS approach
  - There exists error in terms of distribution compared to the explicitly evaluated contact forces
  - Investigation of the effects of this error on the evaluated PDF of quantities of interest: **numerical verification**
- Investigation of the agreement between numerical predictions and experiments
  - **Experimental validation**

Contents

Numerical verification and experimental validation

- Stiction tests with micro cantilever arrays [Xue et al. 2008]
  - Beams were forced to enter to contact with their substrate
  - External factors were then released, the beams exposed the s-shape stiction configuration

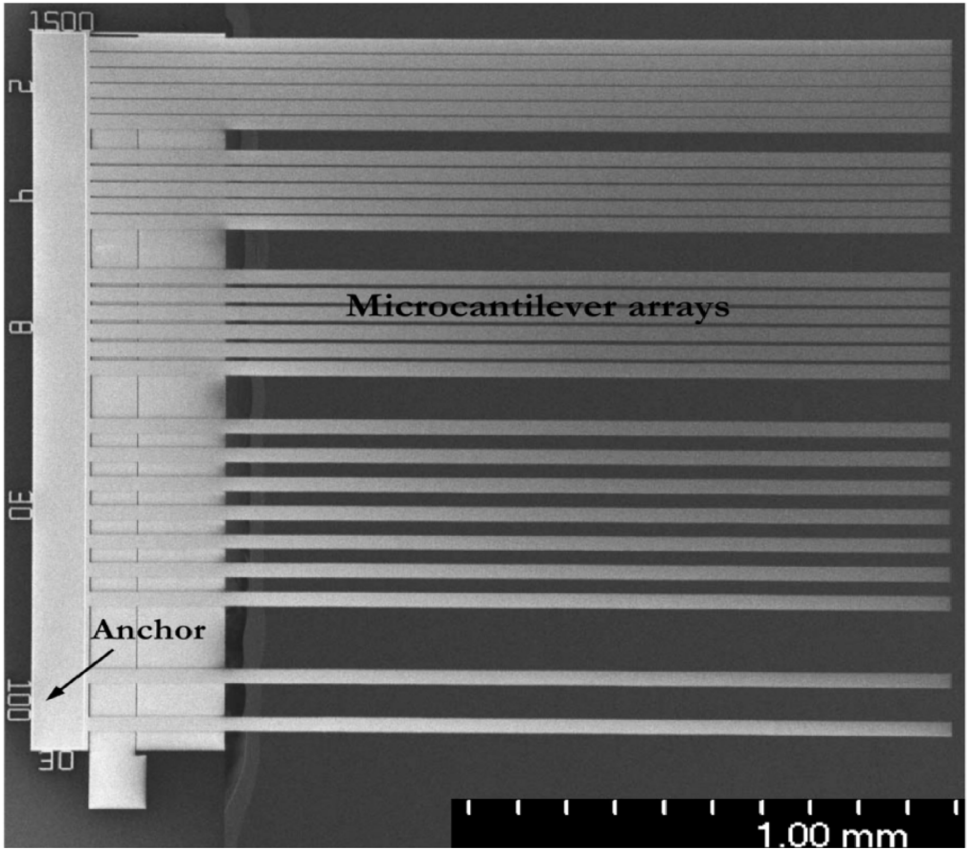

Micro-cantilever beam arrays (top view) [Xue et al 2008]

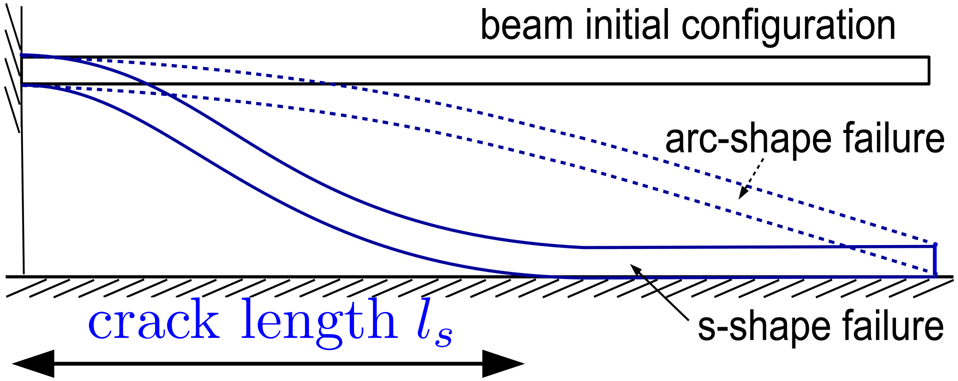

Stiction tests to measure crack length characterizing the adhesion energy

Numerical verification and experimental validation

- Stiction tests with micro cantilever arrays [Xue et al. 2008]
  - From the S-shape failure configurations of the beams, the crack lengths were measured

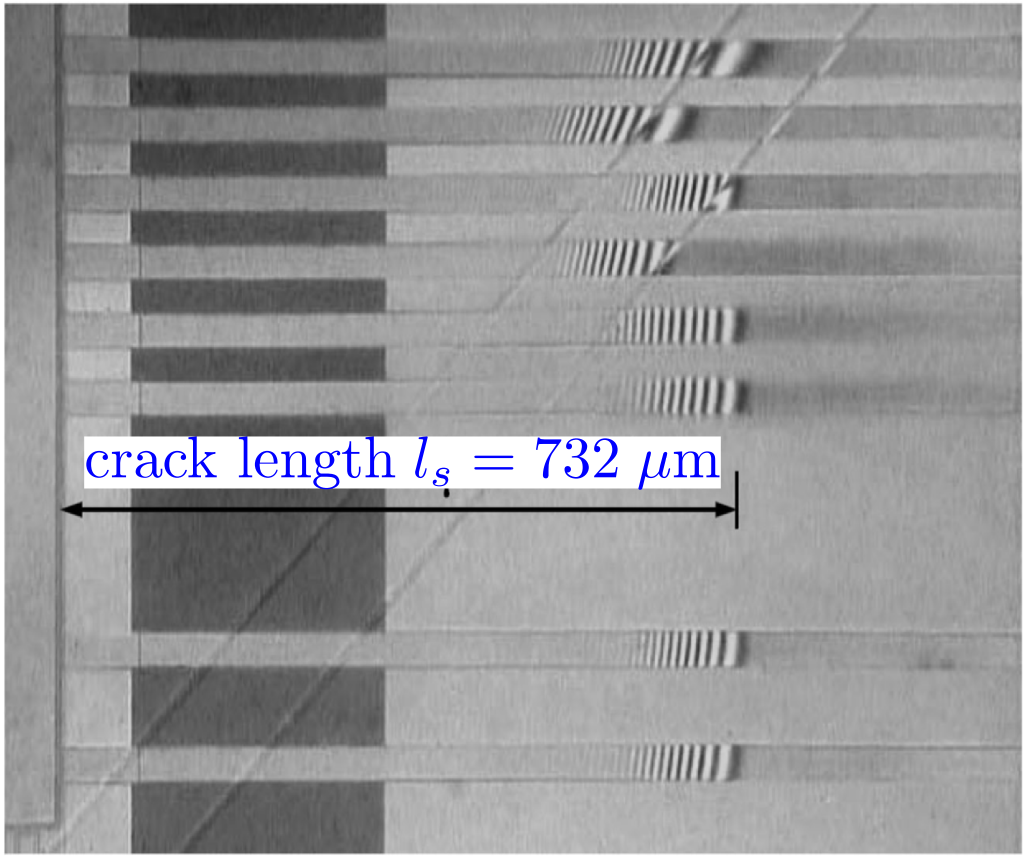

Interferometric image of beams undergoing stiction failure (top view) [Xue et al 2008]

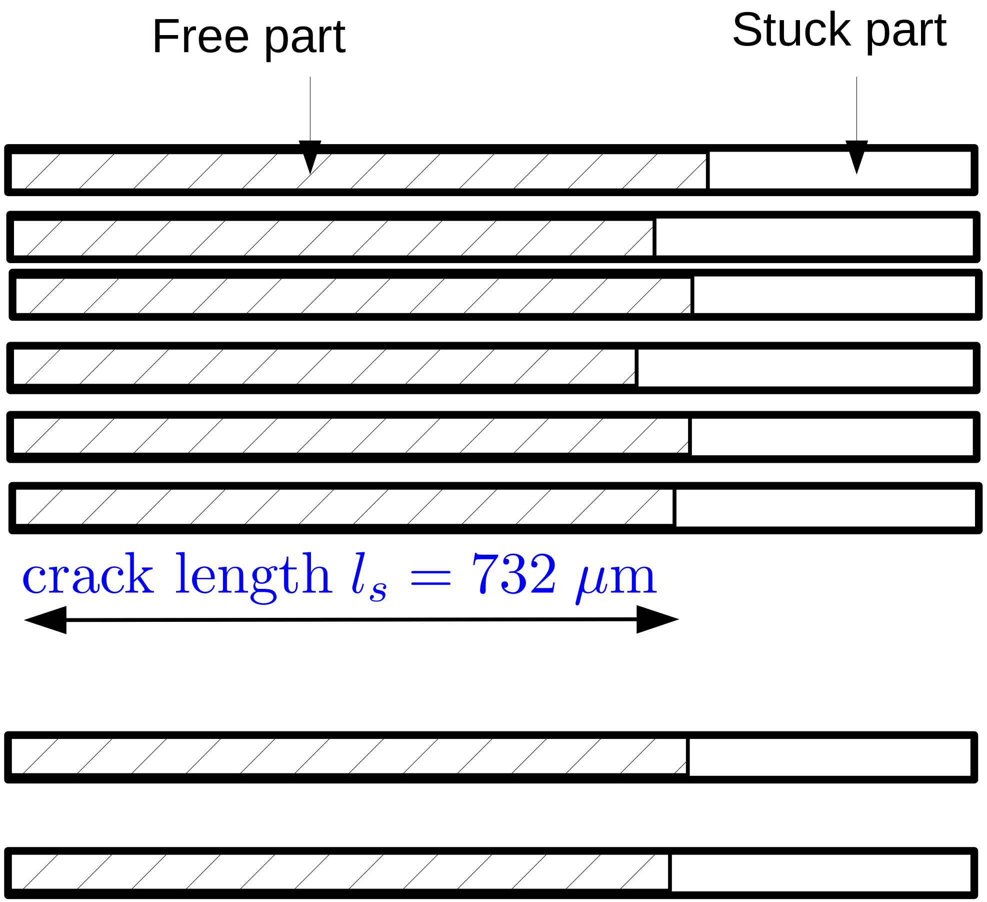

Sketch of the left figure

Numerical verification and experimental validation

- Stiction tests with micro cantilever arrays [Xue et al. 2008]
  - From the S-shape failure configurations of the beams, the crack lengths were measured
  - Effective adhesion energy, required energy to close or open a unit area of free surface, is then evaluated
    - The shorter the crack length, the higher the internal elastic energy of deformed beam, and thus the higher the effective adhesion energy
- Using developed method to model the stiction tests of micro cantilever beams

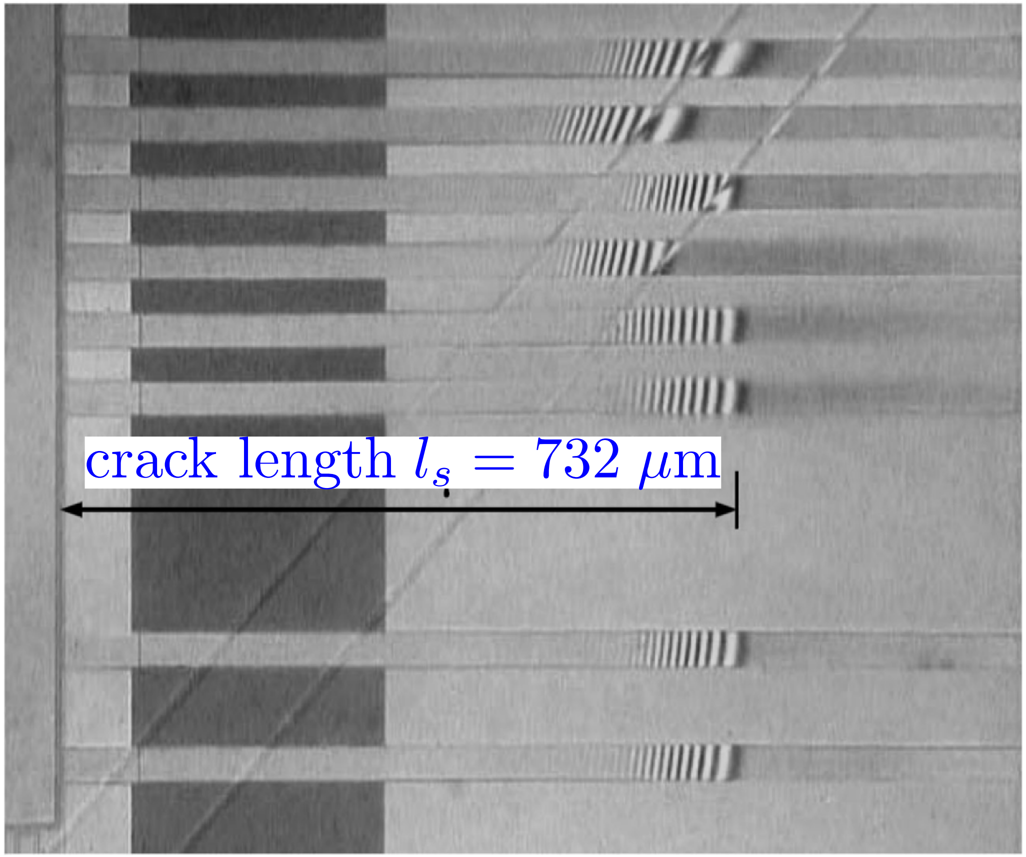

Effective adhesion energy

$$\Gamma = \frac{3}{2} E \frac{h^2 t^3}{{l_s}^4}$$

Crack length

(When contacting surfaces are flat, or in the full saturation condition:

$\Gamma = \text{Theoritcal energy of capillary interaction})$

Numerical verification and experimental validation

- Numerical verification: verify the stochastic model approach versus Direct MCS
    - Direct MCS: all the **contact forces** required for MCS are **explicitly evaluated**
    - Stochastic model-based method: a stochastic model of contact forces is developed to **generate the required contact forces for MCS**
- Experimental validation: compare numerical prediction with experimental data

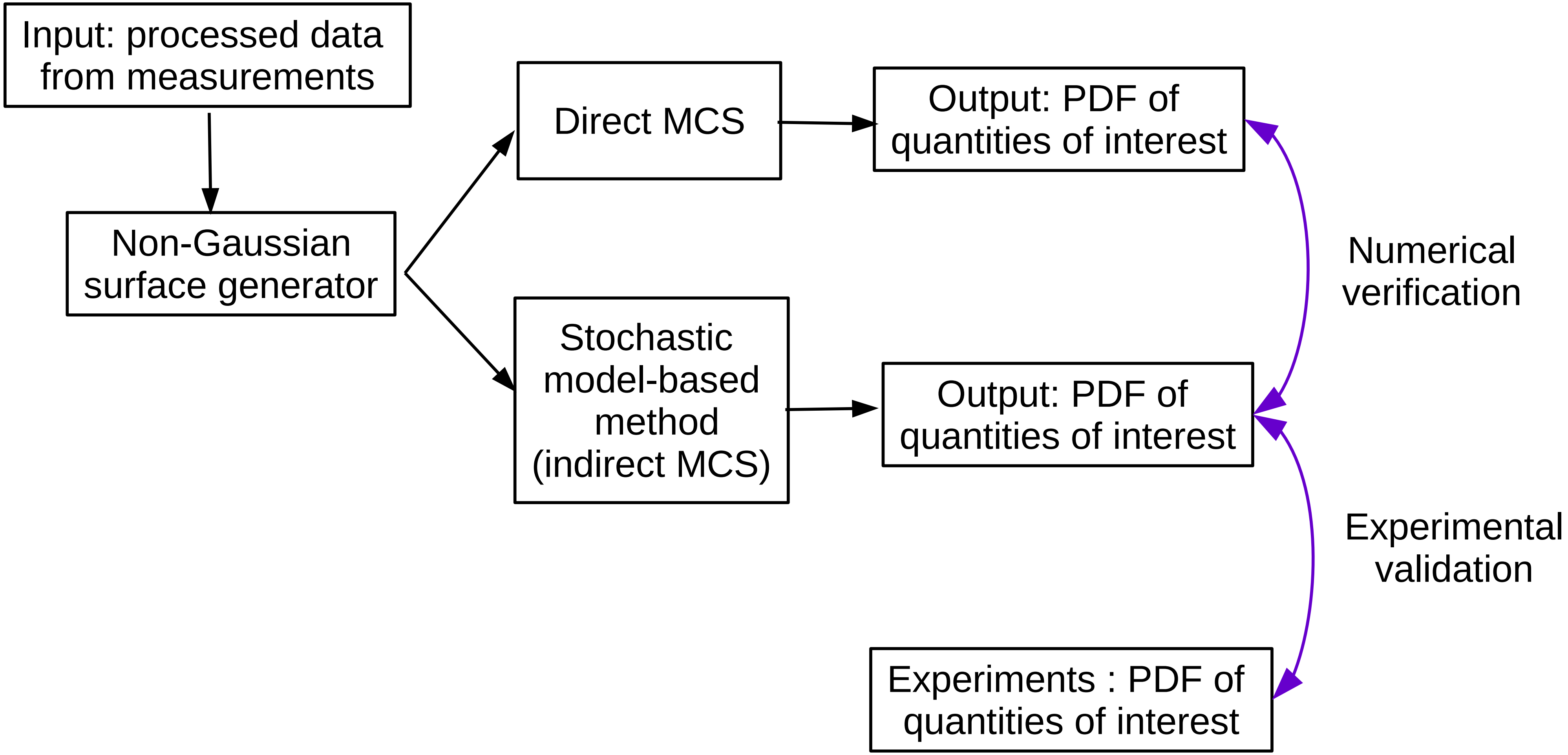

Numerical verification

- Direct MCS (with generated surfaces) as reference vs. Stochastic model-based method
- Prediction given by the stochastic method **well approximates the distribution** of crack lengths given by direct MCS
  - 0.3% difference in terms of mean of crack length
  - 0.2% difference in terms of standard deviation of crack length
- **Computational cost is reduced by 97% with the stochastic method**
  - Direct MCS 671 CPU days, Stochastic method 17 CPU days

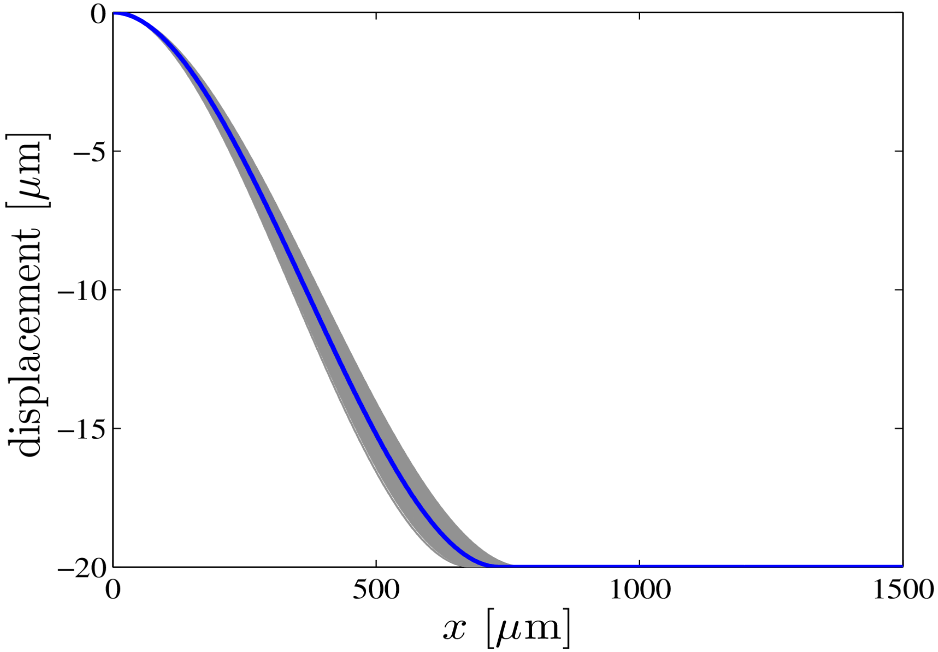

Collection of 1000 realizations of S-shape failure stiction beams (stochastic model-based method)

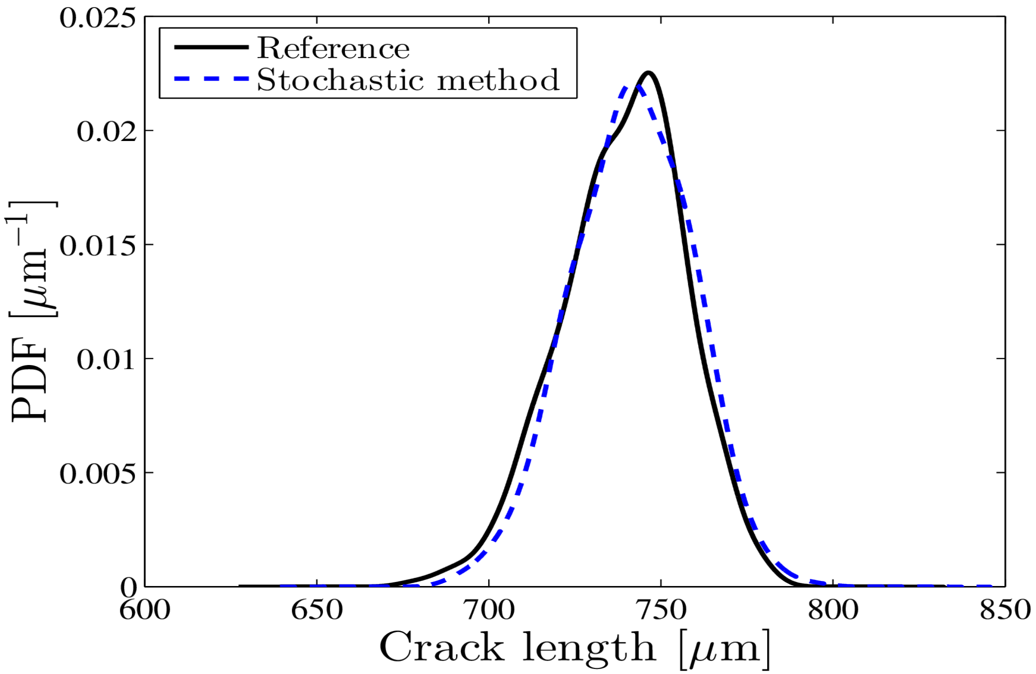

Distribution of crack lengths

Experimental validation

- Experimental validation: compare with experiments [Xue et al. 2008]

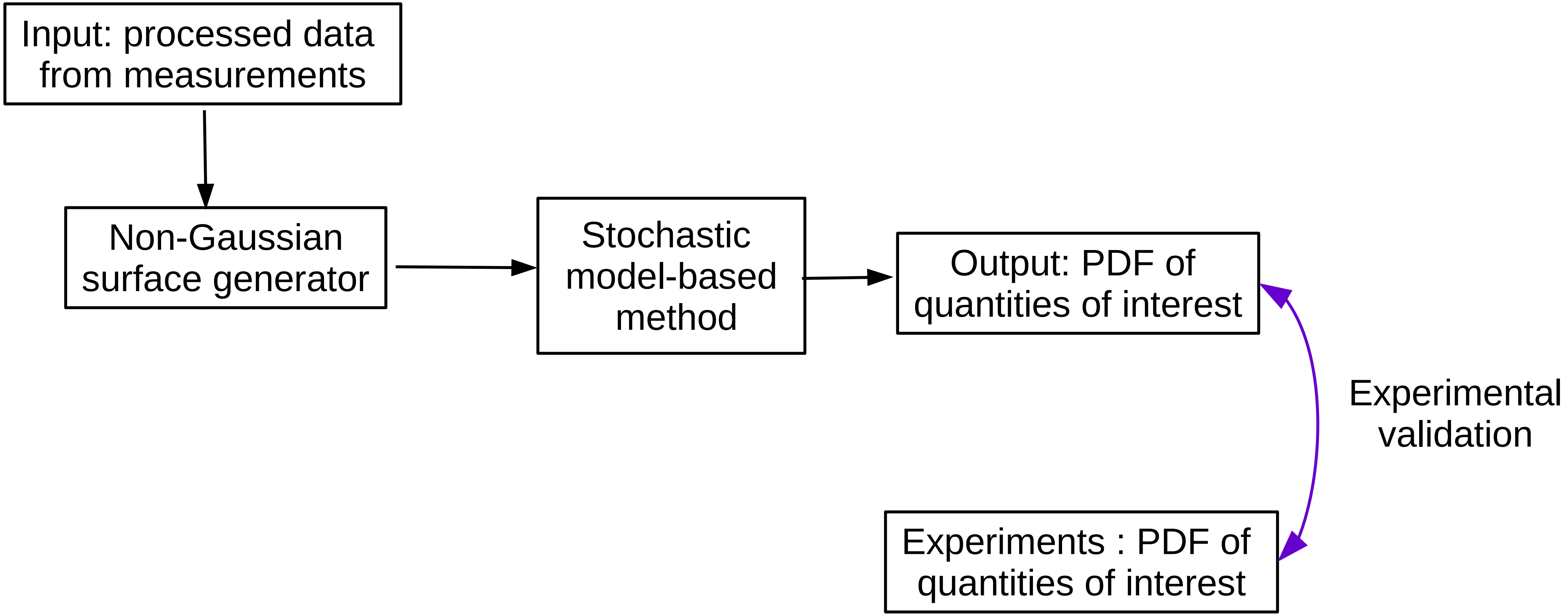

Experimental validation

- Experimental validation: compare with experiments [Xue et al. 2008] with three cases
  - Difficulty: **AFM measurements are not directly accessible but only processed data**
    - Roughness, skewness, kurtosis: used to evaluated the first order mPDF
    - Summit statistical properties: summit density, and mean radius of all summits
  - PSD function is indirectly identified from summit statistical properties
    - There might exist errors due to the indirect identification

Surface topology with an identified summit (○)

illustration of a summit

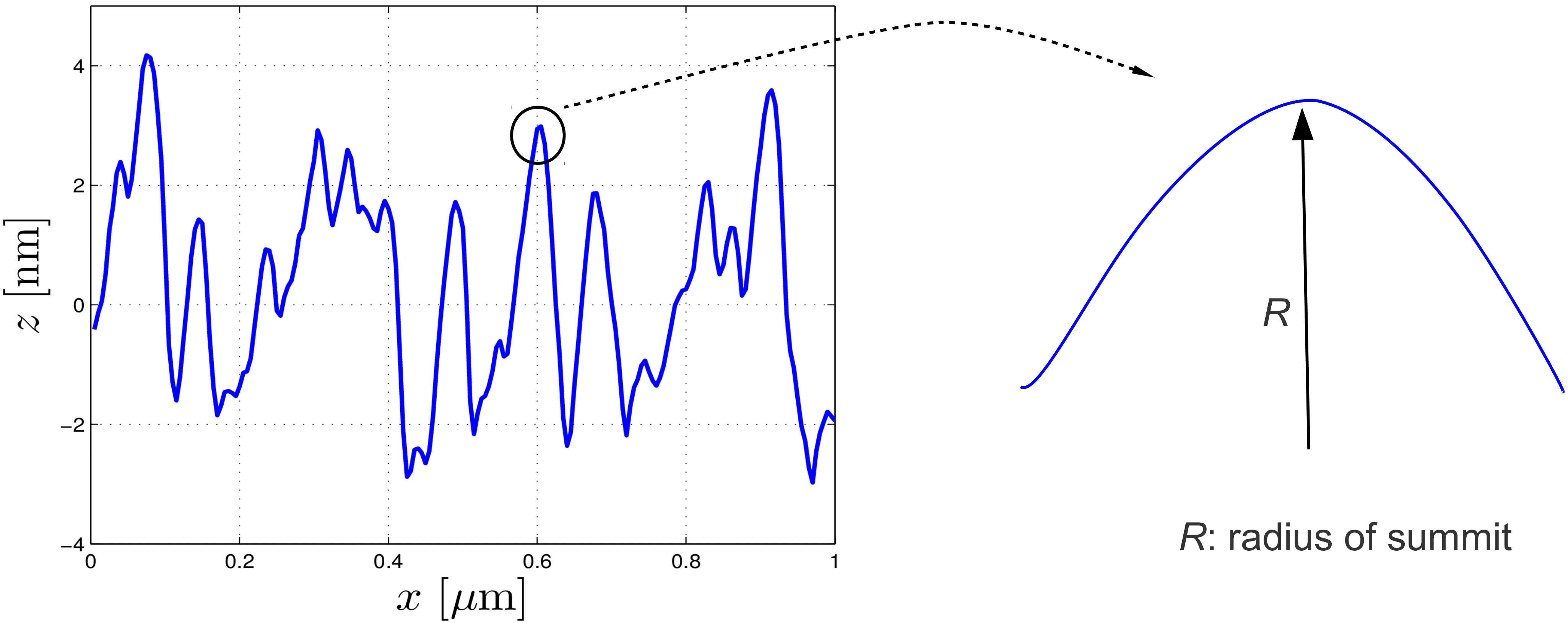

R: radius of summit

Experimental validation

- Case 1 (of three cases): Beam B2 vs Substrate S1 [Xue et al. 2008]

	Beam B2			Substrate S1		
	AFM	non-Gaussian	Gaussian	AFM	non-Gaussian	Gaussian
rms [nm]	3.4	3.4	3.4	0.17	0.17	0.17
skewness [-]	-0.76	-0.76	0	-0.31	-0.31	0
kurtosis [-]	3.9	3.9	3	3.9	3.9	3
$\bar{R}_{\text{sum}}$ [μm]	0.84	0.85	0.56	3.0	3.0	3.0
$\bar{N}_{\text{sum}}$ [μm^{-2}]	20.9	20.0	29.2	111.5	109	115

rms: root mean square roughness, $\bar{R}_{\text{sum}}$: mean radius of summits, $\bar{N}_{\text{sum}}$: summits density.

Experimental validation

- Case 1 (of three cases): Beam B2 vs Substrate S1 [Xue et al. 2008]

	Beam B2			Substrate S1		
	AFM	non-Gaussian	Gaussian	AFM	non-Gaussian	Gaussian
rms [nm]	3.4	3.4	3.4	0.17	0.17	0.17
skewness [-]	-0.76	-0.76	0	-0.31	-0.31	0
kurtosis [-]	3.9	3.9	3	3.9	3.9	3
$\bar{R}_{\text{sum}}$ [μm]	0.84	0.85	0.56	3.0	3.0	3.0
$\bar{N}_{\text{sum}}$ [μm^{-2}]	20.9	20.0	29.2	111.5	109	115

rms: root mean square roughness, $\bar{R}_{\text{sum}}$: mean radius of summits, $\bar{N}_{\text{sum}}$: summits density.

- Generated non-Gaussian surfaces are representative the real surfaces in terms of statistical properties
  - Statistical moments are perfectly matched
  - Summit statical properties are well approximated
    - Errors are due to the indirect identification of PSD function
- For generated Gaussian surfaces, skewness value is always zeros, and kurtosis is always three by default
  - Non representative

Experimental validation

- Case 1 (of three cases): Beam B2 vs Substrate S1 [Xue et al. 2008]

	Beam B2			Substrate S1		
	AFM	non-Gaussian	Gaussian	AFM	non-Gaussian	Gaussian
rms [nm]	3.4	3.4	3.4	0.17	0.17	0.17
skewness [-]	-0.76	-0.76	0	-0.31	-0.31	0
kurtosis [-]	3.9	3.9	3	3.9	3.9	3
$\bar{R}_{\text{sum}}$ [μm]	0.84	0.85	0.56	3.0	3.0	3.0
$\bar{N}_{\text{sum}}$ [μm^{-2}]	20.9	20.0	29.2	111.5	109	115

$\bar{R}_{\text{sum}}$: mean radius of summits, $\bar{N}_{\text{sum}}$: summits density.

- Generated non-Gaussian surfaces are representative the real surfaces in terms of statistical properties
  - Statistical moments are perfectly matched
  - There are errors in terms of summit statistical properties: negligible for this case
    - Due to the **indirect identification of PSD function**
- For generated Gaussian surfaces, skewness value is always zeros, and kurtosis is always three by default
  - Non representative

Experimental validation

- Case 1 (of three cases): Beam B2 vs Substrate S1 [Xue et al. 2008]

	Beam B2			Substrate S1		
	AFM	non-Gaussian	Gaussian	AFM	non-Gaussian	Gaussian
rms [nm]	3.4	3.4	3.4	0.17	0.17	0.17
skewness [-]	-0.76	-0.76	0	-0.31	-0.31	0
kurtosis [-]	3.9	3.9	3	3.9	3.9	3
$\bar{R}_{\mathrm{sum}}$ [μm]	0.84	0.85	0.56	3.0	3.0	3.0
$\bar{N}_{\mathrm{sum}}$ [$\mu\mathrm{m}^{-2}$]	20.9	20.0	29.2	111.5	109	115

rms: root mean square roughness, $\bar{R}_{\mathrm{sum}}$: mean radius of summits, $\bar{N}_{\mathrm{sum}}$: summits density.

- Generated non-Gaussian surfaces are representative the input data from the measurements
  - Statistical moments are perfectly matched
  - There are errors in terms of summit statistical properties: negligible for this case
    - Due to the **indirect identification of PSD function**
- For generated Gaussian surfaces, skewness value is always zeros, and kurtosis is always three by default
  - Non representative

Experimental validation

- Case 1 (of three cases): Beam B2 vs Substrate S1 [Xue et al. 2008]
  - Overall trend: the higher the humidity level,
    - The larger the adhesion energy: toward theoretical value of capillary forces 144 mJ/m²
    - The smaller the uncertainty range
  - The water height increases at high humidity level, and consequently the importance of surface roughness reduces compared to meniscus height

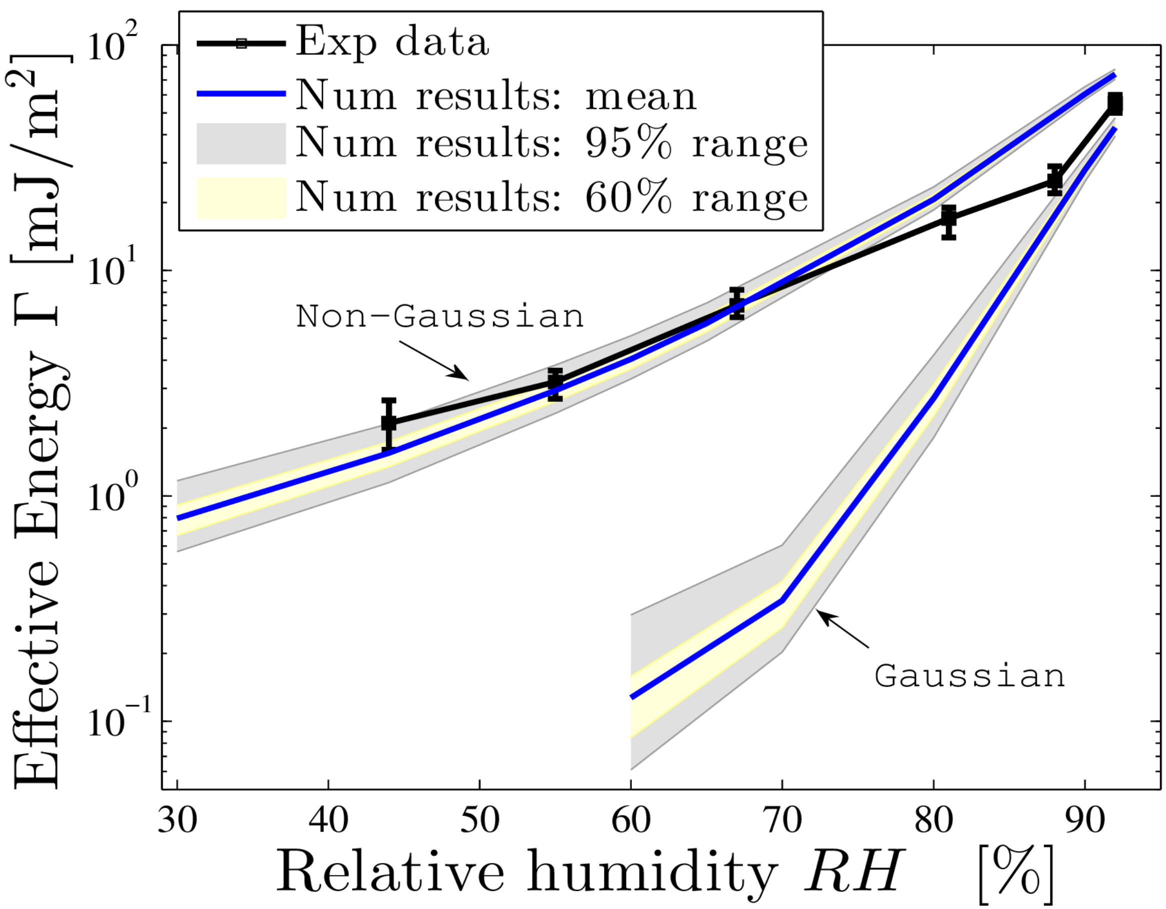

- Experimental data: black error bars

- Numerical predictions: mean values associated with confidence ranges of 95%, 60%

Experimental validation

- Case 1 (of three cases): Beam B2 vs Substrate S1 [Xue et al. 2008]
  - Overall trend: the higher the humidity level,
    - The larger the adhesion energy: toward theoretical value of capillary forces 144 mJ/m²
    - The smaller the uncertainty range
  - The water height increases at high humidity level, and consequently the importance of surface roughness reduces compared to meniscus height

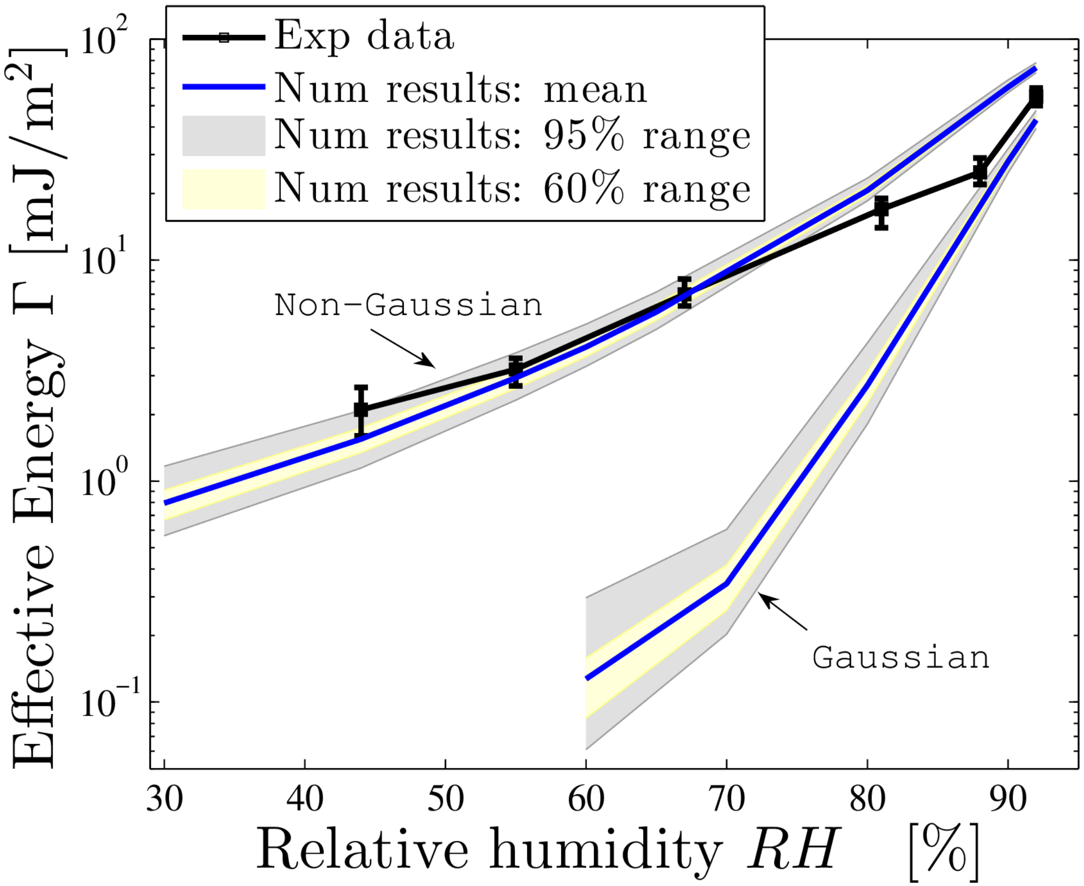

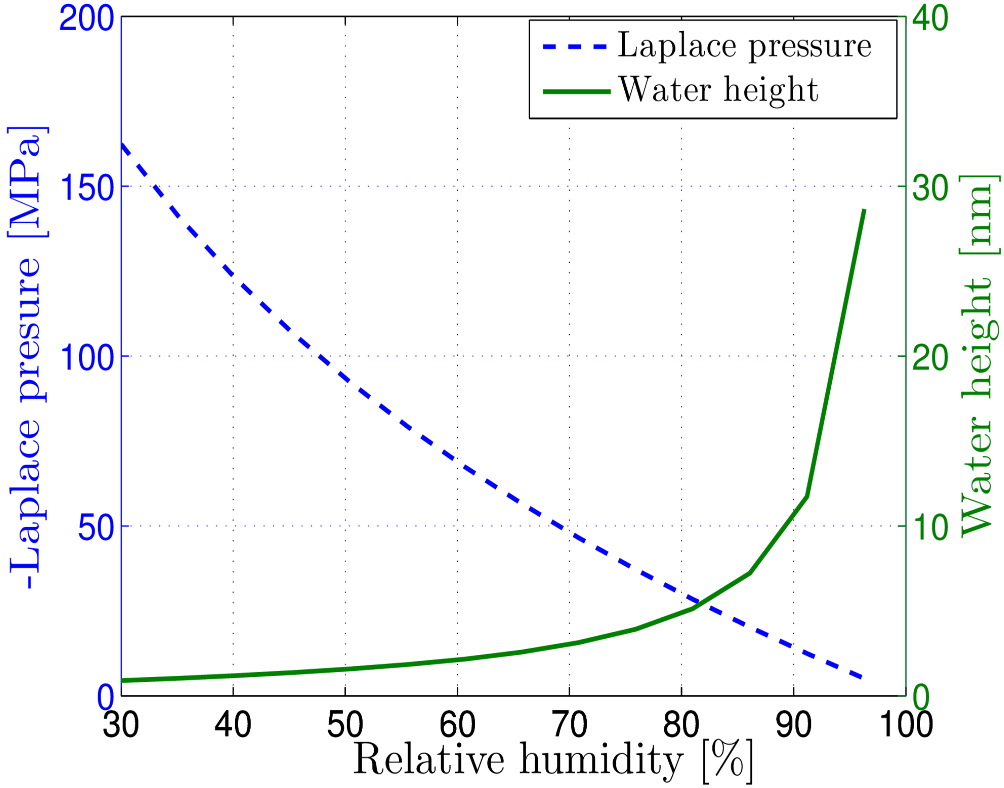

Experimental validation

- Case 1 (of three cases): Beam B2 vs Substrate S1 [Xue et al. 2008]
  - **Good agreement between numerical predictions (non-Gaussian surfaces) and experiment data: model is validated**
  - The predictions obtained from Gaussian surface significantly underestimates the experimental data

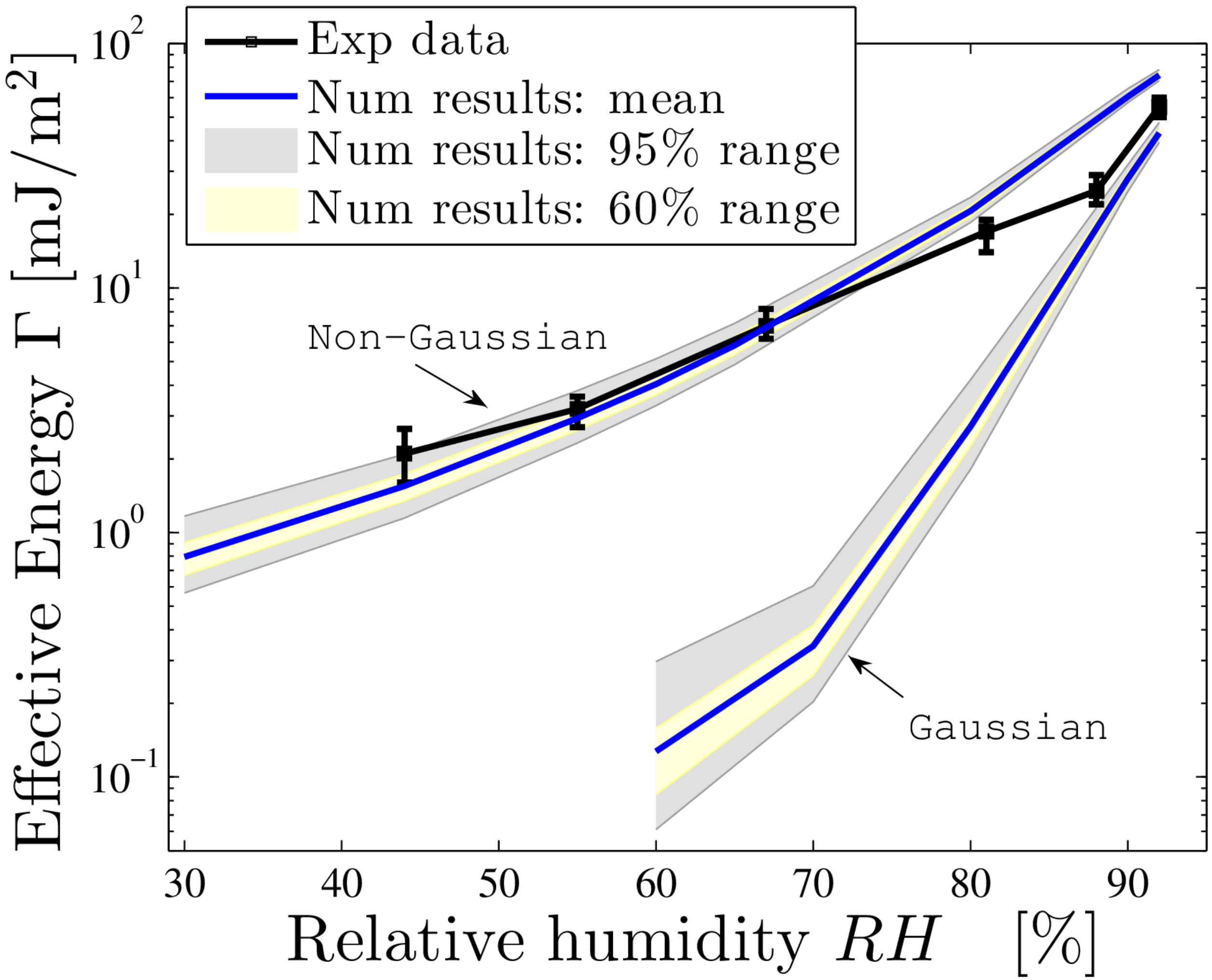

- Experimental data: black error bars

- Numerical predictions: mean values associated with confidence ranges of 95%, 60%

Experimental validation

- Case 1 (of three cases): Beam B2 vs Substrate S1 [Xue et al. 2008]

	Beam B2			Substrate S1		
	AFM	non-Gaussian	Gaussian	AFM	Non-Gaussian	Gaussian
rms [nm]	3.4	3.4	3.4	0.17	0.17	0.17
skewness [-]	-0.76	-0.76	0	-0.31	-0.31	0
kurtosis [-]	3.9	3.9	3	3.9	3.9	3
$\bar{R}_{\text{sum}}$ [μm]	0.84	0.85	0.56	3.0	3.0	3.0
$\bar{N}_{\text{sum}}$ [μm^{-2}]	20.9	20.0	29.2	111.5	109	115

- The heights of the contacting asperities of non-Gaussian surfaces are less scatter than the ones of Gaussian surface due to the negative skewness

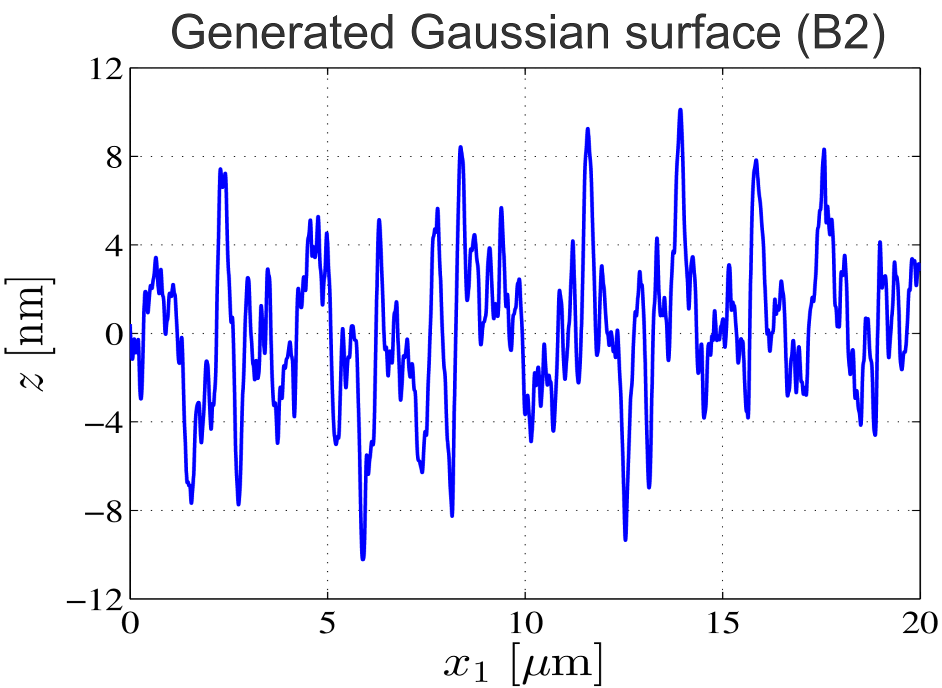

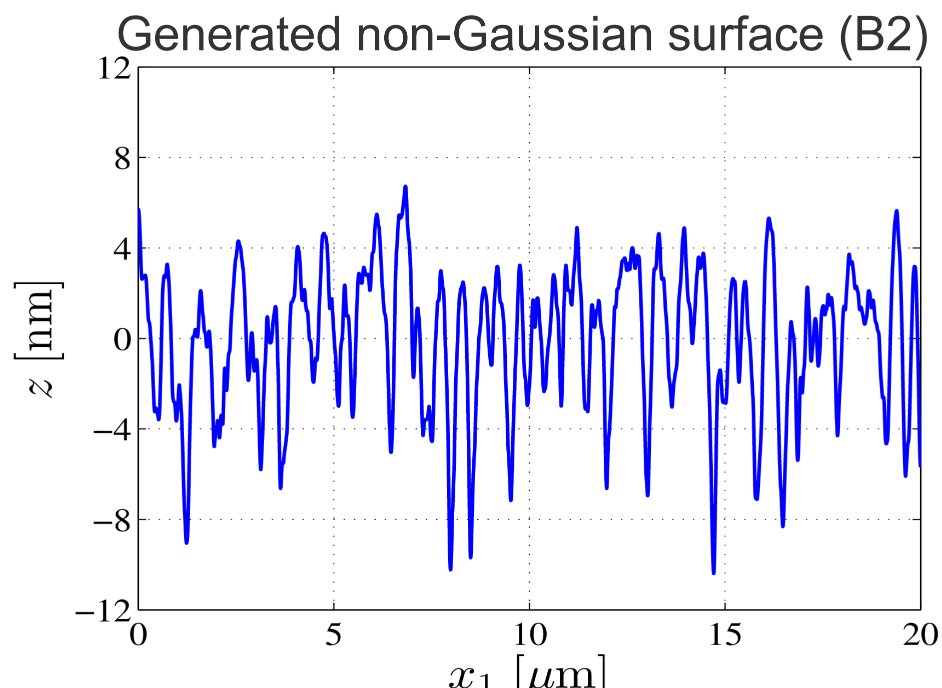

Experimental validation

- Case 2 (of three cases): Beam B1 vs Substrate S1 [Xue et al. 2008]

	Beam B1			Substrate S1		
	AFM	non-Gaussian	Gaussian	AFM	non-Gaussian	Gaussian
rms [nm]	1.7	1.7	1.7	0.17	0.17	0.17
skewness [-]	-0.78	-0.78	0	-0.31	-0.31	0
kurtosis [-]	4.6	4.6	3	3.9	3.9	3
$\bar{R}_{\text{sum}}$ [μm]	0.41	0.41	0.30	3.0	3.0	3.0
$\bar{N}_{\text{sum}}$ [μm^{-2}]	68	63	71	111.5	109	115

$\bar{R}_{\text{sum}}$: mean radius of summits, $\bar{N}_{\text{sum}}$: summit density.

- Generated non-Gaussian surfaces vs. AFM measurements
  - Statistical moments are perfectly matched
  - **Moderate error** in terms of density of the summits for the case of Beam B1: 8% of error
    - Due to the indirect approximation of PSD function

Experimental validation

- Case 2 (of three cases): Beam B1 vs Substrate S1 [Xue et al. 2008]
  - Overall trend (similar to case 1)
  - **Moderate agreement** between numerical prediction and and experiment data
    - Due to the error in terms of density of the summits of generated surfaces
    - Numerical predictions can be improved: accounting for other random sources, e.g. geometrical dimensions of cantilever beams (see my thesis for more details)
    - A kink in the evolution experimental results: the non-proper implementation of experiments

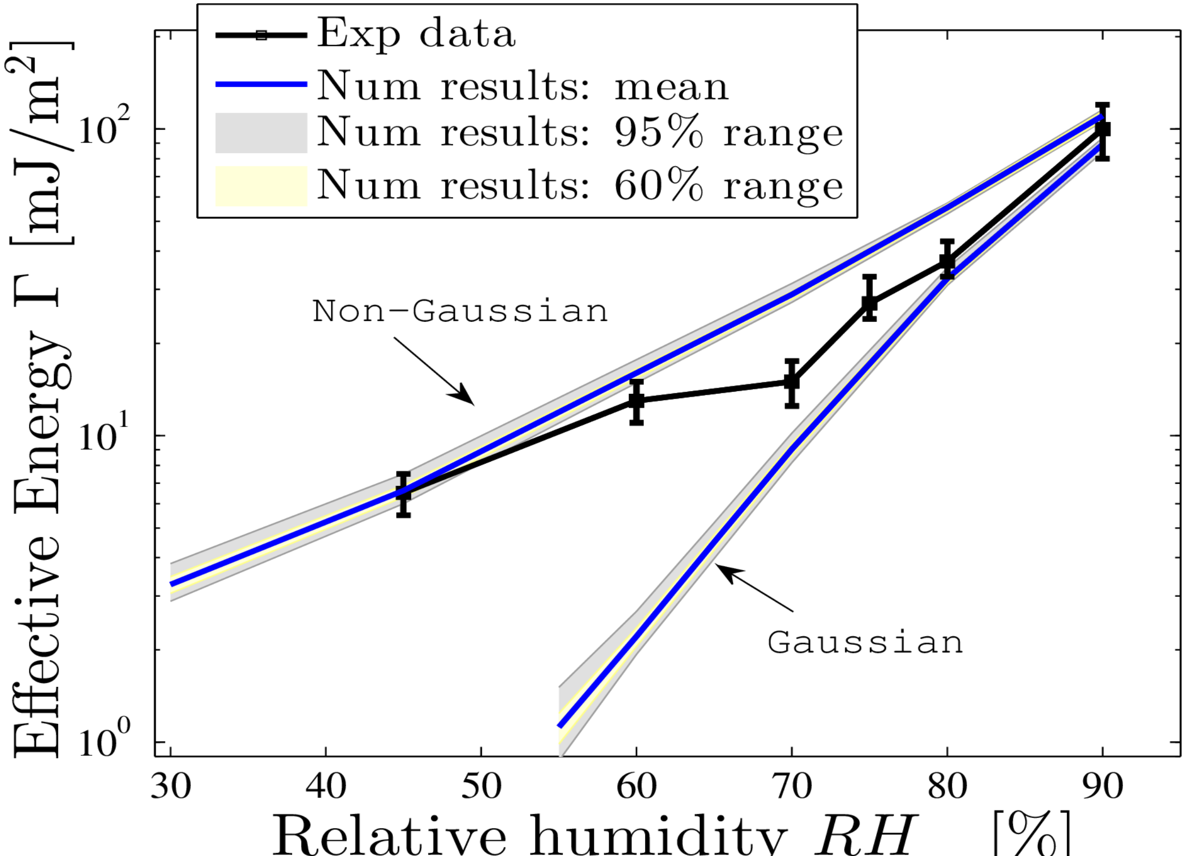

- Experimental data: black error bars

- Numerical predictions: mean values associated with confidence ranges of 95%, 60%

Experimental validation

- Case 3 (of three cases): Beam B1 vs Substrate S2 [Xue et al. 2008]

	Beam B1			Substrate S2		
	AFM	non-Gaussian	Gaussian	AFM	non-Gaussian	Gaussian
rms [nm]	1.7	1.7	1.7	5.5	5.5	5.5
skewness [-]	-0.78	-0.78	0	-1.1	-1.1	0
kurtorsis [-]	4.6	4.6	3	5.1	5.1	3
$\bar{R}_{\text{sum}}$ [μm]	0.41	0.41	0.30	0.12	0.14	0.09
$\bar{N}_{\text{sum}}$ [μm^{-2}]	68	63	71	48	59	68

$\bar{R}_{\text{sum}}$: mean radius of summits, $\bar{N}_{\text{sum}}$: summit density.

- Generated non-Gaussian surfaces vs. AFM measurements
  - Statistical moments are perfectly matched
  - **Significant error** in mean radius of summits for the case of Substrate S2: 23% of error
  - **Significant error** in density of the summits for the case of Substrate S2: 17% of error
    - Due to the indirect identification of PSD function

Experimental validation

- Case 3 (of three cases): Beam B1 vs Substrate S2 [Xue et al. 2008]
  - Significant differences between numerical predictions and and experiment data
    - Due to the significant errors between generated surfaces and real surfaces (AFM measurements)

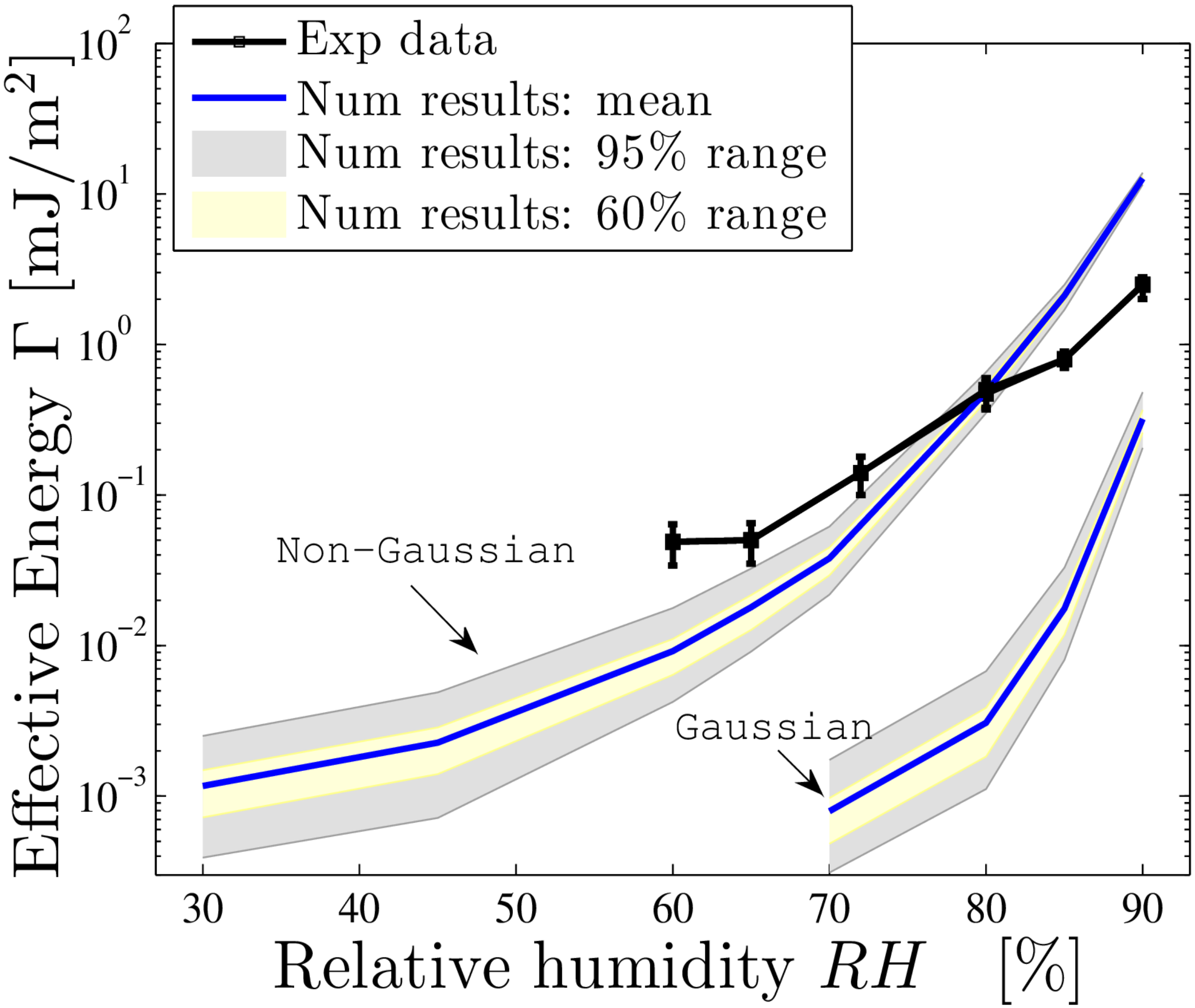

- Experimental data: black error bars

- Numerical predictions: mean values associated with confidence ranges of 95%, 60%

Experimental validation

- Summarization of the comparison between numerical predictions vs. experiments [Xue et al. 2008]
  - The lower the errors of generated surfaces compared with AFM measurements, the smaller the difference between numerical predictions and experimental data

	Case 1	Case 2	Case 3
Input: Error of summit statiscal properties	negligible	moderate	significant
Output: Error of numerical predictions	small	moderate	significant

  - Accounting for non-Gaussian properties of contacting surfaces significantly improves the numerical predictions accuracy

Contents

Conclusions

- A **Stochastic model-based multiscale method for stiction problems** taking the surface topology into account by
  - Lower-scale: using random field method to characterize the AFM surface measurements and generate numerical surfaces
    - The accuracy is improved thanks to the non-Gaussianity is accounted for
  - Meso-scale: a semi-analytical contact model to evaluate the meso-scale apparent contact forces
    - At an acceptable computational cost while accounting for saturation effect and size effect
  - Applying gPCE to build a stochastic model of the random meso-scale contact forces
    - To reduce efficiently the **computational cost**
  - Upper-scale: Integrate contact forces generated using the stochastic model as random contact laws to a FE model
    - Performing MCS to obtain the distribution of the stiction behaviors
- The model is numerically verified and then experimentally validated
  - Numerical predictions are in a good agreement with experimental results when the real surfaces are well represented using generated surfaces
- The model is helpful to broaden our knowledge about stiction phenomenon
  - "… Why one MEMS device sticks and another identical one does not" [van Spengen 2015]

Perspectives

- Applying the model to evaluate the **failure percentage** of MEMS designs such as
  - The stiction of MEMS accelerometers under shock
  - The stiction of MEMS gears system
- Accounting for plastic deformation and fatigue of contacting surfaces
  - Initial design is stiction free
  - Stiction risk increases when contacting surfaces are plastically deformed and/or fatigue
  - To predict the life time of a given device before stiction failure

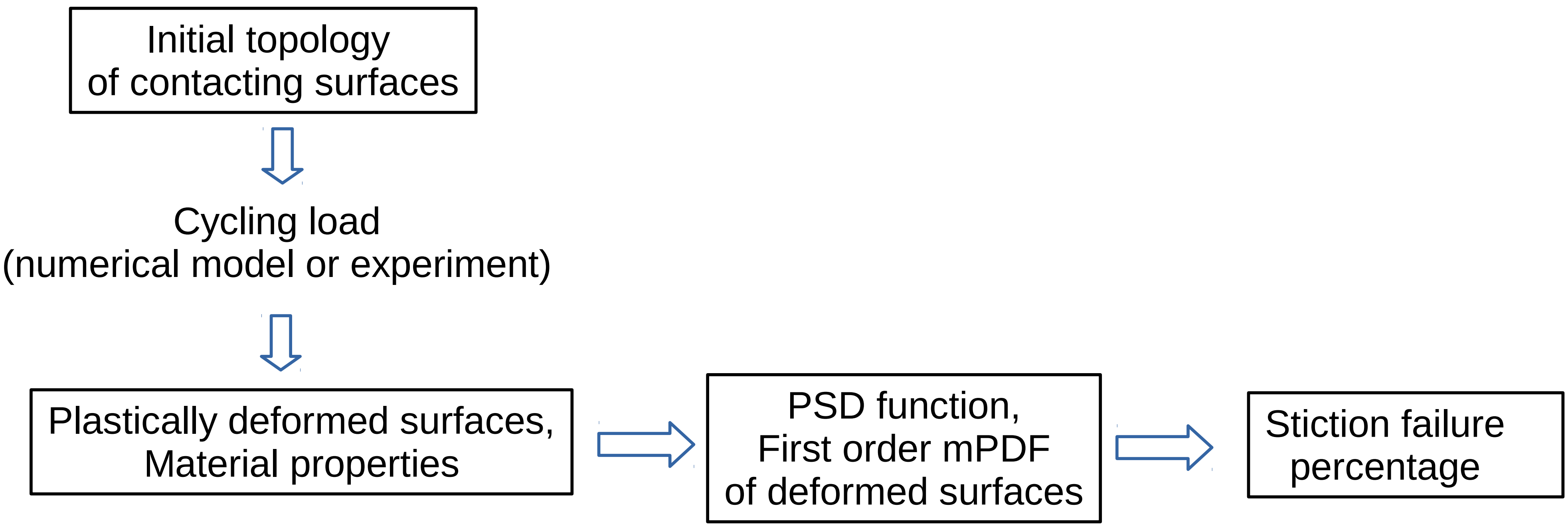

Thank you for your attentions

Q&A section